Behaviour of deepwell handpumps with PVC rising mains

Jue

BEHAVIOUR OF DEEPWELL HANDPUMPS WITH PVC RISING MAINS

by

Jos BESSELINK*, Jacques GRUPA+, Paul SMULDERS+

* InterAction Design
Arnhem, The Netherlands

+Wind Energy Group
Laboratory of Fluid Dynamics and Heat Transfer
Faculty of Physics,
Eindhoven University of Technology
Eindhoven, The Netherlands

An IAD Handpump Project Research Publication

BEHAVIOUR OF DEEPWELL HANDPUMPS WITH PVC RISING MAINS by Jos besselink, Jacques Grupa and Paul Smulders
Arnhem: IAD Handpump Project, 1990; 90 pages, 50 Fig.
Includes references, selected bibliography and 5 appendices.
Publication Number: IADHPP90.02 **ISBN 90-6618-544-9**
Printer: AC Ermelo, The Netherlands
Publisher: APP bv. Ellecom, The Netherlands

Abstract

In applying handpumps with PVC rising mains at greater depths, unexpected problems have been encountered in the field, such as frequent fracturing of the rising mains and pump rods, and severely decreased pump yields. To obtain an understanding of these problems and their causes the IAD Handpump Project, sponsored by the Netherlands Ministry for Development Cooperation, Section for Research and Technology, was set up to test a number of hand driven deepwell piston pumps and to analyze their behaviour.

This report is intended for persons with a technical background, who are involved in the manufacturing, implementation and maintenance of medium and deepwell handpumps. But it also aims at persons involved in handpump research and development, as well as consultants.
The report summarizes the main results of the investigations and explains the basic principles and problems related to deepwell handpumps with PVC rising mains. It indicates in a general sense how to improve handpump design.

The elasticity of PVC rising mains governs the behaviour of the pump to a large extent:
- it reduces the effective piston stroke, resulting in (much) lower volumetric efficiencies;
- it reduces the resonance frequencies, so that resonance may occur at normal pumping frequencies.

These resonances are due mainly to pressure waves in the water column in the rising main. The resulting, very much increased pressure fluctuations may lead to considerably increased stresses. The valve dynamics are of no importance for this type of pump.

Fatigue has shown to be the main reason for fracturing PVC rising mains and steel pump rods. This is due mainly to the frequent stress fluctuations (more than 10 million pump cycles!), the corrosive water, notches in the PVC and stress concentrations in the joints of the rising mains and the pump rods.

By careful detailing and dimensioning the fatigue lifetime and the pump efficiencies can be increased, for example by reducing the ratio piston diameter versus rising main diameter and wall thickness. Where possible, indications are given for such improvements of the design of deepwell handpumps.

Finally, the origins and effects of buckling, swinging and 'snaking' are explained, as well as the consequences of creep and cylinder support.

Key words: community water supply, handpumps - testing, handpumps - developing, handpumps - PVC rising mains

The IAD Handpump Project

The IAD Handpump Project is sponsored by the Section for Research and Technology of the Netherlands Ministry of Foreign Affairs. In line with similar projects that have been carried out in recent years under the auspices of the World Bank, its main goal is to provide a contribution to the improvement of (communal) drinking water supply and small-scale irrigation, notably in Third World countries.

Five partners are involved in the IAD Handpump Project (see below for abbreviations used):

IAD	-	over-all coordination, data acquisition, hard- and software, carrying out of testing programme, final responsibility;
DHV	-	general advice on project implementation, project publications;
WEG/EUT	-	planning advice, analysis of results, physical modelling, fatigue studies;
JVI	-	supplier of the Volanta handpump; analysis of test results;
SWNV	-	supplier of the SWN 81 handpump; assistance in providing, setting up and conversion of test stand.

Since 1986 the project has been involved in the testing of handpumps with PVC rising mains, and in developing the related theoretical background and working models. Experiences gained and recommendations derived from them are published at regular intervals. Comments and reactions to these publications, as well as information on similar tests carried out by others are very much welcomed. For such reactions and for additional information please contact the Project Coordinator: Jos Besselink, at InterAction Design, Arnhem.

For further information contact (in alphabetical order):

Abbreviation	*Partner*	*Persons involved*
DHV	**DHV Consultants,** P.O. Box 85, 3800 AB Amersfoort, The Netherlands Phone: (033) 689111; Fax: (033) 615047	Kees Bonnier* Rob Trietsch
IAD	**InterAction Design,** Onderlangs 125, 6812 CJ Arnhem, The Netherlands. Phone/Fax: (085) 511304	Jos Besselink* Rineke Besselink
JVI	**Jansen Venneboer International B.V.,** P.O.Box 6, 8130 AA Wijhe, The Netherlands Phone: (05702) 3705; Fax: (05702) 3712	Kees Bliemer*
SWNV	**Sociaal Werkvoorzieningsschap Noordwest-Veluwe,** P.O. Box 87, 8070 AB Nunspeet, The Netherlands Phone: (03412) 54046; Fax: (03412) 60218	Pim Brouwer*
WEG/EUT	**Wind Energy Group,** Laboratory of Fluid Dynamics and Heat Transfer, Faculty of Physics, Eindhoven University of Technology P.O. Box 513, 5600 MB Eindhoven, The Netherlands Phone: (040) 472680/473191; Fax: (040) 447035	Paul Smulders* Jacques Grupa Hans Cleijne Jan de Jongh

* Contact person

TABLE OF CONTENTS

TABLE OF CONTENTS (Continued)

PAGE

APPENDICES

LIST OF FIGURES

LIST OF FIGURES

FIGURES IN APPENDICES

1 INTRODUCTION

1.1 General

The importance of handpumps in community water supply cannot easily be overestimated. Millions of people, in particular from the Third World, depend on handpumps for their drinking water supply. In addition there is a change-over from maintenance-sensitive piped supply systems to handpumps as the prime choice for rural water supply systems. Therefore, increasingly, and for decades to come handpumps are likely to remain the only feasible solution to the problem of water supply to small communities in rural areas.

Although a handpump based water supply system is seemingly a technology of utmost simplicity, a combination of criteria imposed on it makes it more complex. This applies especially to pumps with high lifts, i.e. pumps which lift water some 40 to 50 metres, or more.

Handpumps must be:
- easy to manufacture .... preferably also in Third World countries
- easy to install .... by the village mechanic
- of sufficient yield .... for 250 people or more
- reliable .... not unnecessary sophisticated
- durable .... lasting 5 to 10 years
- economical .... capital costs and maintenance affordable by local population

The wells and boreholes on which these handpumps are installed, have an estimated lifetime of about 30 years. The handpumps themselves should last not less than 5 - 10 years. In practice, however, even though quite a number of designs have proven satisfactory, handpumps break down more frequently than expected. Apart from the acute lack of drinking water which a pump failure may cause in a village, a lack of confidence in the handpump may result. This may adversely affect the users' attitude towards pump operation and maintenance, the use of safe drinking water, personal hygiene, etc.

Many different reasons can be given for the early breakdowns of handpumps. The most common are:
- inferior design, materials and/or manufacture
- incorrect installation
- corrosion/abrasion and fatigue
- lack of maintenance, spare parts and/or money.

Not all of these reasons are technological, some being institutional in nature.

Especially under the corrosive conditions that are often encountered in practice (such as low pH of the groundwater) the lifetime of handpumps is considerably shorter than that of the wells and boreholes on which they are installed. Under rural conditions handpumps inevitably pump some sand along with the water, which poses additional requirements on the abrasion resistance of piston and cylinder wall. Increasingly, corrosion-resistant materials such as stainless steel and PVC are, therefore, being used in handpumps, especially in those parts that are in direct contact with water.

PVC is frequently used for rising mains to avoid corrosion, because it is much cheaper than stainless steel. However, it was hardly ever used before under conditions as occurring in rising mains. How PVC should be applied for rising mains for deepwell pumps has, therefore, so far been determined by trial and error. This approach resulted in many early fractures, mainly in or just outside the threaded or cemented joints at the extreme ends of the riser and at the surface of the water in the well.

Even today the joints of the PVC risers and (stainless) steel rods break regularly in handpumps installed on deep wells and boreholes. This is mainly due to fatigue, the degradation of the material properties of those pump parts that are subjected to fluctuating loads. This degradation is worse under corrosive conditions and leads to so-called corrosion fatigue. The tens of millions of strokes to which a pump is subjected cause load fluctuations, result in fatigue and ultimately cause the failure of such parts as the rising main or the pump rod. Even for most high lift handpumps with corrosion-resistant materials (i.e. handpumps that have PVC rising mains and stainless steel pump rods) the problem of fatigue, including corrosion fatigue, is the prime issue that needs to be addressed to reduce breakdown of the pumps.

Another point of concern is that the relative elastic PVC (compared to steel) will cause a large axial cylinder displacement during pumping. Under the fluctuating loads the riser will alternately stretch and shrink (lengthwise) with every pump cycle. The displacements may equal the piston stroke in length!. Therefore it will be obvious that to a large extent cylinder movements will govern the functioning of the pump and its discharge.

By applying PVC large pressure fluctuations may build up in the pump already at normal pumping frequencies. These pressure waves are caused by the dynamic behaviour of the water column, which strongly depends on the elastic properties of the rising main. The pressure waves considerably increase fatigue!

Finally, in addition to axial displacements of the cylinder and the rising main, buckling, swinging and 'snaking' may occur.

1.2 IAD Handpump Project

The IAD Handpump Project was initiated to obtain a better understanding of all these effects in deepwell handpumps. This should give the means to predict and to limit the fluctuating stresses in the pump rod and the PVC rising main, and thereby help to increase the fatigue lifetime of the handpump.

The behaviour of deepwell handpumps was investigated by means of tests on the SWN 81 and Volanta handpumps, and on a hybrid of both pumps. These two models of Dutch manufacturers share a piston diameter of 50 mm, but have different sizes of rising mains. The SWN 81 rising main has an outside diameter of 47.5 mm and a wall thickness of 5.75 mm, whereas the Volanta rising main has an outside diameter of 80 mm and a wall thickness of 5.15 mm. Between the two, these handpumps are representative for the range of rising main diameters (as compared to cylinder diameter) that can be found in practice.

The testing programme was carried out in two phases, separated by an interim period that was used mainly to overcome teething troubles in the data acquisition line.

The first project phase was used to prepare the infrastructure necessary for testing deepwell handpumps with lifts up to 100 metres. The test unit consisted of an enclosed boring with a depth of 100 metres, in which the water level could be varied at will. The phase was concluded with a series of measurements on the SWN 81 handpump with a riser length of 20 metres, and with the analysis of the data obtained.

The second phase, from August 1988 to November 1989, was used to execute a large test and analyzing programme, and to gain a better understanding of the behaviour of deepwell handpumps and the remedies against unwanted consequences such as fatigue fracture.

To analyze the experimental results it was also necessary to develop physical models describing the pumping process. First a model was developed that explains the pressure fluctuations in the water column. A second model, describing the relation between the pressure in the water column and the axial loads of the rising main and the pump rod was developed, the results of which support the experimental results.

Details of the experimental set-up are given in Appendix II.

1.3 Aim and structure of this publication

The results of the test and analysis programme of the IAD Handpump Project may be of interest for a broad audience, being aimed at all those interested in the technical backgrounds of hand driven piston pumps, be it from a practical or a theoretical point of view, and working in the office or in the field.

To suit readers with such varying levels of interest and backgrounds, first a mainly qualitative description is given of the elements that are important for understanding the factors that govern the behaviour of the piston pump with an elastic rising main: see Chapter 3.

Chapter 4 quantifies the main stresses in the riser and the rod, and the relation with the pump yield.
Chapter 5 explains the relation between the stresses in the riser and the pump rod, and the fatigue lifetime.
Finally, in Chapter 6 an analysis is made of technical problems with deepwell handpumps, as frequently occurring in the field.
Where possible, design advices are given for increasing the efficiency and the lifetime of the pump.

Appendices III through V give the theoretical background of the relations between pressures, stresses, dimensions, etc. For those still not satisfied, the References give the opportunity for further research. The IADHPP publications mentioned are detailed reports on the test and analysis results.

Appendix I.1 lists the parameters used throughout this publication, Appendix I.2 the indices, and Appendix I.3 the various abbreviations and acronyms used, whereas Appendix I.4, the glossary, explains the main expressions used.

It is intended that in due course a joint British/Netherlands report will be prepared, which is to provide guidance for the use of PVC for rising mains. To that effect the Netherlands IADHPP team will closely collaborate with representatives from the Consumer Research Laboratory at Harpenden, Hertfordshire, and with Dr. P.R. Lewis, Senior Lecturer in Materials at The Open University, Walton Hall, Milton Keynes.

2 PUMP TYPES

2.1 Main piston pump types

2.1.1 Suction versus lift pumps

There are two main pump types, depending on whether the piston is situated above or below the water level in the well or borehole.

Piston above water level: **suction pump:** water is sucked upwards by the piston because of the relative under-pressure underneath the piston. Theoretically the suction head of such a pump is about 10 metres; in practice due to hydraulic losses it is less, say 6 to 7 m.

This pump type is relatively inexpensive. It depends, however, on an airtight fit of the piston in the cylinder. If the pump gets dry it needs to be primed with water. When the only clean water is in the well or borehole itself, the only alternative to render the pump operational again is to use contaminated water thus contaminating the well/borehole.

Piston below water level: **lift pump:** water is forced upwards by the piston, which is always under water.

This pump type is more expensive[1], as it requires long pump rods to keep the piston below the water level. It is, however, more reliable, as it does not require priming at all. The quality of the water in the well or borehole is thus better guaranteed than in the case of a suction pump.

For either pump type the piston is operated by means of a pump rod that can be driven:

- *directly* (reciprocating movement along the axis of the pump rod).
  Examples are the Nira AF85 direct action pump and the Kangaroo pump, among others.

- *with a lever* (the most common type of handpump).
  Examples are the SWN 81 and India Mark II handpumps, among others.

- *with a flywheel.*
  An example of this type is the Volanta handpump.

The tests that were carried out by the IAD Handpump Project used lift pumps, either operated by a lever (SWN 81) or by means of a flywheel (Volanta). A typical lift pump lay-out is indicated in Figure 2.1. It should be mentioned that for some pumps the inside diameter of the rising main is either the same or even larger than the cylinder diameter, in deviation from what is shown in Figure 2.1.

2.1.2 Materials used

Traditionally, handpumps were used to provide water to individual families, farms, etc. Materials used were often cast iron for the cylinder and mild steel or galvanized steel for the pump rod, with galvanized steel pipes as rising main.

[1] Even with relatively short rising mains of about 30 m the cost of riser and pump rod represents about half the total pump cost.

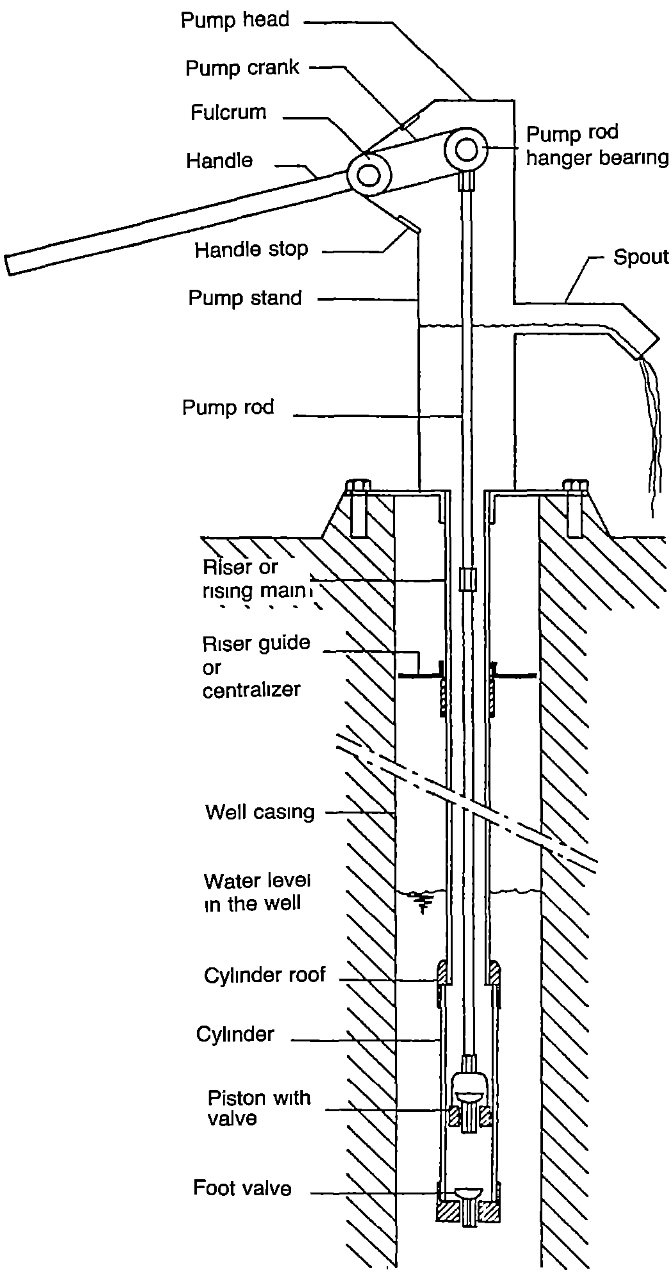

Figure 2.1 Typical lift pump

With the increased use of handpumps for community water supply, also the requirements made to the material properties have gone up. Currently, cylinder assemblies often use corrosion-resistant materials such as brass, nylon, PVC, rubber and stainless steel.

Pump rods are increasingly made of stainless steel, with stainless steel or PVC, ABS or similar plastics being used for the rising mains.
The pumps tested by the IAD Handpump Project use PVC rising mains and stainless steel pump rods, with cylinders composed of corrosion-free materials.

2.2 Description of the tested handpumps

2.2.1 SWN 81 handpump (see Figure 2.2)

The SWN 81 handpump is a lever-operated reciprocating deepwell handpump. Its superstructure is made of galvanized steel, and consists of a pump head with bush bearings at the fulcrum and rod hanger, a handle with counterweight and a pump stand with spout, anchored with four M18 bolts to a (concrete) foundation.

The components below-ground include a high impact PVC cylinder (inner diameter 50 mm), with plunger and foot valve seats made from stainless steel and nylon, and brass valves with neoprene on the sealing faces. The piston has a bi-directional neoprene seal.

Pump rods are stainless steel, 10 mm diameter, with M10 x 1.5 screwed connections, held in a protective HDPE tube.
The rising main is made of special high impact thick-walled PVC pipe with screwed connections (1.5") and an outer/inner diameter of 48/36 mm.

A flexible rod hanger ('swivel') was provided separately, as well as a perforated tube (to be installed beneath the cylinder, as a cylinder support), centralisers for the rising main, and a flexible riser hanger.

2.2.2 Volanta handpump (see Figure 2.3)

The Volanta handpump is a reciprocating deepwell pump driven by rotation of a large flywheel (1.5 m diameter). A crank and connecting rod convert the rotary motion into a reciprocating action. Its superstructure consists of a stand with pillow block bearings for the crankshaft, an adjustable connecting rod, guided upper pump rod and a stuffing box, fixed in a socket with spout. The flywheel is provided with an eccentric for 5 different crank radii.

The below-ground components include an epoxy bonded glass-fibre cylinder, suspended with its conical top end socket from the conical seat socket at the bottom end of the rising main, thus permitting removal of the cylinder through the rising main. The cylinder is provided with a seal-less plunger of stainless steel (hydraulic sealing) and moulded neoprene valves.

Pump rods are stainless steel, 9 mm diameter, with rolled M10 x 1.5 screw connections and plastic pump rod guides.
The rising main is made of standard PVC pipe with glued sockets and an outer/inner diameter of 80/70 mm, suspended from a collar glued at the top end.

A half-size flywheel (0.75 m diameter) and different detachable valve weights were provided separately.

2.2.3 Hybrid handpump

A hybrid was also tested, consisting of the SWN 81 superstructure with Volanta substructure.

From the SWN 81 pump stand, the screw socket underneath the bottom plate was removed, to permit the stand to be placed directly on top of the Volanta rising main. The standard Volanta seal on top of the riser provided the sealing with the SWN pump stand. The Volanta cylinder could be installed/removed through the SWN 81 stand with only the SWN head removed.
The hybrid was operated by the SWN handle.

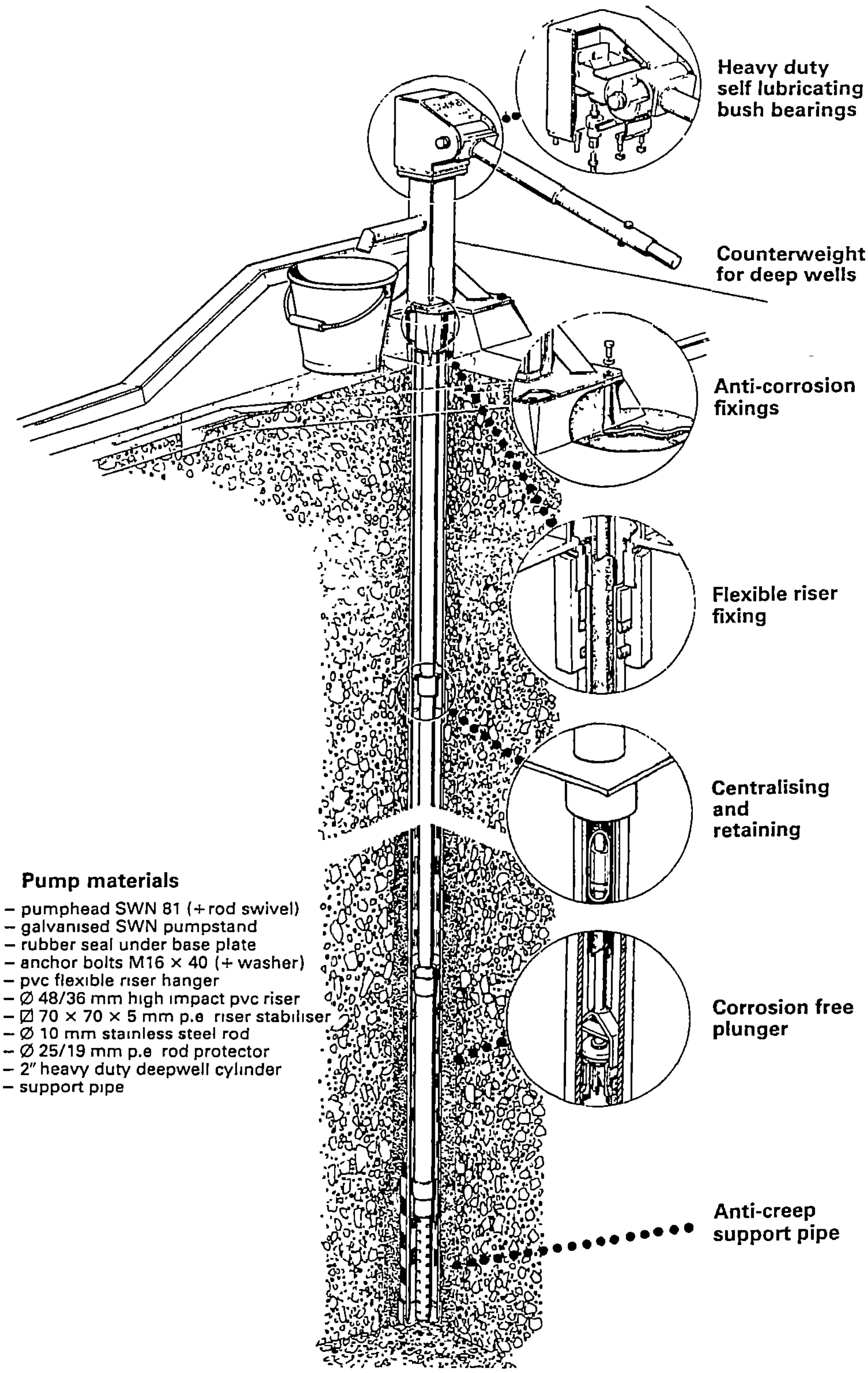

Figure 2.2 SWN 81 handpump

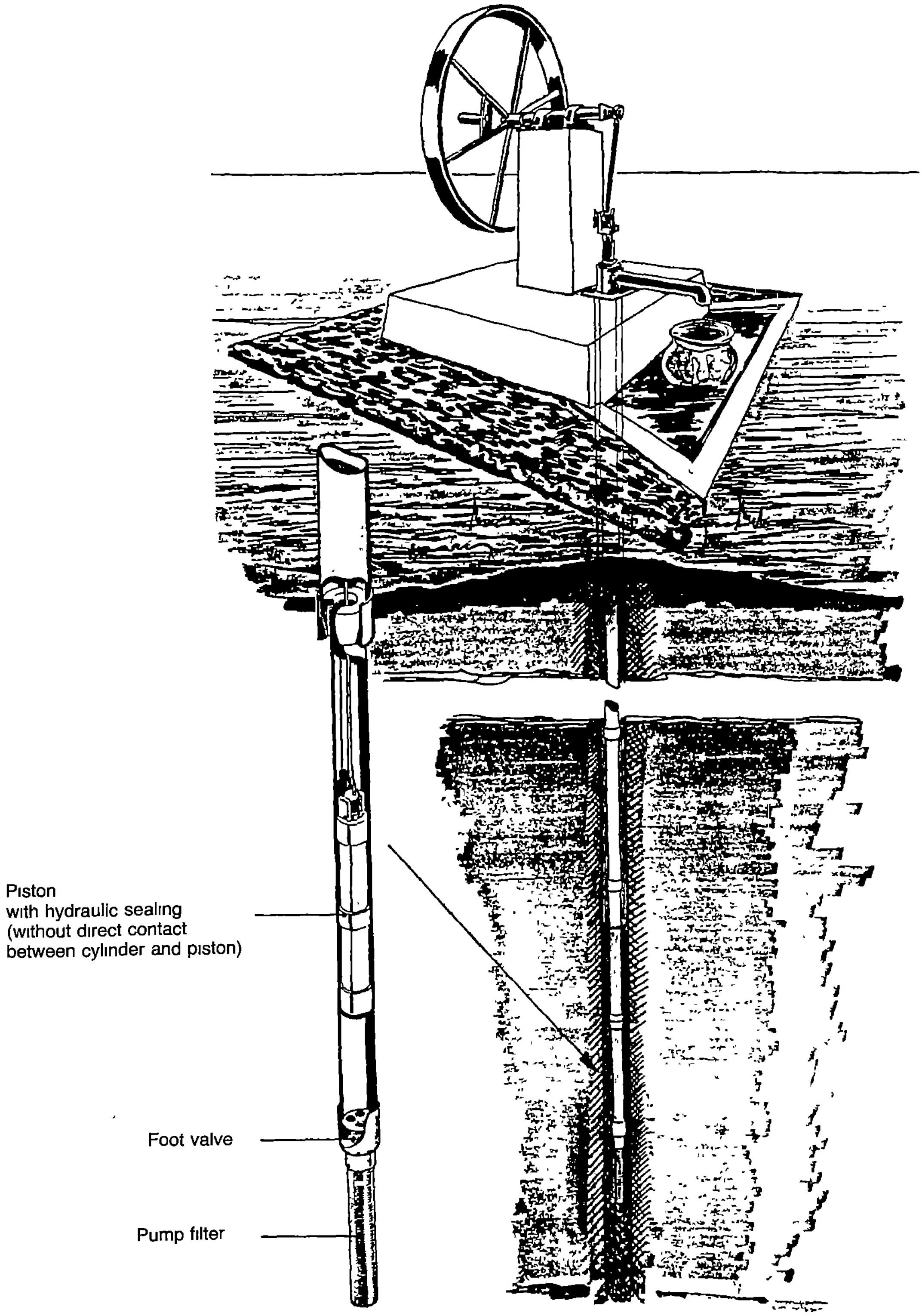

Figure 2.3 Volanta handpump

3 PRINCIPLES OF HANDPUMP OPERATION

3.1 Introduction

A deepwell handpump with a relatively elastic PVC rising main behaves differently from a pump with a 'stiff' steel rising main. Because of the elasticity of the rising main, axial and lateral cylinder and riser displacements will develop. The axial displacements of the piston and the cylinder will induce pressure waves in the pump during the entire pump cycle.

To get a clear picture of all these phenomena it will be necessary to describe both pump types: the cycle of a piston pump with a 'stiff' riser and that with an elastic riser. Both descriptions will only take quasi-static effects into account ('no inertia').
Thereupon the two cycles will be compared in relation to the load and stress fluctuations, and an example of measured stress fluctuations in a pump rod and an elastic PVC riser will be shown.
The differences, which are due to dynamic effects, will be shown in section 3.4.

3.2 Basic pump cycle of a piston pump with a 'stiff' riser (no inertia)

3.2.1 General description of pump cycle

The basic pump cycle is the following cycle (see Figure 3.1):

I. Just after the bottom dead centre (BDC, the lowest piston position) when the piston starts its upwards stroke the piston valve is closed and the foot valve will open, permitting the water to enter the cylinder through the foot valve seat.
II. Thereupon the piston will lift water out of the cylinder and water will be discharged through the pump spout as long as the piston moves upward.
III. At the top dead centre (TDC, the topmost position of the piston) the pump action stops. Thereupon the foot valve will close, while the piston starts moving downward. The body of water now enclosed in the cylinder below the piston will open the piston valve.
IV. While the piston moves further downward, water will pass through the piston valve seat. This process continues until the piston reaches BDC.

3.2.2 Valve opening/closing

The valve opening and closing is directed by the water flow through the valve seat. Because it takes time for the valves to close and open it can be understood that the opening and closing of the valves will not always be exactly at TDC and BDC. Especially the delayed closing of the valves is generally feared because this is held responsible for the occurrence of so-called water hammer: pressure peaks that develop in the pump directly after the (delayed) valve closing.

3.2.3 Output

During the downward piston stroke some water may also be discharged through the spout (see Figure 3.11). This is due to the displacement of water from the cylinder caused by the volume of the pump rod entering the cylinder at the downward stroke.

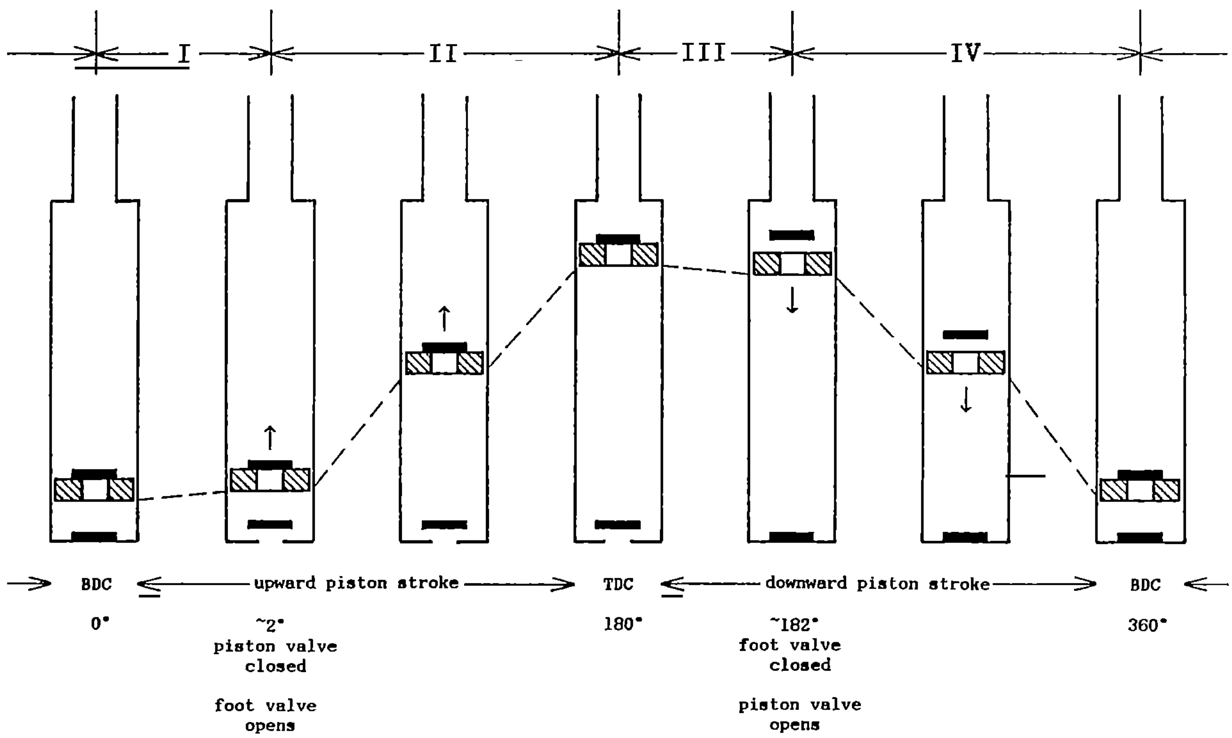

Figure 3.1 The basic pump cycle of a piston lift pump ('stiff' riser)

When the pump rod has a relatively large diameter, this displacement may become an important part of the total volume of water pumped per cycle. Most designers of *direct action pumps* exploit this effect to realize a more equal division of the necessary manpower over both pump strokes[2].

3.3 Pump cycle of a piston pump with an elastic riser (no inertia)

3.3.1 General description of pump cycle

The differences between the pump cycle of a piston pump with a stiff and an elastic rising main are mainly due to the very much increased axial elasticity of the rising main. The axial strains result in significant axial displacements of the cylinder, as will be shown.

The pump cycle of a deepwell piston pump with an elastic riser is shown in Figure 3.2. Note the difference with the situation with 'stiff' riser (Figure 3.1).

---

[2] Note that the total volume of water pumped per cycle will not be influenced by this effect as the volume pumped by the upward stroke is reduced by exactly the same volume as that pumped during the downward stroke.

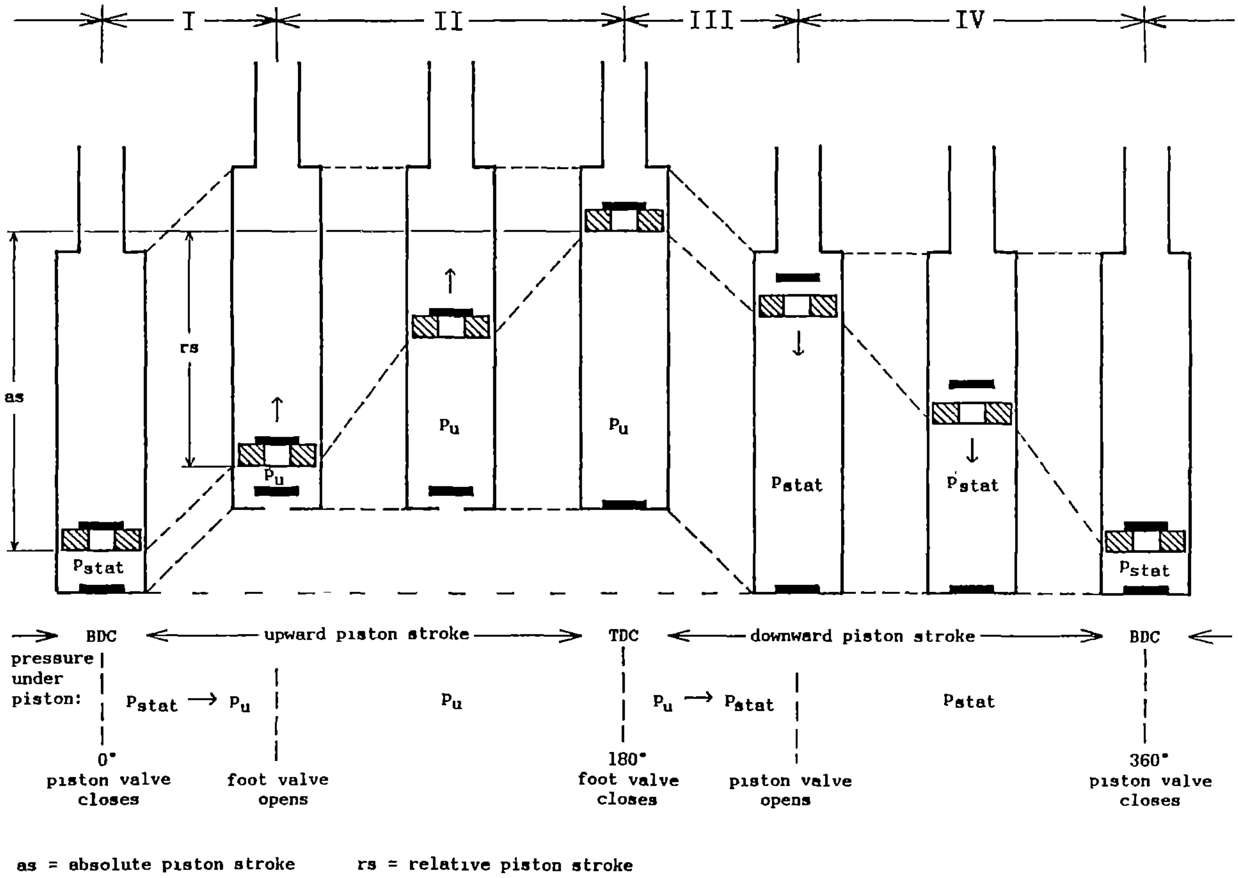

Figure 3.2 The pump cycle of a deepwell piston pump with an elastic riser

Description of the pump cycle:

I. Starting from the lowest piston position (BDC) the cylinder bottom (and therefore the rising main) is gradually relieved from the pressure now taken by the piston: the cylinder moves upwards with the piston, without mutual displacement. The pressure below the piston gradually decreases to the pressure outside the cylinder.

II. The rising main is now relieved and does not move further upwards, while the piston continues. Now water is sucked into the cylinder.

III. When the cylinder starts to move downwards from TDC, with the foot valve just closed, the cylinder bottom is gradually reloaded; the pressure below the piston gradually increases to the pressure above the piston. The piston and the cylinder move down, without mutual displacement.

IV. The pump rod is relieved and the cylinder bottom is fully loaded, so now the piston valve opens and only the piston moves further downwards

Figure 3.3, which is based on experimental data, clearly supports the claim that during a part of the pump cycle the piston and cylinder move together in an axial sense, without (hardly any) mutual displacement. (The small displacements shown are due to dynamic effects.)

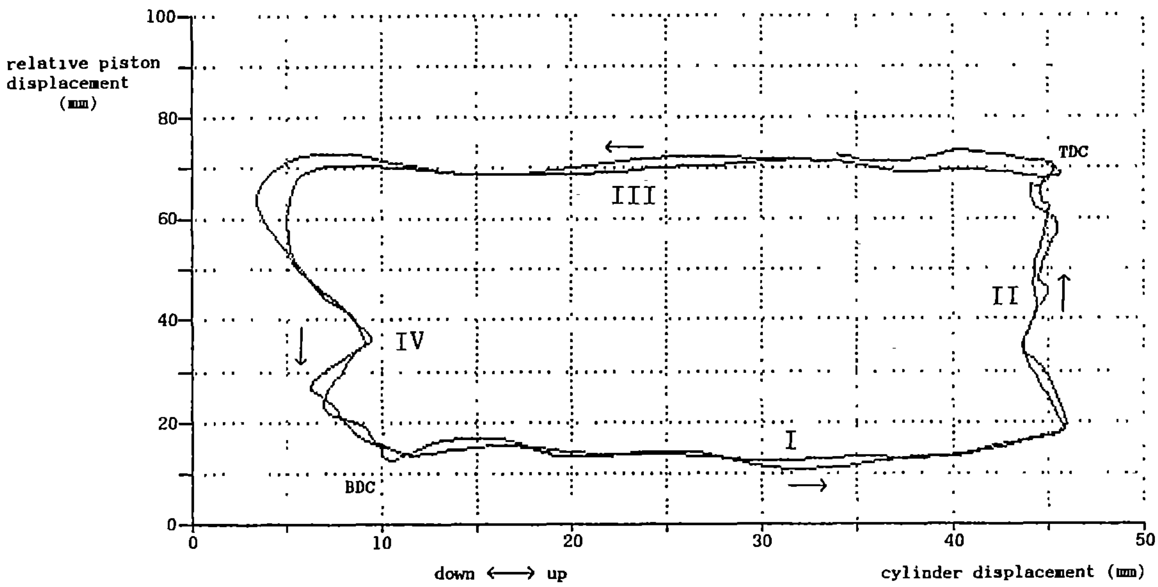

Figure 3.3 *The relative axial displacement of the piston against the axial cylinder displacement.*
The more or less horizontal lines (Stages I and III) indicate zero displacement of the piston relative to the cylinder, i.e. no mutual displacement.
The more or less vertical lines (Stages II and IV) indicate that now (mainly) the piston moves.
(From experimental observation: Volanta with 78 m rising main)

Upward piston stroke

With a completely stiff pump, the bottom valve would open immediately after the start of the upward piston stroke, to permit water to enter the cylinder. This is not the case, however, when the pump has an elastic rising main.
Before the foot valve can open, the pressure underneath the piston has to become equal to the pressure outside the cylinder (p_u, determined by the immersion depth of the cylinder).

A decrease of the pressure below the piston means a reduction of the load on the cylinder bottom, resulting in a lower stress in the rising main and thus in a shorter rising main, i.e. an upward displacement of the cylinder. Conversely, a less strained riser means a reduced reaction force on the cylinder bottom against the water enclosed underneath the piston, resulting in a lower pressure.

As long as both valves are closed a fixed volume of (incompressible) water is trapped below the piston. Therefore the cylinder will move upwards together with the piston (without mutual displacement) with the pressure gradually decreasing, as long as the foot valve cannot open. Only when the pressure underneath the piston and the pressure outside the cylinder have become equal, the foot valve will open, permitting water to enter the cylinder.

As the pressure below the piston gradually decreases, the pressure difference over the piston builds up, thus loading the pump rod. This gradual transfer of load from the riser to the pump rod continues until the cylinder bottom has been fully released from the inside pressure, i.e. until the foot valve opens.

Once the piston moves upwards (relative to the cylinder), water will enter the cylinder and pumped water will be discharged through the pump spout. This process continues until TDC has been reached.

Downward piston stroke

At TDC, the highest piston position, the piston no longer moves relative to the cylinder and the foot valve closes.
Then, during the first part of the downward stroke the opposite will happen of what took place at the beginning of the upward piston stroke: while both valves are closed, the piston and cylinder move down together, again without mutual displacement. Meanwhile a gradual load transfer takes place, back from the pump rod to the rising main. The pressure below the piston gradually increases from the outward immersion pressure (p_u) to the pressure above the piston. Once the pressures above and below the piston have become equal, the piston valve opens and water passes through the piston.

Figure 3.4 gives a good example of the load fluctuations in the riser and the pump rod:

a) Pump with stiff riser (no inertia): a sudden load transfer from the riser to the rod and vice versa;
b) Pump with an elastic riser (no inertia): a gradual load transfer;
c) Elastic riser plus inertia, based upon experimental results: a gradual load transfer plus dynamic effects.

The measured load fluctuations are clearly different in shape from those based upon quasi-static approximations, and are also much higher. The figure shows that dynamic effects become important already at normal pumping frequencies: in the example shown the pumping frequency is 1 Hz, in a SWN pump with a riser length of only 21 m. At greater depths the dynamic effects are even larger. Chapter 3.4 will explain the causes of these differences.

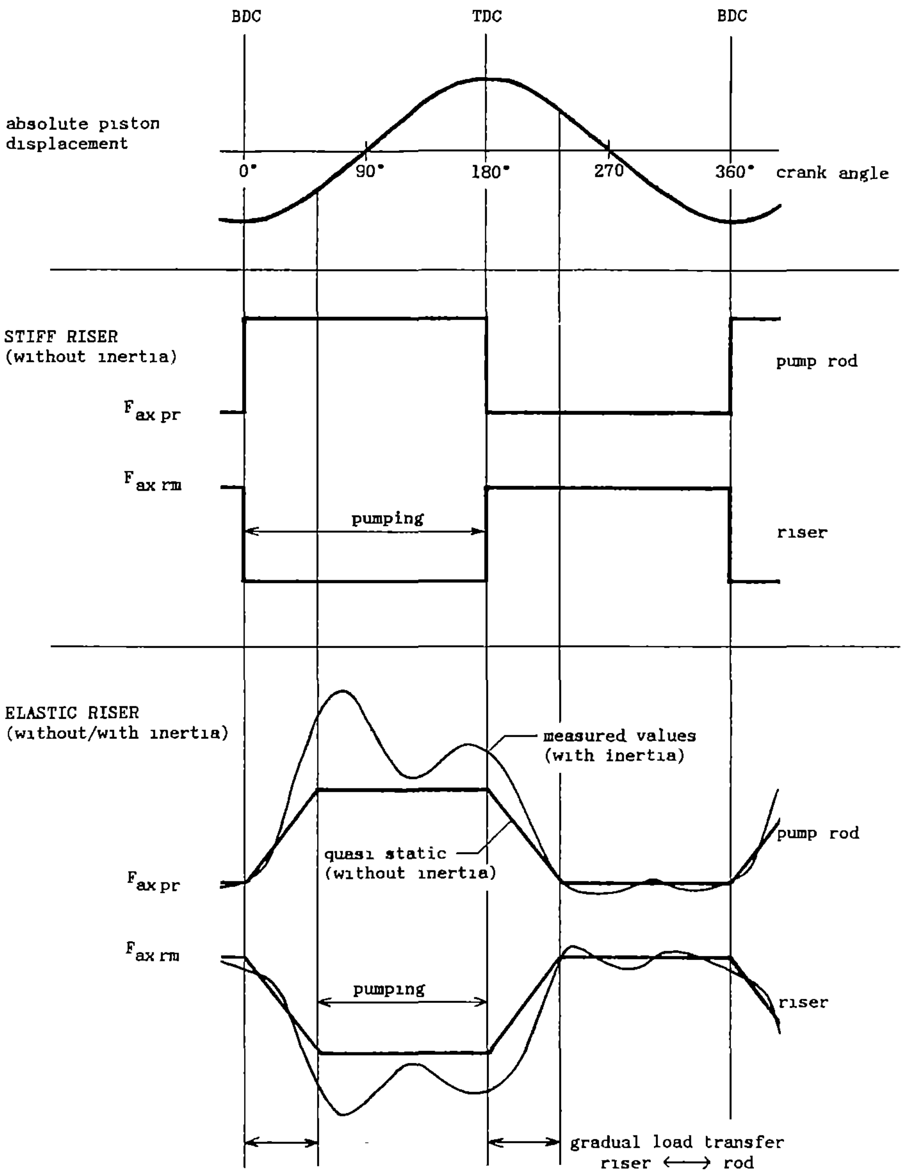

Figure 3.4 *The corresponding axial loads in the rising main and pump rod:*
a) in a pump with a 'stiff' riser (no inertia)
b) in a pump with an elastic riser (no inertia)
c) in a pump with an elastic riser (with inertia)
(Experimental observations; SWN 81, pumping freq. 1 Hz, riser length 21 m)

3.3.2 Valve opening/closing

If a piston pump has a *stiff* rising main, the piston valve closes near BDC, when the piston starts its upward stroke. Directly thereafter the bottom valve opens. At TDC the opposite takes place. With such pumps the delay, related to BDC and TDC, is hardly noticeable (see Figure 3.1).

In the case of a deepwell pump with a PVC rising main, a distinction must be made between the *net pump cycle*[3] and the *gross pump cycle*[4]. These cycles can differ very much from each other.

Experiments have shown that the valves indeed close and open 'on time', that is: when compared to the *net* (rather than the gross) pump cycle. Compared to the net pump cycle there is no relevant 'delay', but when comparing these moments to the BDC and TDC of the crank drive of the pump, angles of delay[5] of 80° and more may be found at large lifts.

The opening and closing delays caused by valve dynamics are considerably smaller than those caused by the cylinder movement, and will in no way influence the pump cycle and resulting strains and stresses.

Experiments with the Volanta handpump have proven this supposition: changing the valve dynamics by halving the piston valve lift (from 10 to 5 mm) and/or reducing the valve mass from 80 to 25 grammes, neither gave significant changes in delays nor in strains or stresses in the rising main or pump rod (see Figure 3.5).

CONCLUSION: ***In case elastic elements form part of the pump substructure, the valve dynamics are no longer of importance.***

---

3 Net pump cycle = the pump cycle based upon the effective piston displacement relative to the cylinder

4 Gross pump cycle = the pump cycle related to the crank drive (Note: for a 'stiff' pump there is no distinction between the gross and net cycles.)

5 These angles refer to a full pump cycle being completed in 360° (as is the case with the Volanta pump where the flywheel is turned 360° for one full pump cycle).

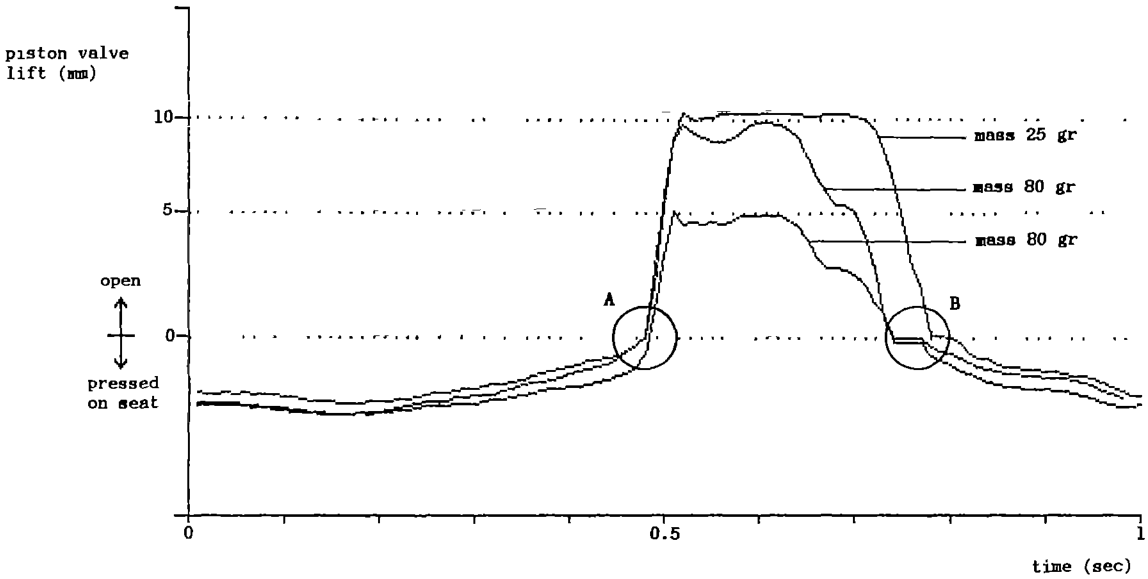

Figure 3.5 *Piston valve lift diagram*
(Maximum lift of 5 and 10 mm, and a weight of 25 and 80 grammes; from experimental observations on Volanta handpump with a 78 m long rising main)

Point A indicates the time at which the valve opens. This is nearly identical for all valve configurations measured. At point B the valve closes. The figure shows that the pressure build-up starts at about the same moment and is about identical for the measured valve configurations. (This is indicated by the way the valve is pressed on its seat after closing.) This proves that the valve configuration has no influence and that the valves close 'on time' (in relation to the net pump cycle).

3.4 Dynamic effects

3.4.1 Introduction

In sections 3.2 and 3.3 the situation was assumed to be quasi-static, i.e. forces due to inertia were neglected. This is right when pumping occurs at very low frequencies, so that accelerations are small. However, even at common pumping frequencies dynamic effects may already increase the magnitude of the stress fluctuations in the pump rod and rising main. In dynamic effects inertia plays a role, in contradiction to the quasi-static approximation.

The most striking feature of a dynamic effect is resonance[6]. Tests where a pump was driven at its resonance frequency showed stress fluctuations of more than twice the magnitude expected from the quasi-static approach. These stress fluctuations may be detrimental to the pump components, as discussed in Chapter 5.
Even pumping at half the resonance frequency already showed a significant increase of the stress fluctuation amplitude.

---

6 For readers who are not familiar with dynamic effects in general, these are illustrated using a simple example in Appendix V.

3.4.2 Possible dynamic effects

Some dynamic effects that occur in handpumps are:

a. *Dynamic behaviour of the water column in the rising main.* The forced accelerations of the water caused by the piston and cylinder motions result in pressure fluctuations in the water, due to the inertia of the water.

b. *Dynamic effects concerning the cylinder motion.* Here the elastic rising main may be considered to be a spring, while the mass of the cylinder and the riser may be regarded to be concentrated at the lower end of the 'spring'. The dynamics of such a mass-spring systems are discussed in Appendix V.

c. *Dynamic effects concerning the piston motion.* As under b.

d. The riser could *swing* like a kind of pendulum or *snake*[7] like a rope. The driving mechanism could act via *buckling*[8] and *bending* of the rising main (and pump rod) caused by a compressive force during the upward stroke (rising main) or downstroke (pump rod).

The question now arises which of these dynamic effects causes the large stress fluctuations that are observed experimentally.

Traditional theories hold effects b (cylinder and rising main mass, and rising main elasticity) responsible for the large stress fluctuations. However, this was shown to be incorrect. Detailed monitoring of the rising main, using 18 strain gauges (see Appendix II) showed that the behaviour of the rising main is almost perfectly quasi-static. The same holds true for dynamic effects c.

As the observed stress fluctuations were mainly directed axially, and dynamic effect d (swinging, snaking) only gives rise to bending stresses, the dynamic behaviour of the water column had to be responsible for the large stress fluctuations observed. The quantitative agreement between the theories we developed to describe this dynamic behaviour, and the measurements support this conclusion.

3.4.3 Dynamic behaviour of water column inside rising main

When the cylinder starts to move upwards, due to the inertia of the water, the water layer just above the piston is compressed. The layer above this compressed layer will be pushed upward by the underlying layer and also be compressed, etc. In this way a pressure 'front' runs upward through the rising main (in the same way a ripple propagates over the surface of a pond when a stone is thrown into the water). This process is shown in Figure 3.6[9]

---

7 Snaking = undulating, probably because of travelling transverse waves

8 Buckling = bending of the centreline caused by an excessive axial compressive force

9 Most people hold the closing of the valves responsible for the pressure fluctuations, i.e. the closing delay of the valves, which causes a sudden stop of the so-called back-flow through the valves. However, because of the elasticity of the PVC rising main the valves close on time (see section 3.3) causing only minor pressure disturbances.

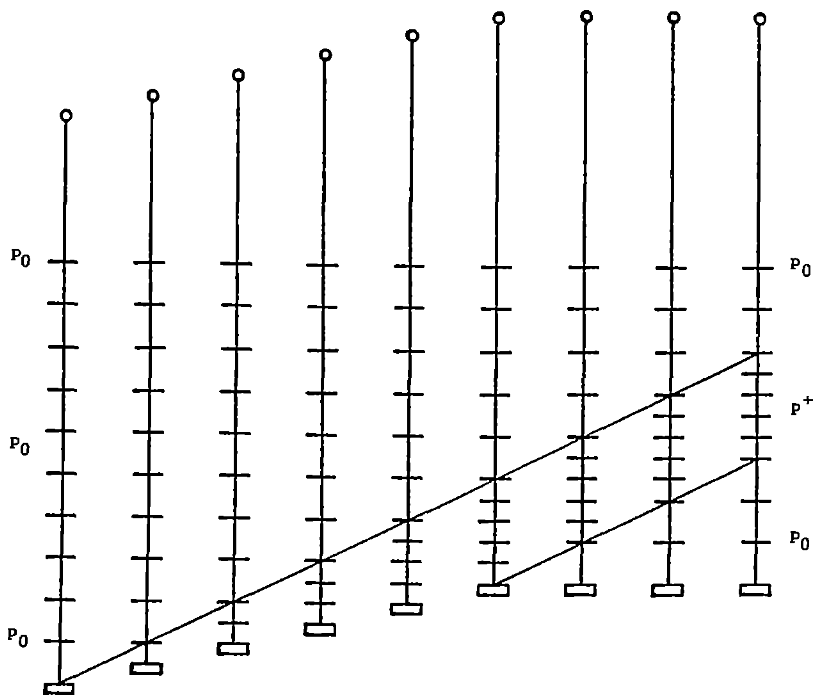

Figure 3.6 The upward moving piston causes a compression wave (p^+). The crowding of the 'rafters' is proportional to the pressure.

The propagation speed of this pressure front is the velocity of sound (in water).

Suppose the water is completely incompressible (i.e. it does not give way when subjected to pressure), then the water at the top of the rising main immediately has to follow the piston movement, as the water column cannot change its volume. In that case the velocity of sound is infinite.
Water is hardly compressible, in fact calculations (and measurements) show that the velocity of sound in pure water is about 1500 m/s (which is about five times as high as that in air under normal atmospheric conditions!). However, the pipe wall itself is elastic and gives way when pressure is applied, having the same effect as if the water itself were more compressible. Therefore, the velocity of sound in water contained within an elastic pipe is lower than 1500 m/s.

In general this speed depends on the pipe diameter, wall thickness and the elasticity of the pipe material. For example, the velocity of sound when contained in a (relatively stiff) thick-walled steel riser will be about 1400 m/s, whereas for PVC pipes used in handpumps this velocity will only be about 400 m/s. Figure 3.7 shows the propagation speed for water-filled PVC risers.

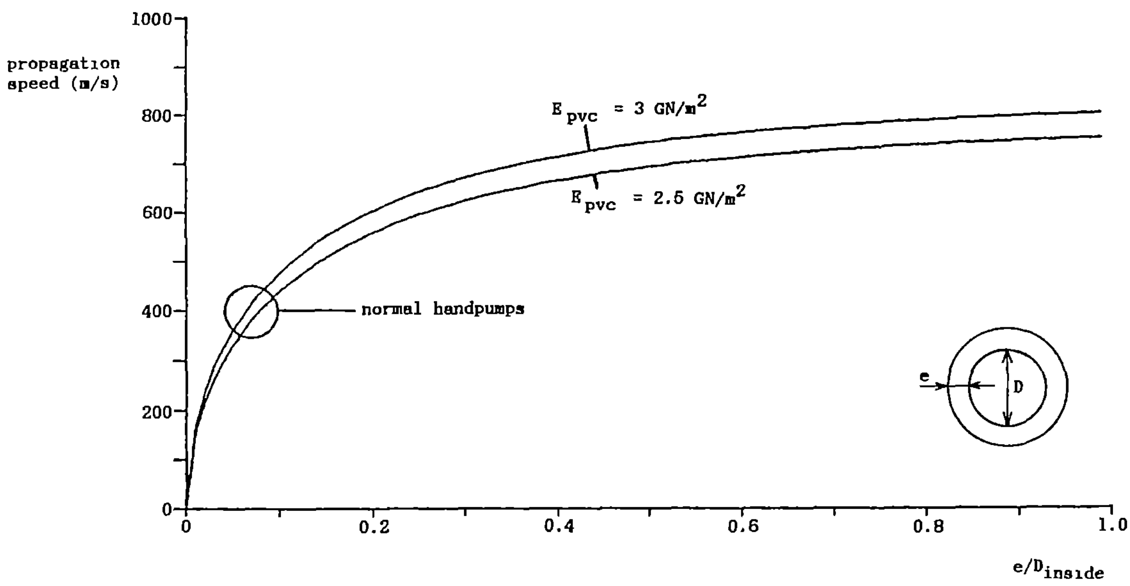

Figure 3.7 The propagation speed (a) as a function of the quotient of wall thickness (e) and the inside diameter of the rising main (D_{inside}). E is the elasticity modulus of the pipe material.
(data extracted from the plot is valid within 10% if D_{inside} is larger than 2.8 x $D_{pump\ rod}$. An explicit formula for the propagation speed 'a' is given in Appendix III.5)

Let us now return to Figure 3.6.
In the last part of the upward stroke the piston velocity decreases. Again due to the inertia of the water, the water layer just above the piston is now decompressed: the pressure decreases. The layer above it will also slow down and decompress as well. Hence the pressure 'drop' follows the pressure front, again with the velocity of sound.

Once a pressure wave has been produced, it takes some time before the wave is damped out. During that time the wave travels up and down through the rising main, because the wave cannot leave the system since it is reflected at the top end of the riser and at the piston or cylinder bottom. During pumping, waves are continuously produced by the piston and cylinder movements. The result is a complicated mixing of waves in the riser, determined by the interference of newly produced waves and those already present in the riser. The waves interact with each other and result in a fluctuating (at first glance rather obscure) pressure pattern in the rising main.

It is to be expected that the largest pressure fluctuations occur when pumping takes place at the resonance frequency. To illustrate this, in Figure 3.8 the measured peak values of the pressure signal just above the piston have been plotted against the pumping frequency.

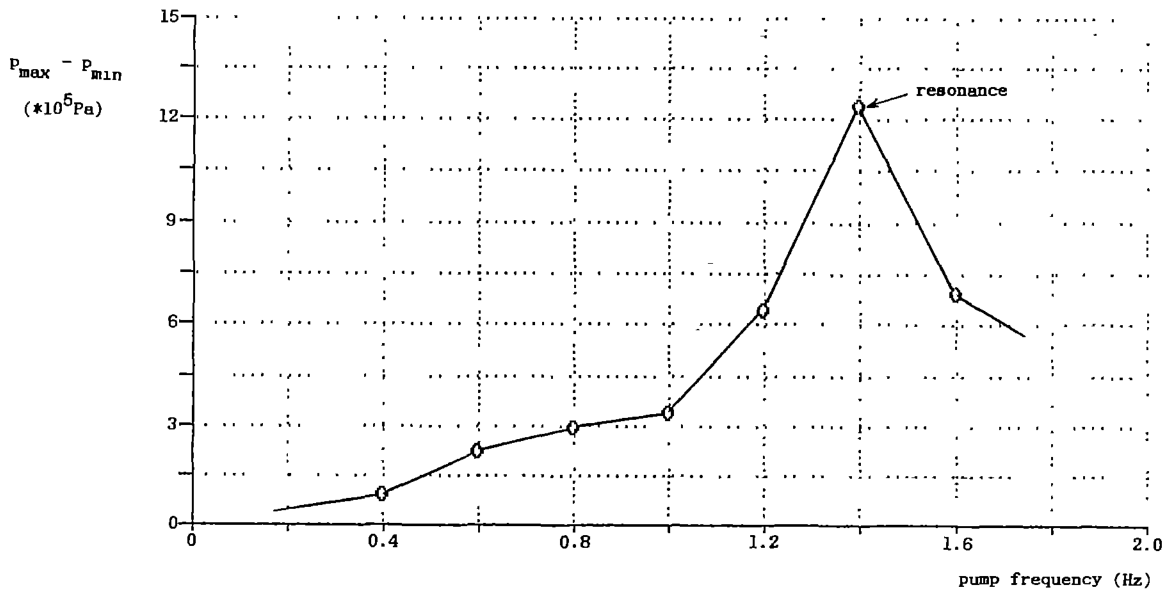

Figure 3.8 *Pressure fluctuations as a function of pumping frequency (pressures measured just above the piston).*
(Experimental results: Volanta, riser length 78 m, stroke length 138 mm)

From Figure 3.8 it follows that in this geometry resonance occurs at 1.4 Hz.

Remark that for low pumping frequencies the pressure fluctuations just above the piston are small (compared to the static pressure of 7.8 * 10^5 Pa in this situation. The quasi-static description then is a good description of the situation.
Note that for every situation (quasi-static as well as resonance!) the pressure underneath the piston fluctuates between the actual pressure above the piston (during the downward piston stroke) and the pressure outside the cylinder (during the upward piston stroke)!

It is interesting to know in what way this resonance is induced by the pressure waves. This process is illustrated in Figure 3.9:

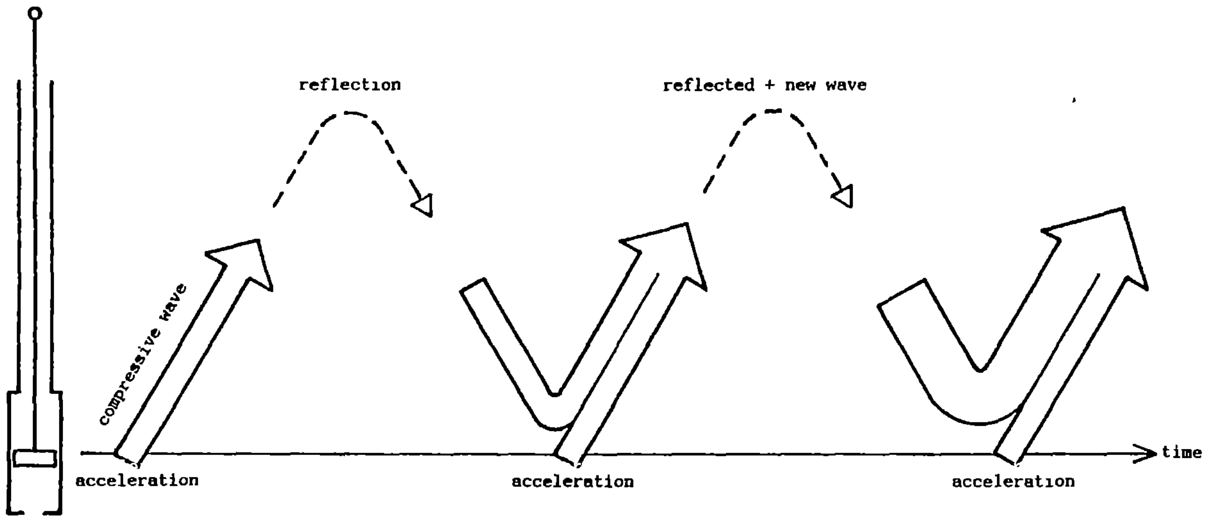

Figure 3.9 Resonance mechanism of pressure waves

During the acceleration of the water (induced by piston or cylinder motion) a compressive wave is produced. This pressure wave is reflected at the boundaries of the riser and arrives at the bottom end of the riser after a fixed period of time. (This period depends only on the distance travelled and the velocity 'a').

If the pumping frequency has been chosen such that exactly at the moment that the reflected wave arrives, a new compressive wave is produced, the two waves combine to form one larger pressure wave. After a few cycles the pressure wave will thus become very large, causing large pressure fluctuations, which are recognized as resonance.

It is, therefore, clear that the resonance frequency is determined mainly by the velocity 'a' and the distance travelled (which is proportional to the riser length L).

From the theory it follows that the resonance frequency can be calculated using eq. (3.1):

$$f_{res} = \frac{a}{4 \cdot L} \tag{3.1}$$

where f_{res} = resonance frequency (Hz)
a = velocity of sound (m/s)
L = riser length (m)

For example, in case of the Volanta pump of Figure 3.8, with L=78 m and a ≈ 400 m/s, it follows:

$$f_{res} \approx \frac{400}{4 \cdot 78} = 1.3 \text{ Hz}$$

In Figure 3.10 some resonance frequencies have been plotted, on the basis of both calculations and experiments.

Following the theory, an exact relation has been derived between the piston or cylinder movements and the pressure fluctuations. A detailed description of this theory does not fall within the scope of this publication, but is discussed elsewhere[10]. An example is shown in Figure 3.11.

[10] *Final technical report, second project phase*, by J. Grupa, Wind Energy Group, Eindhoven University of Technology, and J. Besselink, InterAction Design.
Report IADHPP89.07; 1989

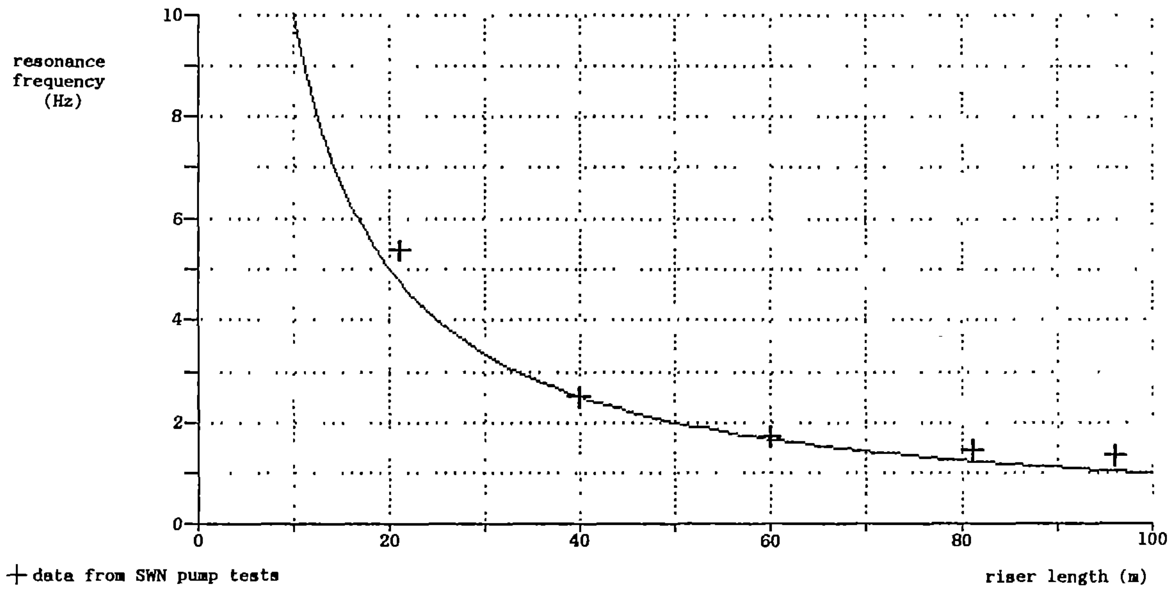

Figure 3.10 Resonance frequencies as a function of riser length
Symbols refer to measurements, while the solid line is calculated with $f_{res} = 400/4L$

3.5 Consequences of pressure fluctuations for the stresses in pump rod and rising main

It is obvious that at the moment the pressure reaches its maximum value during the pump cycle, the load on the pump rod or rising main (depending on whether the piston is moving up or down) is also at its maximum. In fact, the experimental data show that the load on the rising main and pump rod is in accordance with the actual pressure at any moment during a cycle.

This is illustrated in Figure 3.12 where the maximum and minimum values of the pressure just above the piston and the stresses in pump rod and rising main have been plotted against the pumping frequency. The symbols refer to measurements, whereas solid lines represent calculated values.

The pressure fluctuations have been estimated using only the handle (or flywheel) displacement during a cycle, in the same way as shown in Figure 3.11. Using this *calculated* pressure the stresses have been calculated.

The agreement between measured and calculated[11] stresses in Figure 3.12 illustrates that the increased stress fluctuations near resonance are indeed caused by the pressure fluctuations, and therefore a consequence of the dynamic behaviour of the water column.

---

[11] If the measured pressures had been used instead of the calculated values, the agreement would have been even better.

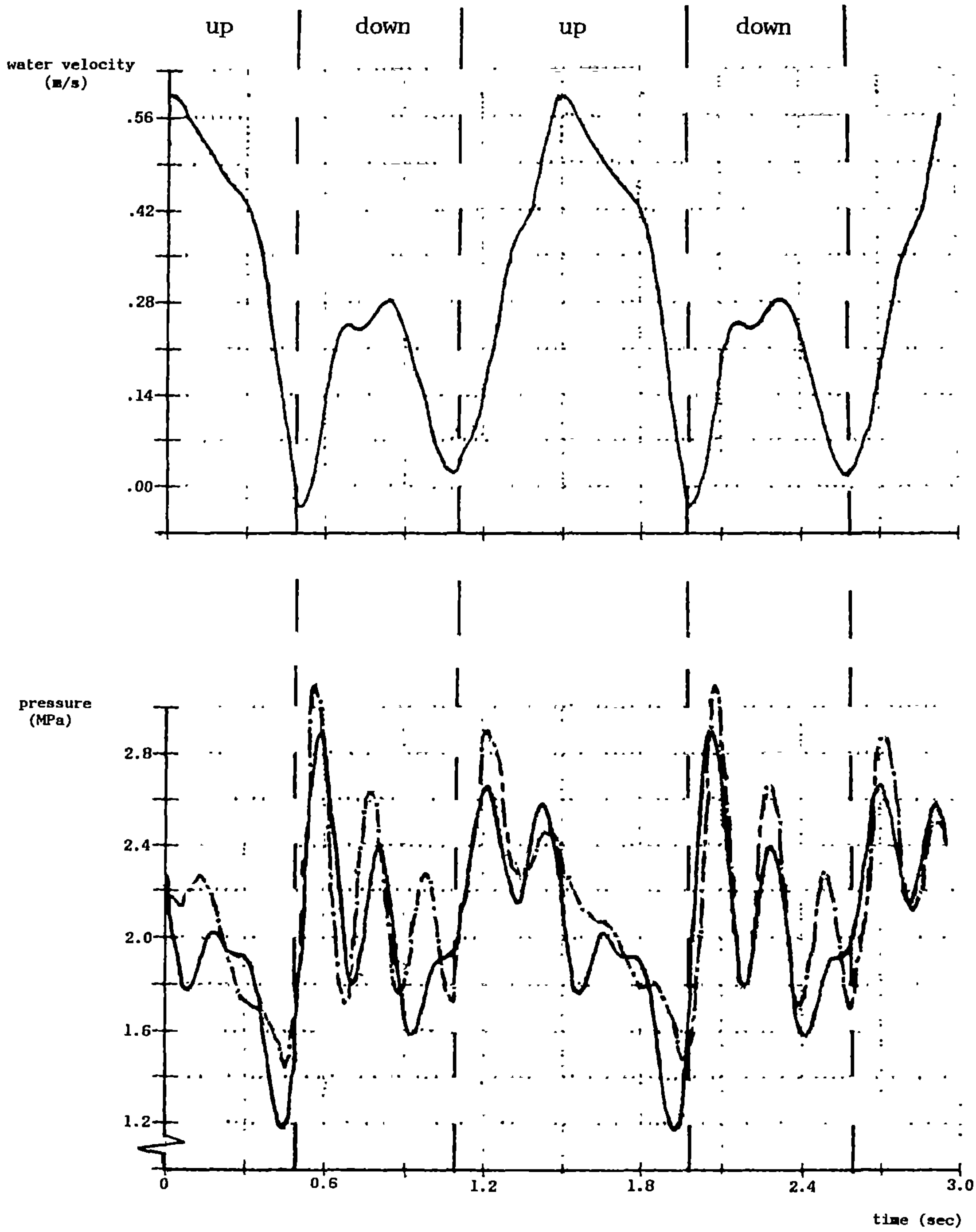

Figure 3.11 Top: *Velocity of water at the bottom end of the rising main, calculated from the piston and cylinder movement. Also the displacement of water in the cylinder by the pump rod during the downstroke is clearly visible.*

Bottom: *Pressure at the bottom end of the rising main. The solid line refers to the calculated pressure using the 'pressure waves method', while the dashed line refers to the measured pressure.*

(Experimental data: L = 21 m; f_{pump} = 0.67 Hz; stroke = 114 mm; man-driven; pump = SWN 81

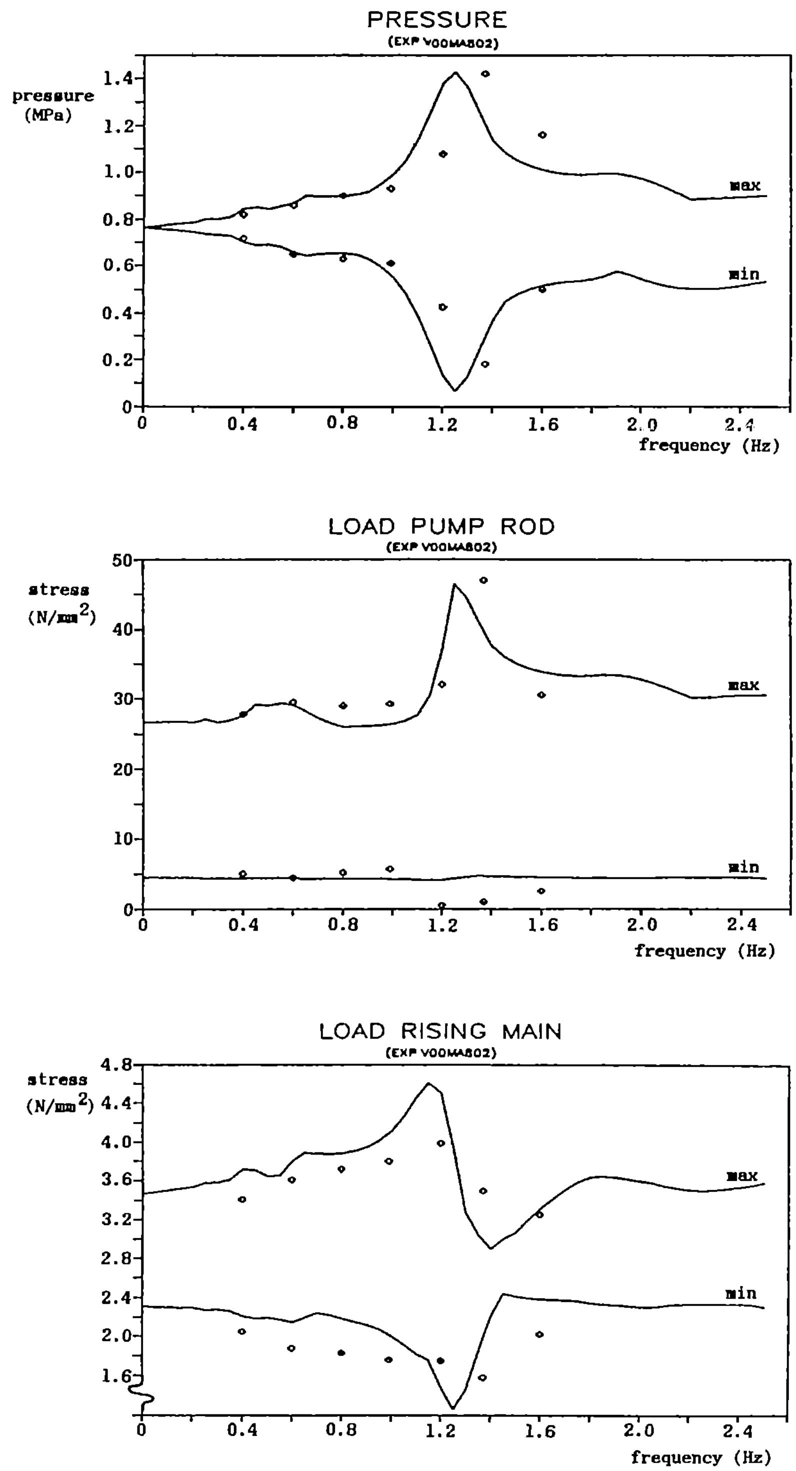

Figure 3.12 Pressure fluctuations and pump rod and riser loads, calculated with the model (solid lines) and measured values (symbols).

4 QUASI-STATIC ESTIMATION OF THE STRESS AND STRAIN FLUCTUATIONS, THEIR INFLUENCE ON PUMP YIELD, MECHANICAL EFFICIENCY AND CREEP

4.1 Introduction

In the **rising main** three main deformations occur:

1. *Axial strain*: along the entire length of the riser (maximum at the top), by the weight of the riser itself and the cylinder, the pressure of the water inside and outside the pump, and dynamic effects;
2. *Tangential strain*: negative at the top end because of transverse contraction, to positive, and downwards increasing (until the water surface in the well/borehole), by the pressure inside and outside of the pump;
3. *Bending*: due to many different causes such as inclined joints, buckling, swinging, snaking and cylinder support, and inclined and/or curved boreholes.

In the **pump rod** the tangential strain plays no role. Torsion will probably only occur while assembling or dismounting the pump.

This chapter will elaborate on the relations between the stress and the strain in the riser and pump rod.

Chapter 3 has shown that already for normal pumping frequencies dynamic effects occur[12]. The problem is that the resulting stresses in the rising main and the pump rod are difficult to calculate: a complex computer programme will be needed. However, experiments show that the axial stress fluctuations hardly ever exceed twice the values of quasi-static estimations. For examples see Figures 4.4 and 4.5. Only for the tangential stresses, important at the bottom end of the rising main, this simplification will not hold, as will be explained in paragraph 4.3.2.

Bending stresses and their causes will be explained in Chapter 6, in relation to field experiences. Although their values are hard to predict, they cannot be neglected, as sometimes bending stress fluctuations have been measured that exceed the axial stress fluctuations!

The following paragraphs will explain how to estimate the stresses and the resulting strain of the riser and the pump rod:
- for the pump at rest: static stresses;
- during pumping: by means of quasi-static estimations.

Also the relation with the pump yield, the volumetric and mechanical efficiency and creep will be explained for different pump configurations.

4.2 Static load

The *static axial load* is caused by:
- the weight of the rising main itself, including cylinder, etc.;
- the axial resultant of the water pressure (i.e. the weight of the water column) in the rising main (see Figure 4.2);
- reductions by the upward force of the water in the well, which is proportional to the volume of the immersed pump parts.

---

[12] Only for pumping frequencies less than half the resonance frequency, the quasi-static estimation will be accurate.

The static pressure inside and outside the rising main, caused by the heads of water in and outside the rising main, will cause radial and tangential strains and stresses. For details see Appendix III.1, equations (III.1) through (III.7).

An example of the static stresses (excluding bending) in the rising main is given in Figure 4.1. In the threaded or cemented joints axial, radial and tangential *prestresses* will increase the static stresses. Apart from that, dangerous *stress concentrations* may occur due to abrupt changes of shape, diameter, etc. For details see paragraph 5.3.3 and Chapter 6.

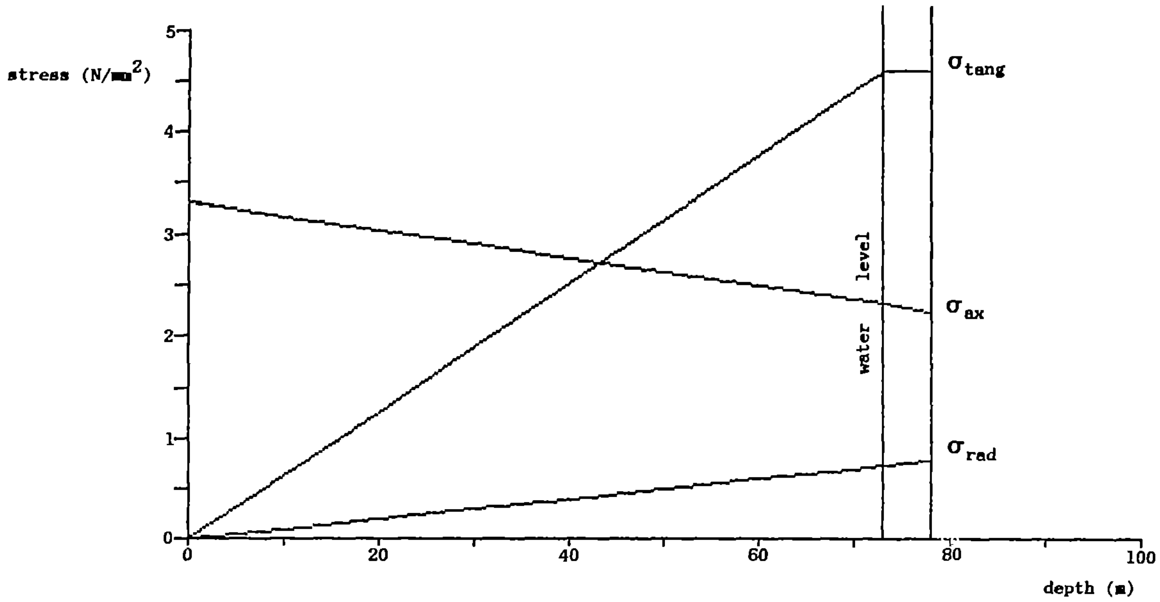

Figure 4.1 *Static stresses in the rising main*
(Volanta configuration, riser length 78 m)

As shown in Figure 4.2 the rising main is loaded by the pressure inside the cylinder. At rest the axial load equals the static pressure multiplied by the cross section of the water column in the rising main (see also Appendix III.1)[13]:

$$F_{rest} = p_{stat} \cdot A_{i\,rm} = p_{stat} \cdot \pi/4 \cdot D_{i\,rm}^{\;2} \tag{4.1}$$

$$p_{stat} = \rho . g . L \tag{4.2}$$

This load is independent of the piston diameter! Added to the weight of the rising main itself, it causes the static strain in the rising main.

13 see Appendix I for an explanation of symbols and indices

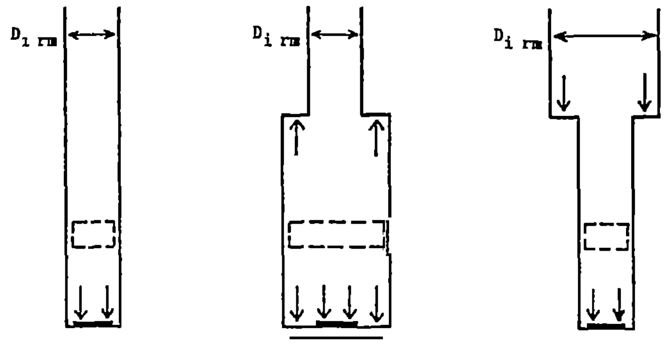

Figure 4.2 The axial load in the bottom end of the rising main, caused by the pressure in the cylinder at rest

4.3 Load fluctuations in the riser and the pump rod

4.3.1 Axial load fluctuations

In section 3.3 it was explained that when the piston moves upward, with opened foot valve, the cylinder bottom is relieved from the load caused by the (static) pressure in the pump. As shown in Figure 4.3 this axial load fluctuation fully depends on the piston diameter, and not on the riser diameter! (The dotted arrows represent the load fluctuations in the riser.)

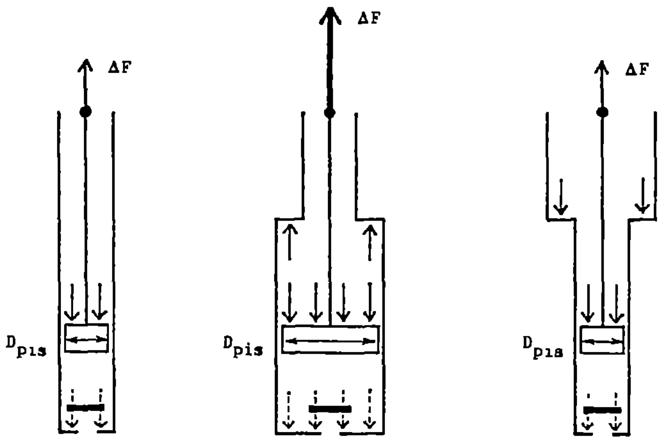

Figure 4.3 The load fluctuation in the rising main and pump rod, due to the upward moving piston
(When the piston diameter is larger than the inside diameter of the rising main, a pressure increase above the piston will cause the cylinder to go up; in case the piston diameter is smaller, the cylinder will go down.)

For small immersion depths the axial load fluctuation equals the pressure multiplied by the piston cross section:

$$\Delta F = p \cdot A_{pis} = p \cdot \pi/4 \cdot D_{pis}^2 \qquad \text{(see Figure 4.3)} \qquad (4.3)$$

The axial load taken off the rising main is now taken up by the piston and the pump rod. The resulting stress fluctuation in the rising main, resulting from this load fluctuation, is equal to the load fluctuation divided by the cross section of the rising main:

$$\Delta\sigma_{rm} = \frac{\Delta F}{A_{rm}} = \frac{p \cdot \pi/4 \cdot D_{pis}^2}{\pi/4 \cdot (D_{u\,rm}^2 - D_{i\,rm}^2)} \tag{4.4}$$

Similarly, the stress fluctuation in the pump rod becomes:

$$\Delta\sigma_{pr} = \frac{\Delta F}{A_{pr}} = \frac{p \cdot \pi/4 \cdot D_{pis}^2}{\pi/4 \cdot D_{pr}^2} \tag{4.5}$$

When for p the value p_{stat} is substituted, these equations give the quasi-static estimation of the axial stress fluctuations in the riser and the pump rod. Examples can be found in Figures 4.4 and 4.5, for low pumping frequencies (based on experiments with the Volanta handpump, with 78 m riser length).

These figures clearly show that the maximum stress fluctuations, near the resonance frequency, are about twice the values for low pumping frequencies. This is in line with the measured maximum pressure fluctuations, which may become twice the static pressure as is shown in Figure 4.6. This is due to pressure waves, as has been explained in section 3.4.

The magnitude of the pressure fluctuation depends strongly on the pumping frequency, on the length of the rising main and the pump stroke, and on the elastic properties of the riser material.

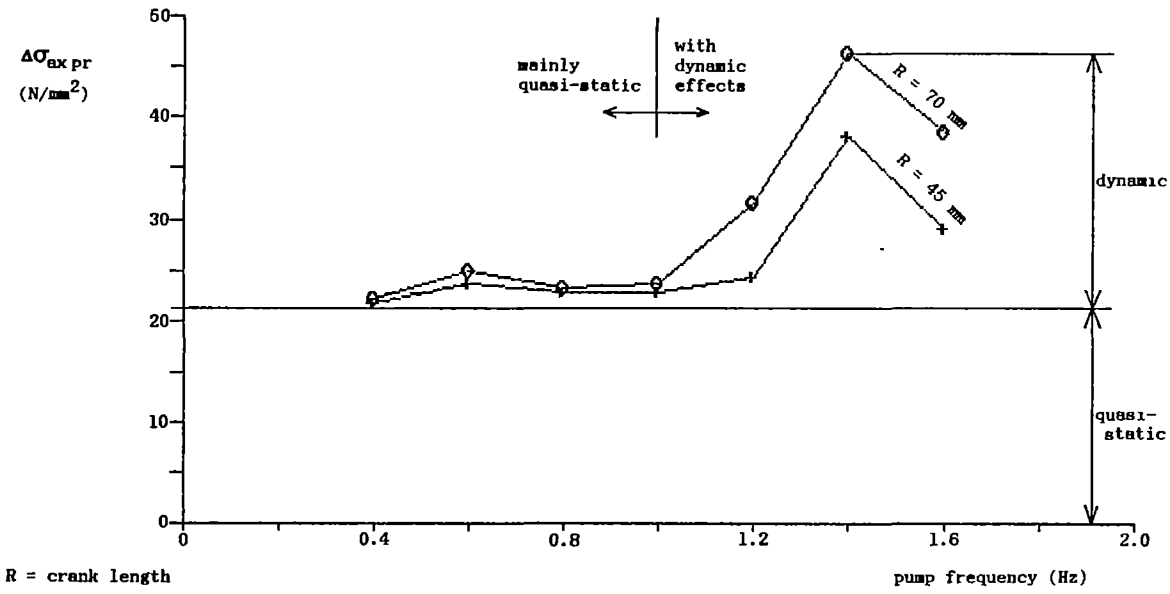

Figure 4.4 Axial stress fluctuation in the top end of the pump rod, at increasing frequencies and for two different crank lengths
(From experimental observation: Volanta handpump, with rising main of 78 m length)

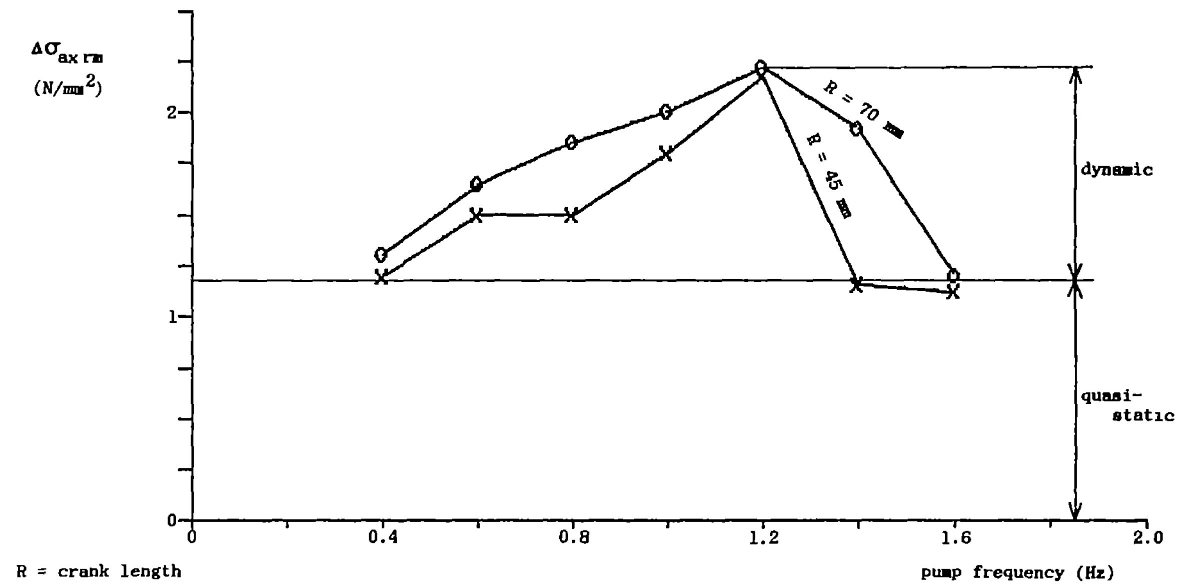

Figure 4.5 *Measured axial stress fluctuations in the top end of the rising main, for two different crank lengths*
(Volanta pump with rising main of 78 m)

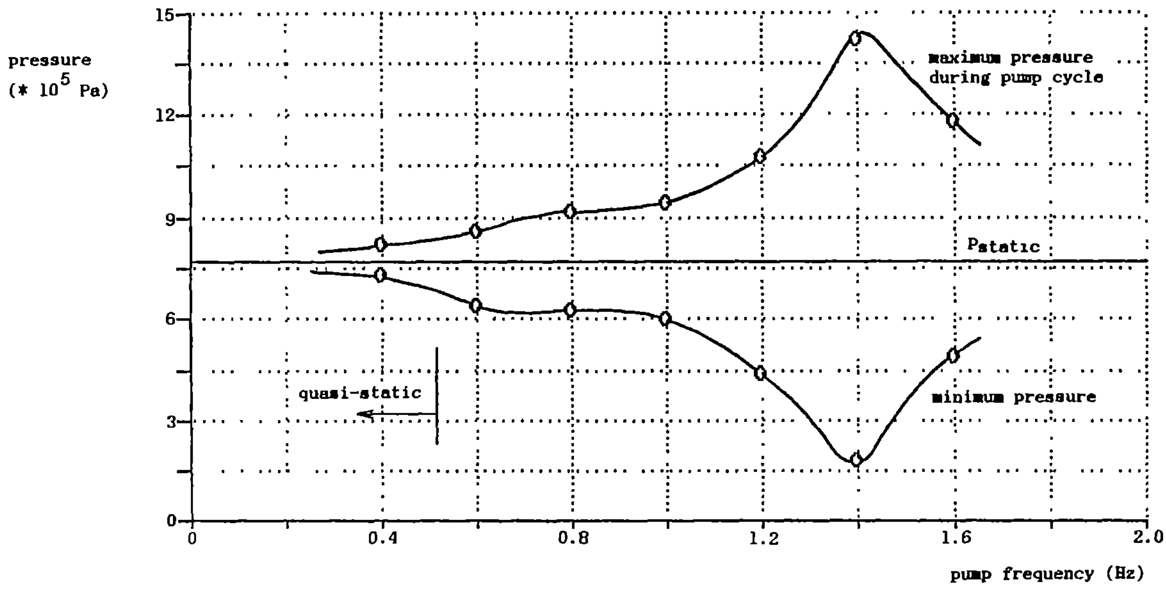

Figure 4.6 *Maximum and minimum pressure above the piston, at increasing pump frequency*
(From experimental observations: Volanta handpump with 78 m rising main. The pressure inside the cylinder at rest, caused by the water column inside the pump, is called the static pressure, P_{static})

The outside pressure p_u is (almost) constant, and is mainly a function of the immersion depth of the cylinder. Therefore the axial, radial and tangential stress fluctuations depend mainly on the pressure fluctuations inside the cylinder, for frequencies below the resonance frequency. For frequencies close to and above the resonance frequency the inertia of the rising main and pump rod will complicate the picture.

Pressures have been measured in the cylinder (above the piston!) as low as p_u and as high as 2 times p_{stat} (when pumping near the resonance frequency).

4.3.2 Tangential load fluctuation

The tangential stress fluctuations are proportional to the pressure fluctuations, as shown by the experiments (see also Appendix III.1, equation III.7). As the pressure fluctuations may exceed 2 times the static pressure when pumping near the resonance frequency, the tangential stress fluctuations may also become twice the static tangential stress (see Figures 4.7 A and B).

Figures 4.4 through 4.7 clearly show the consequences of pumping near the resonance frequencies[14]. It is obvious that these frequencies should be avoided. They are, however, above the normal pumping frequencies as observed in the field (about 0.4 to 0.8 Hz). But even pumping at half the resonance frequency can cause increased pressure and stress fluctuations. For example the so-called *fluttering* (pumping with short, quick strokes as regularly observed in the field) is pumping at about half the resonance frequency. For a riser length of 20 metres, the fluttering frequency is about 2.5 Hz; for 40 m 1.3 Hz and for 60 m 0.8 Hz.

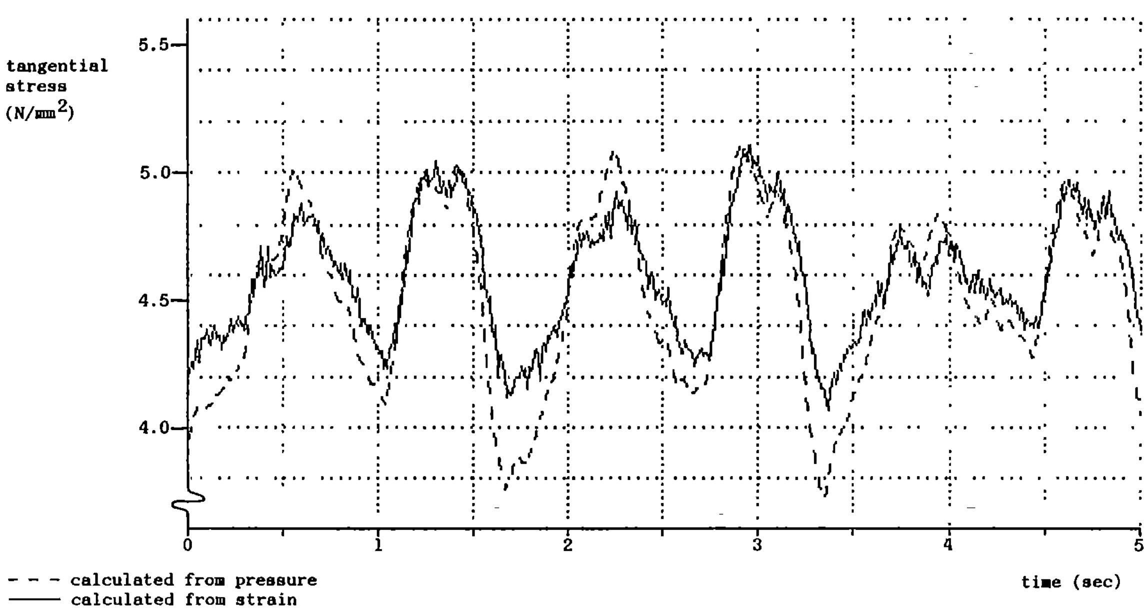

Figure 4.7A *Tangential stress fluctuations at the bottom end of the rising main, at a pumping frequency of 0.6 Hz (see Figure 4.7 B for explanations)*

[14] Note the difference in vertical scales between Figures 4.7 A and 4.7 B.

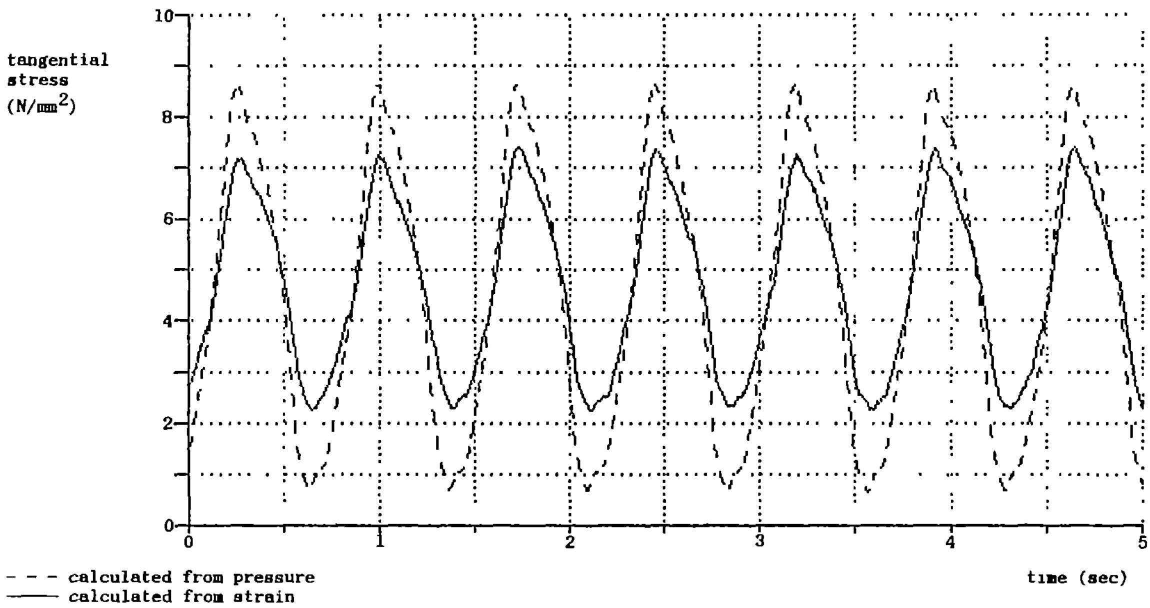

Figure 4.7B *Tangential stress fluctuations at the bottom end of the rising main, at a pumping frequency of 1.4 Hz (Note the difference in vertical scale between Figures 4.7 A and B)*
(The stresses are either based upon measurements of axial and tangential strain <solid lines>, or calculated by means of the pressure fluctuations <dashed lines>.
Measurements were carried out on a Volanta pump with a rising main of 78 m length.)

4.4 Axial strain in the rising main and the pump rod

The changing axial load causes a shortening of the rising main and a (much smaller) lengthening of the pump rod. These length fluctuations depend on the resulting stress fluctuation in the riser and rod, on their lengths and on Young's elasticity moduli of the respective materials.

The shortening of the riser will become:

$$\Delta L_{rm} = \frac{L_{rm}}{E_{rm}} \Delta \sigma_{rm} \tag{4.6}$$

and the elongation of the pump rod:

$$\Delta L_{pr} = \frac{L_{pr}}{E_{pr}} \Delta \sigma_{pr} \tag{4.7}$$

E_{rm} and E_{pr} are the Young's elasticity moduli for the rising main and pump rod, respectively. They indicate the extent to which a material deforms under pressure. There is a difference in elasticity of a factor 70 between PVC and steel (E_{PVC} = 2.5 - 3 GPa[15]; E_{steel} = 200 GPa). Therefore the axial strain in the plastic rising main is much larger than in a steel riser and in the steel pump rod.

[15] 1 GPa = 1 GigaPascal = 10^9 Pascal = 10^9 N/m^2 = 10^4 kgf/cm^2

During the downward piston stroke the bottom of the cylinder will be loaded once more by the pressure in the pump. This causes re-straining of the riser by the same length as calculated before for the shortening.

These strain fluctuations in rising main and pump rod are indicated in Figure 4.8, for different configurations (as a function of their lengths). As can be seen in this figure, strain fluctuations of 80 mm and more may occur in long PVC rising mains. This implies that the cylinder will move up and down over that distance, every pump cycle! It is obvious that this may considerably reduce the outflow of water from the pump (see also section 3.4).

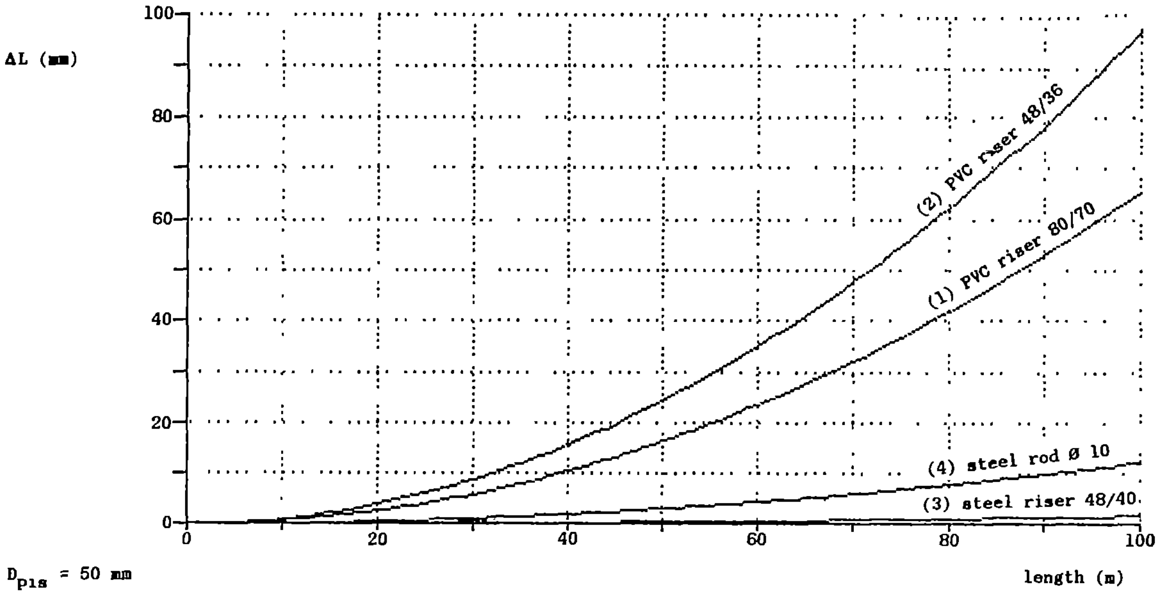

Figure 4.8 *Strain fluctuations in rising main and pump rod, as a function of their length, at low pumping frequencies (quasi-static)*
1: PVC riser; $D_{u\ rm}$ = 80 mm; wall thickness = 5 mm
2: PVC riser; $D_{u\ rm}$ = 48 mm; wall thickness = 6 mm
3: steel riser; $D_{u\ rm}$ = 48 mm; wall thickness = 4 mm
4: steel rod: D_{pr} = 10 mm

4.5 Pump yield and volumetric efficiency[16]

4.5.1 Effect of effective piston stroke

At 100% volumetric efficiency the discharge equals the gross stroke length times the piston cross section, or - as it is often called - the stroke volume. In practice, however, the discharge is much smaller. As pointed out before, water is sucked into the cylinder only during a part of the total upward stroke. It is obvious that only that water will be discharged during one stroke.

16 see also Appendix III.2

Its volume is proportional to the *effective relative piston stroke* (= piston displacement minus the distance the cylinder travels along with the piston during the upward stroke[17]). Moreover, while the piston and cylinder are both moving upward, the load caused by the water column is transferred to the pump rod, which is elongated because of this. The actual piston displacement is thus shorter than the gross stroke length. In summary:

> ***The discharge is equal to the net stroke length (i.e. the gross stroke length minus both the upward cylinder displacement and the stretch of the pump rod) multiplied by the piston cross section*[18].**

The loss of effective piston stroke length may become as much as 100 mm! Hence in such cases a gross stroke length of up to 100 mm would give no discharge at all (volumetric efficiency = 0%)!

In Figure 4.9 the measured and calculated discharges are shown for a SWN 81 handpump, with its discharge calculated as follows:

$$q = S_{eff} \cdot A_{pis} = (S_{gross} - \Delta L_{rm} - \Delta L_{pr}) \cdot \pi/4 \cdot D_{pis}^{2} \tag{4.8}$$

whereby ΔL_{rm} and ΔL_{pr} are calculated with the equations given in Appendix III.1.

Figure 4.9 shows that the measured and calculated discharges for a SWN 81 handpump correspond reasonably well. Only with greater riser lengths the measured discharge is markedly lower[19].

The volumetric efficiency can be calculated as follows:

$$\eta_{vol} = \frac{S_{eff} \cdot A_{pis}}{S_{gross} \cdot A_{pis}} = S_{eff}/S_{gross} = 1 - \frac{\Delta L_{rm} + \Delta L_{pr}}{S_{gross}} \tag{4.9}$$

The figure shows that at low pumping frequencies the discharge and volumetric efficiency can be accurately calculated by way of quasi-static approximations.

4.5.2 Influence of reduced stroke length

In practice the gross stroke length will be less than the maximum, because usually the stops are not reached when pumping. This may have dramatic consequences for the discharge and the actual volumetric efficiency as can be seen in Figure 4.10[20] and 4.11.

---

17 see also Figures 3.2 and 3.3

18 This is only true when dynamic effects are small. During pumping at higher frequencies, the volume pumped may be influenced by the pressure fluctuations. In fact, dynamic effects may lead to volumetric efficiencies of more than 100%! In such cases, during a fraction of the pump cycle, both valves will be open at the same time. For riser lengths up to 40 m this can be attained even when pumping by hand.

19 In practice the relative piston displacement may be further reduced by piston seal friction and buckling. Both effects increase with larger pump heads.

20 Calculated for SWN 81 handpump; experiments show an even greater loss of discharge.

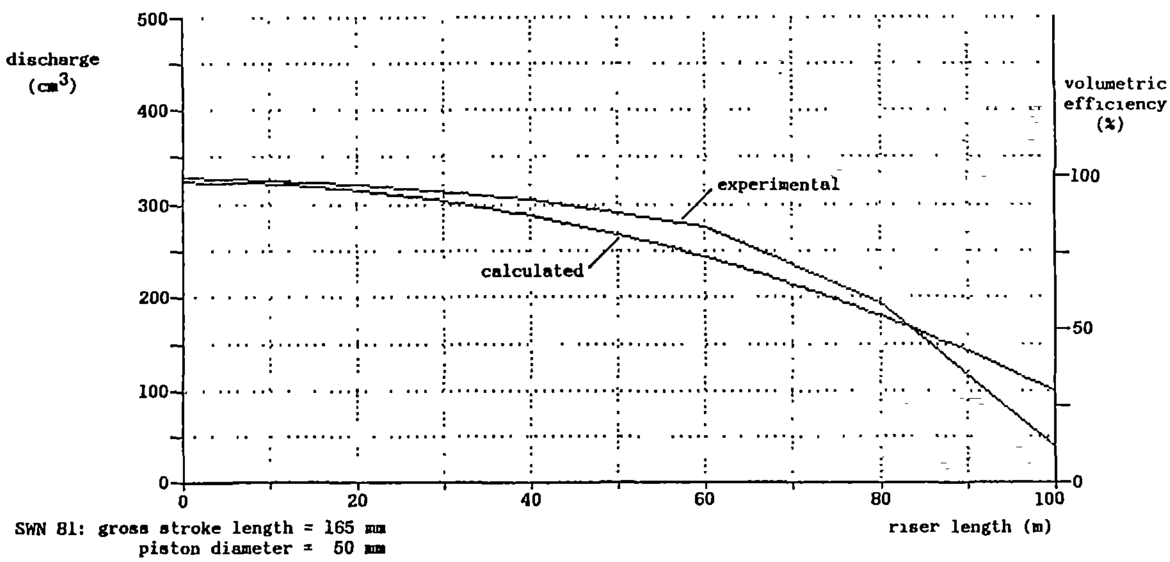

Figure 4.9 Discharge and volumetric efficiency as a function of riser length

4.5.3 Effect of piston diameter

As mentioned in section 4.3, the strain fluctuations in the rising main and the pump rod are proportional to the piston cross section. Figure 4.12 shows the consequences for the discharge and Figure 4.13 those for the volumetric efficiency when the piston diameter is reduced from 50 to 40 mm (SWN 81).

It shows that for a riser length of more than about 80 m (and a gross stroke of 165 mm) the discharge of a 40 mm piston will become more than that of a 50 mm piston! For a 'normal' pumping stroke of about 100 mm, the smaller piston will already pump a larger volume of water at about 70 m riser length. ***The smaller piston cross section is more than compensated for by the increase in effective piston stroke!*** [21]

[21] In practice this will probably already happen at shorter riser lengths.
A smaller piston diameter means reduced axial stress fluctuations as well.

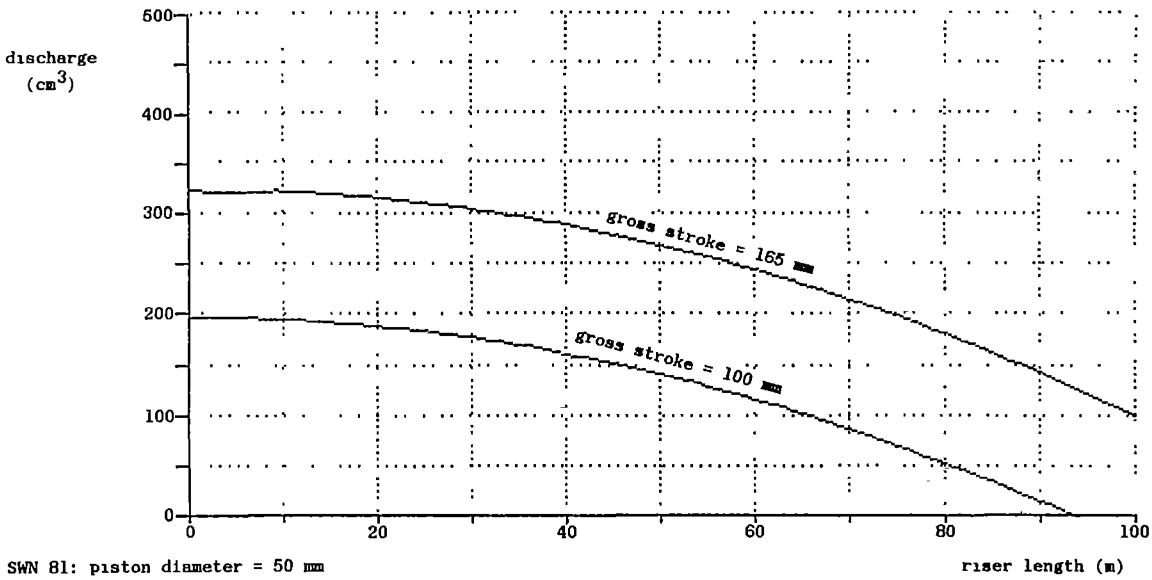

Figure 4.10 The calculated discharge for gross stroke lengths of 100 mm and 165 mm (SWN; 50 mm piston diameter)

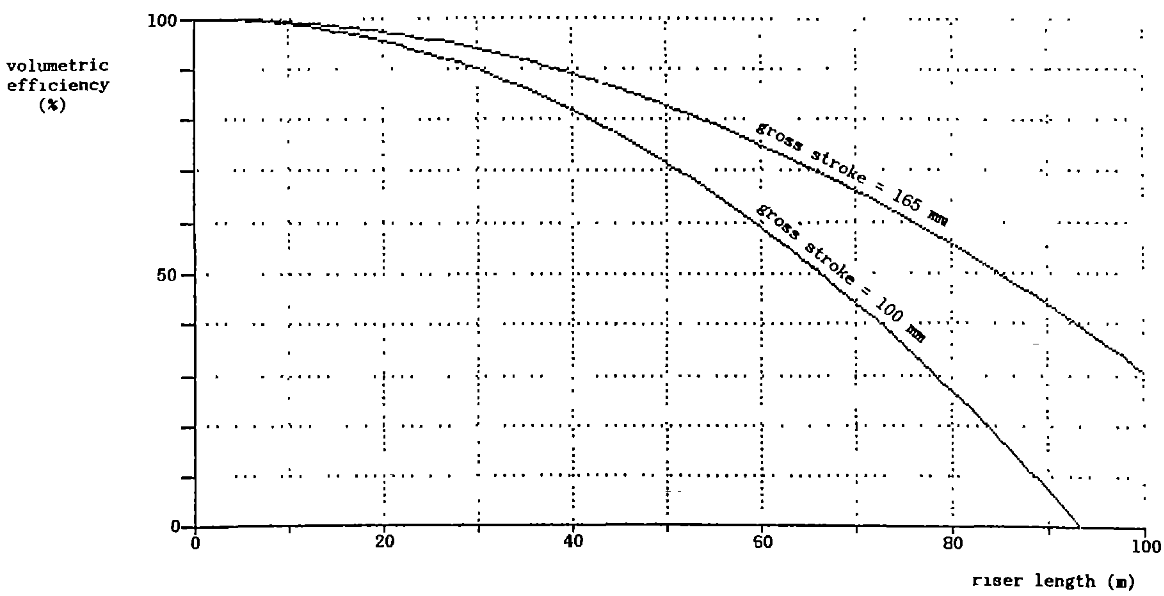

Figure 4.11 The calculated volumetric efficiency for gross stroke lengths of 100 mm and 165 mm (SWN; 50 mm piston diameter)

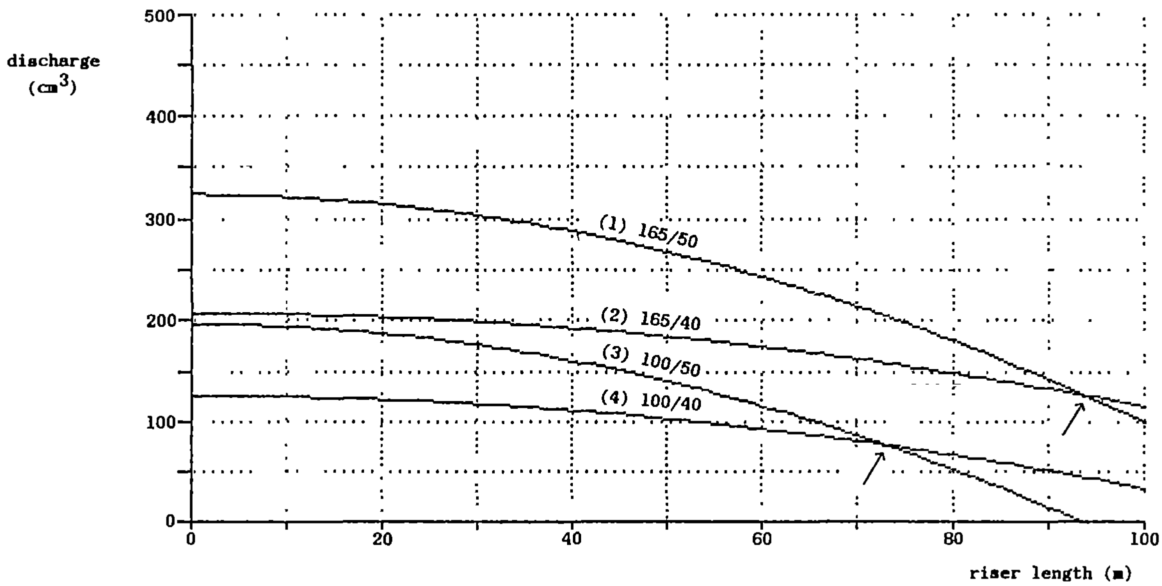

Figure 4.12 *The discharge as a function of the gross stroke length, the piston diameter and the riser length (calculated for SWN 81).*

Number:	*Gross stroke length:*	*Piston diameter:*
1	*165 mm*	*50 mm*
2	*165 mm*	*40 mm*
3	*100 mm*	*50 mm*
4	*100 mm*	*40 mm*

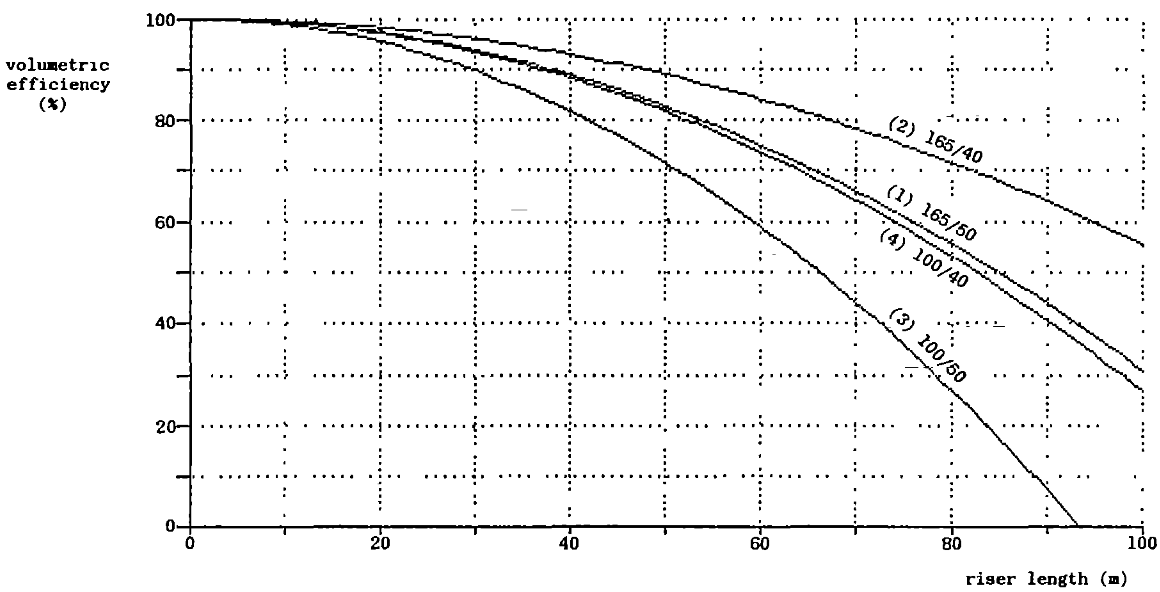

Figure 4.13 *The volumetric efficiency, as a function of the piston diameter, the gross stroke length and the riser length.*
(Calculated for SWN 81)

4.5.4 Effect of wall thickness of rising main

A thicker riser wall will reduce the stress fluctuations in the riser and thus limit the strain fluctuations. In that way the axial cylinder displacements can be reduced, and the discharge increased, as shown in Figure 4.14.

4.6 Mechanical efficiency[22]

The mechanical efficiency of a handpump is the ratio of energy represented by the amount of water pumped out of the well and the energy put in, per pump cycle.
Some energy is lost due to resistance in the bearings, to the piston moving in the cylinder, the rod moving inside the riser, and hydraulic losses.

For handpumps these losses are difficult to calculate and differ largely, depending on the type of pump. But even without taking these losses into account, some conclusions can be drawn in relation to the mechanical efficiency, which relate to the elasticity of the pump.

For handpumps with an elastic riser the main loss is the energy put in from the beginning of the upward piston stroke until the pump starts to pump water, i.e. until the piston starts to move relative to the cylinder (see section 3.3), as if the riser must be spring-loaded first.

Figure 4.15 shows how the mechanical efficiency depends on the ratio between the axial elasticity in the substructure and the gross pump stroke ($\Delta L/S_{gross}$)[23].

For a completely 'stiff' pump the mechanical efficiency would be 100% (neglecting friction losses). For a pump of which the axial elasticity of the substructure equals the gross pump stroke, the mechanical efficiency would be zero.

At the return stroke the 'spring-loaded' riser will stretch. Part of this energy will help to accelerate the flywheel, or to lift the pump handle after passing top dead centre (TDC). For a flywheel pump this may increase the mechanical efficiency (up to 100%, theoretically, neglecting friction losses).
For a handle pump, however, it may cost even more energy, as the 'bouncing' handle may have to be slowed down to prevent injury.

For details of the calculations, see Appendix III.3.

---

22 see also Appendix III.3

23 $\Delta L = \Delta L_{rod} + \Delta L_{riser}$

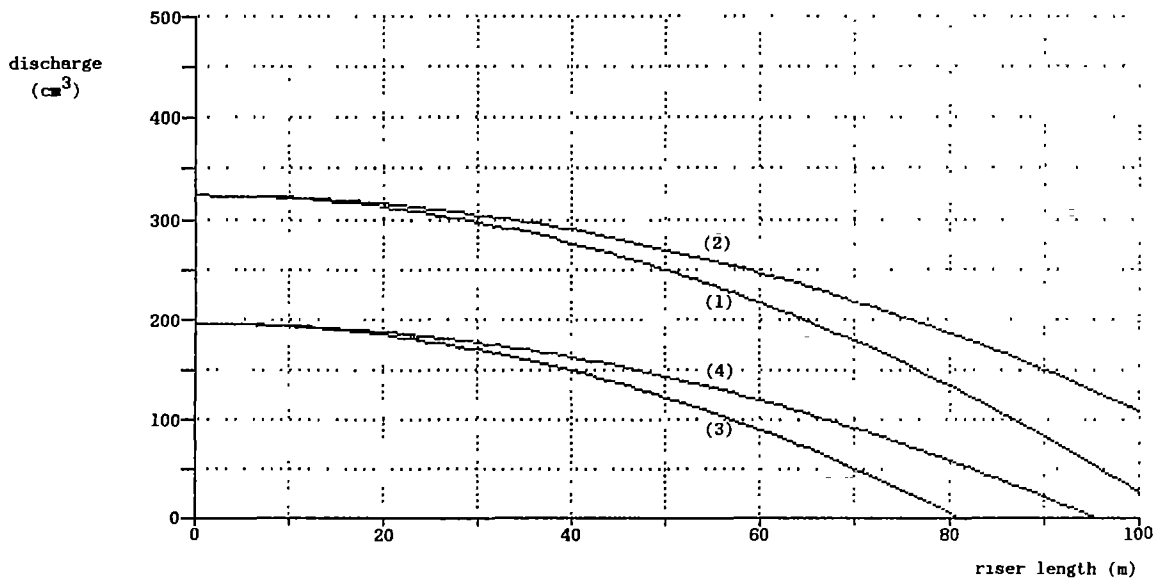

Figure 4.14 Influence of riser wall thickness on the discharge
(Calculated for SWN 81 handpump with 50 mm piston diameter and 48 mm outside diameter of rising main)

Number:	Gross stroke length:	Wall thickness:
1	165 mm	4 mm
2	165 mm	6 mm
3	100 mm	4 mm
4	100 mm	6 mm

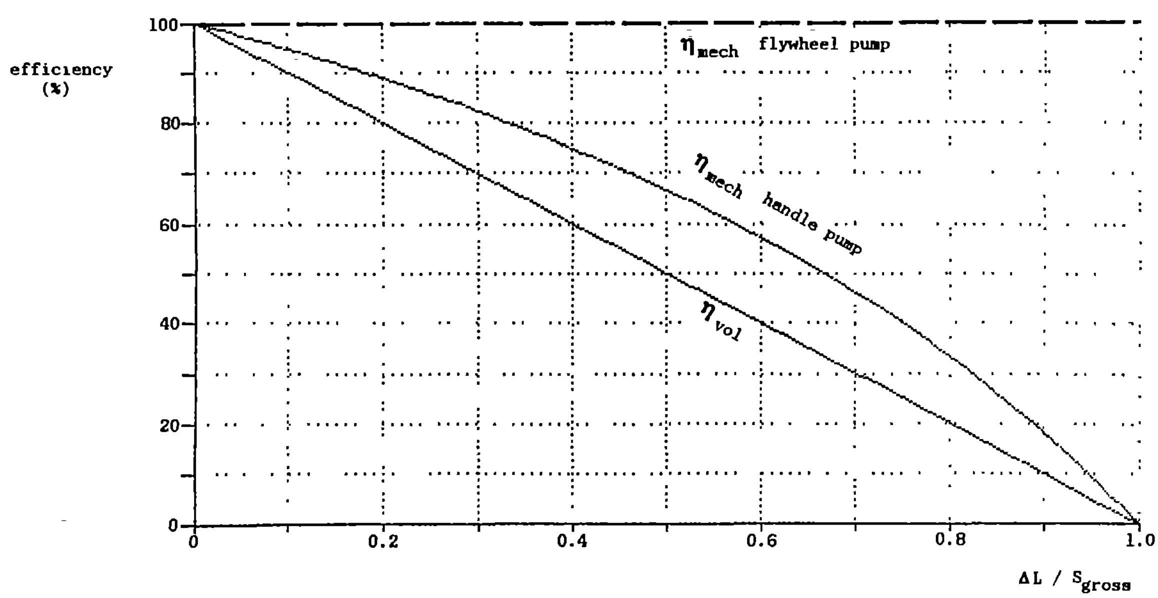

Figure 4.15 Mechanical and volumetric efficiency

4.7 Creep

Static loads will result in so-called 'creep' of the PVC rising main. This means that, depending on the magnitude of the load and on the ambient temperature, a continuing elongation of the riser must be reckoned with. As shown in Figure 4.16, under field conditions an elongation of the rising main of 0.2 to 1.0% may occur over a period of 10 years. This elongation (note that 0.1% of 100 metres equals 100 mm, which is the order or magnitude of the - actual - stroke length) needs to be taken into account for determining the length of the cylinder and/or the relative position of the piston in the cylinder when the pump is installed. Not taking the creep effect into account may easily result in the piston hitting the top of the cylinder (when the riser diameter is smaller than the piston diameter) or in short-circuiting of the piston near TDC (when the riser diameter is larger than the piston diameter).

It should be noted that creep also occurs in a driven pump. During a part of each cycle the riser is 'creep-stretched' by the pressure on the cylinder bottom. Although the riser will be unloaded as well during each cycle, this will lead to a continuing elongation of the riser. The reason for this is that undoing the 'creep-stretching' in the PVC takes about ten times as long as the period during which the load had been applied!

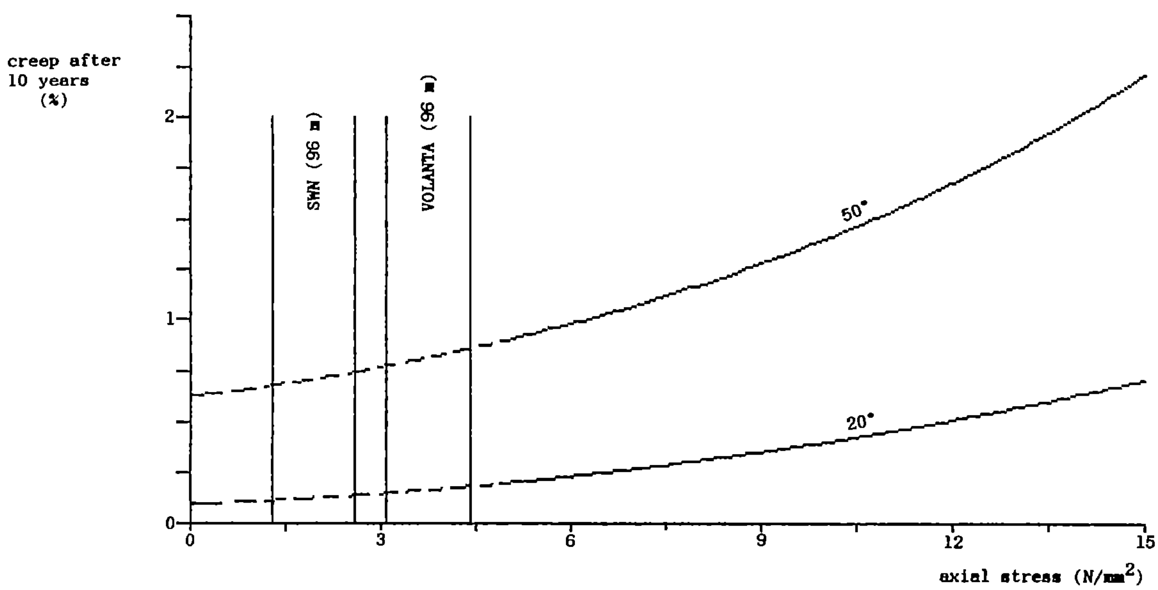

Figure 4.16 Creep in UPVC as a function of the tensile stress and the water temperature
(source: WAVIN R&D)

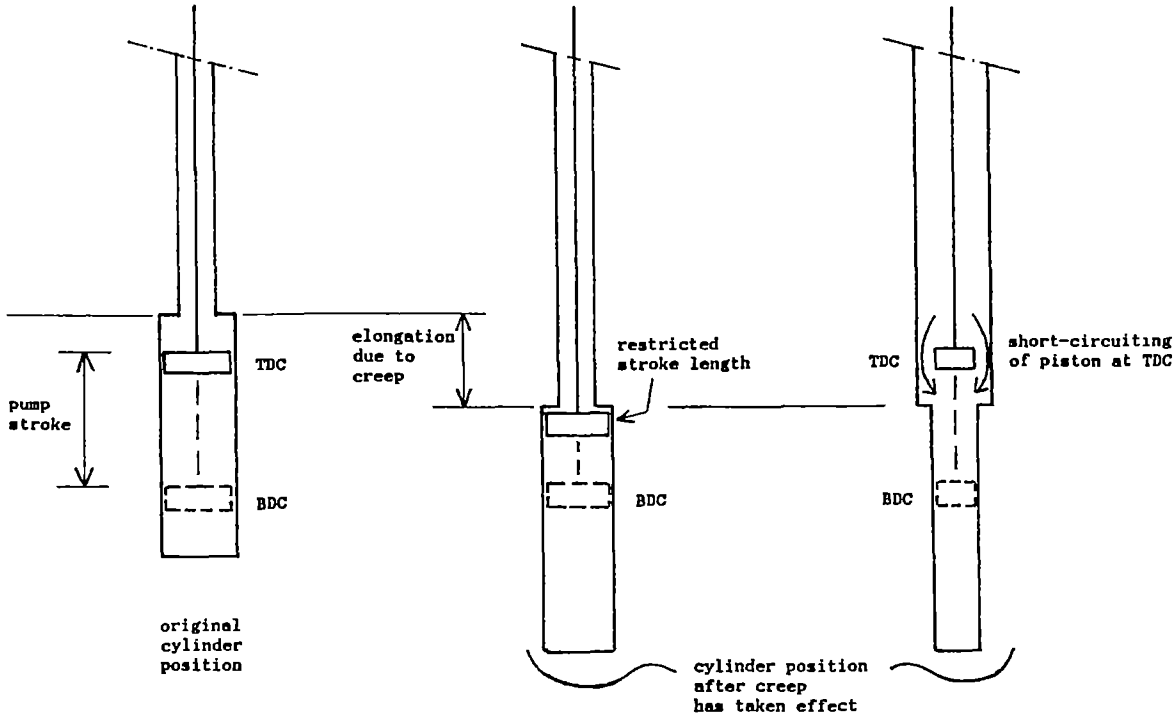

Figure 4.17 Possible effects of creep in PVC rising mains

5 FATIGUE, THE MAIN CAUSE OF FAILURES

5.1 Introduction

In this chapter some mechanisms causing fracture of the pump rod or the rising main will be discussed, with the emphasis on so-called 'fatigue' fractures. Although fatigue will inevitably result in fracture eventually, guidelines will be given on how to avoid such fatigue fractures during the initial 5 - 10 years of a pump's lifetime.
The discussion will be restricted to such pumps that can stand the static load and peak loads occurring during pumping. It will be shown that even these pumps will eventually fail, after years and millions of pump cycles.

In the field many pumps fail already during the first year of operation, however. We trust that the information given in this chapter will provide insight into the problems that cause such early failures.

5.2 Fracture of pump rod and rising main; general

If a rod (or pipe) is loaded with a tensile stress that increases with time, it will break at a certain stress level, the so-called *tensile strength*. The mechanism related to such a fracture is commonly known.

> At low stress levels the stressed material will be strained in more or less direct proportion to the actual stress level. However, at a certain stress level the material will suddenly elongate strongly. This is called 'yielding'. If the stress is maintained after yielding, it is inevitable that the material will break.

This fracture mechanism is called *ductile fracture*.
All pumps are designed in such a manner that the stresses occurring in them never exceed the tensile stress.

Failures of the pump rod or rising main are due to another fracture mechanism: *brittle fracture*. Here a small crack, initiated at the surface due to small damages or overloading, slowly grows with time. If the crack attains a critical size, the remaining material can no longer withstand the load and will break.
The highest growing rates can be found:
- *if a fluctuating load is applied*. In fact, the growth of cracks under a fluctuating load is what we call fatigue. Often the crack growth rate under 'fatigue load' is orders of magnitude larger than under a static load;
- *in a corrosive environment*, due to chemical activity the rate of growth is increased;
- *near stress concentrations*: near sharp edges the stress (and stress fluctuations) may be higher. This situation can be found in joints (see section 5.4).

In handpumps all aspects that contribute to failure of components are present: during pumping the pump components are fatigue-loaded, water is certainly a corrosive environment, and near joints stress concentrations occur. It may also be concluded that the joints are most sensitive to fatigue (i.e. brittle) failures.

5.3 Fatigue[24]

Every material can withstand only a certain maximum stress fluctuation, depending on the number of cycles to which it is subjected. This resistance to failure is what is called the fatigue strength of the material (or better: of the component).

To guarantee the desired lifetime of pump components, these must all have a certain minimum fatigue strength. This fatigue strength appears to be the critical aspect in selecting and dimensioning a hand pump component.

As an example we take a pump rod made of AISI 304 steel. The tensile strength of this steel is 580 MN/m^2, whereas the pump rod will withstand 10^7 - 10^8 cycles only when the load fluctuation amplitude does not exceed 50 MN/m^2. The load amplitude of a PVC rising main (with a tensile strength of 40 MN/m^2) may not exceed 2.5 MN/m^2.

The main features of fatigue are:

- Fatigue cracks are initiated at the surface[25]. Of course the material is more sensitive to fatigue when:
  - there are extra notches and pits caused during manufacturing, transport or installation;
  - the material is attacked chemically, e.g. by glue, by saline or acid water, or by UV (sun)light.

  Note: When the surface damages are caused by the environment this is called corrosion fatigue (see paragraph 5.3.2).

- Fatigue cracks grow under a fluctuating load, the growing rate depending mainly on the amplitude of the load fluctuation.
- Samples prepared in the same way will not break after exactly the same number of cycles. This scatter has to be considered in fatigue analysis.

In air, most metals will not break down due to fatigue when the fluctuating load amplitude does not exceed a certain value, the so-called fatigue limit. However, no material can resist fatigue loading in a corrosive environment.

5.3.1 Fatigue life; S-N curves

The handpump designer has to know the fatigue life of the pump components to check whether they are strong enough to last the desired number of cycles (typically 10^8 cycles over a period of 10 years). The best way to obtain this information is by testing several specimens of each component in a test machine.
By systematic testing so-called *S-N curves* can be determined, in which the applied stress (plotted as S_a, the amplitude of the cyclic stress) is plotted against N, the number of cycles to failure (or fracture).
To estimate the fatigue life of a component without testing, S-N curves of many materials, especially metals, can be found in data books.

---

24 For a more general discussion of fatigue, see also:
Metal fatigue in engineering, by H. Fuchs and R. Stephens, New York, John Wiley & Sons, 1980 and
Fatigue of metals, by P.G. Forrest, Pergamon, 1962

25 see *Metal fatigue in engineering* by H. Fuchs and R. Stephens

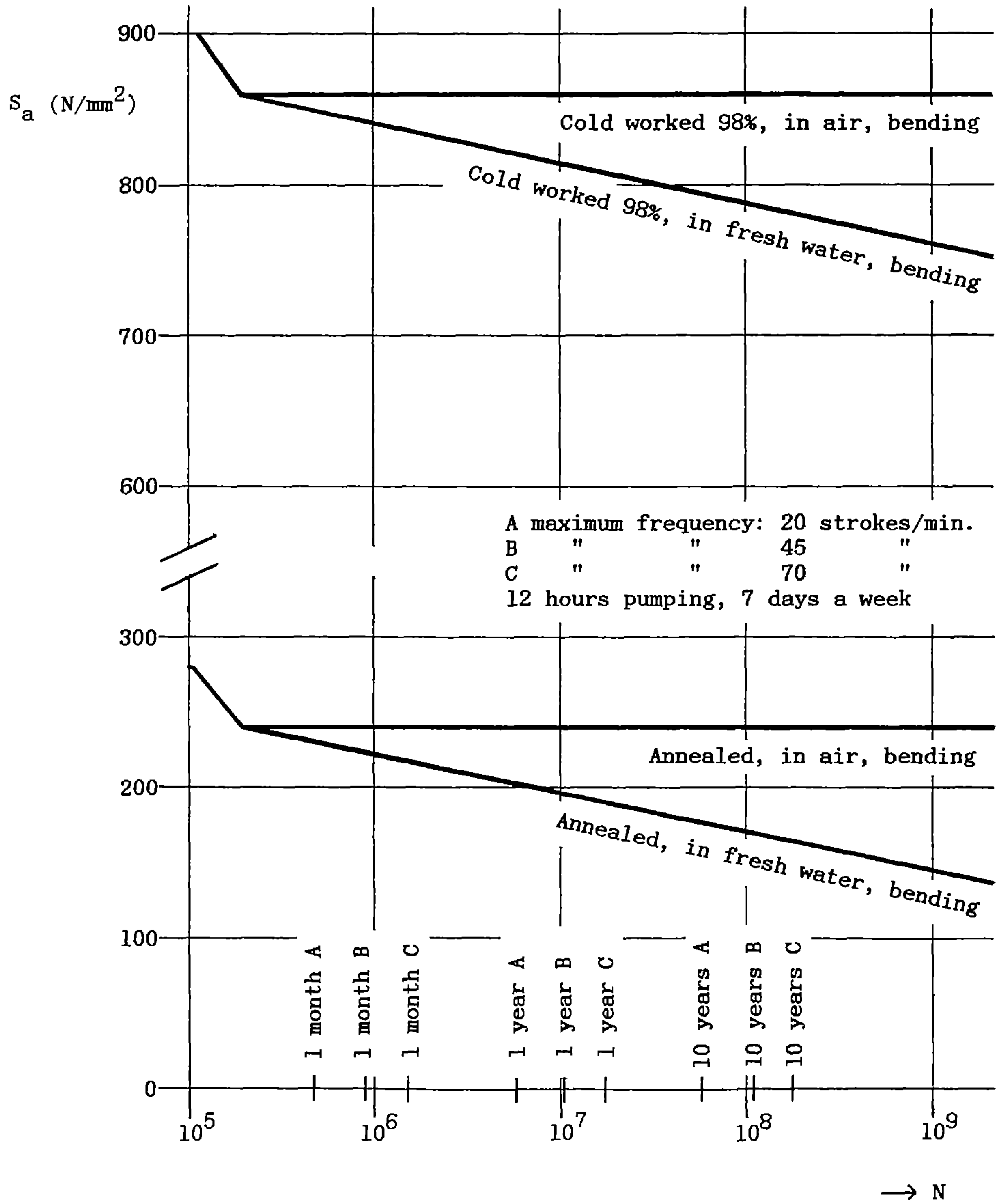

Figure 5.1 S-N curves for stainless steel AISI 304

However, in most cases no data is available for the precise configuration on which fatigue information is sought. For that reason the estimates are by nature rather rough.

Usually fatigue data is available on the rough material only. The fatigue strength of the rough material is a *maximum value*, which has to be reduced to take account of corrosion effects, joints and grooves. These fatigue strength reductions are discussed in paragraph 5.3.4.

Typical S-N curves for AISI 304 stainless steel and for smooth PVC are given in Figures 5.1 and 5.2, respectively[26].

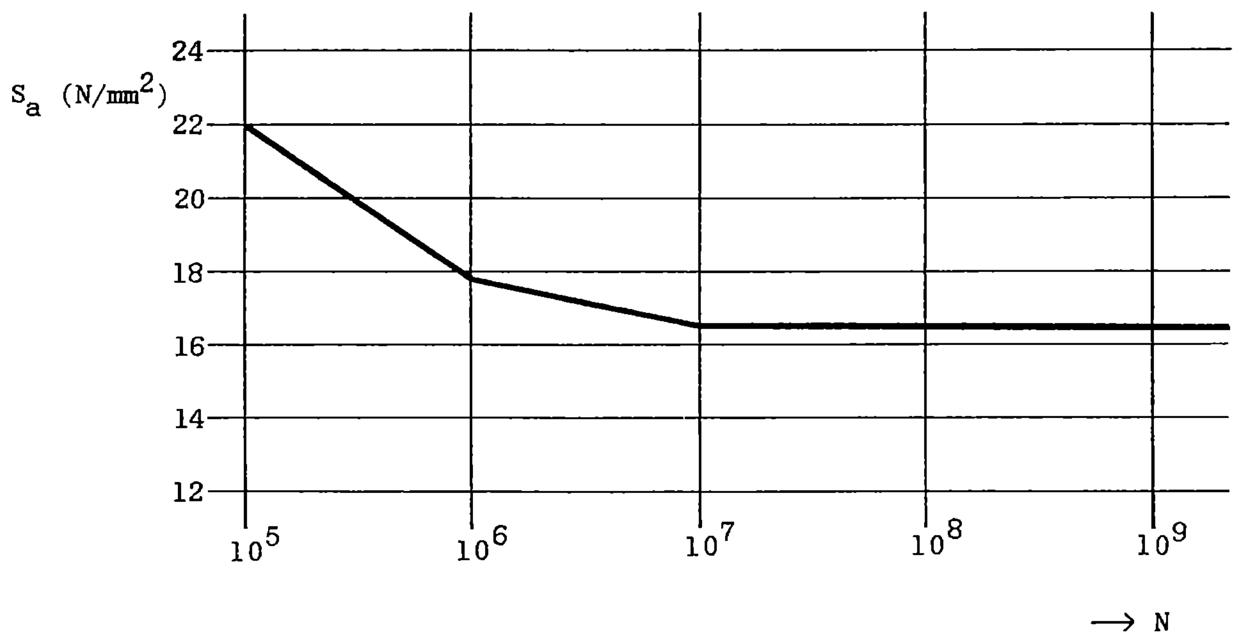

Figure 5.2 S-N curve of smooth PVC (uPVC and rigid PVC)

5.3.2 Corrosion fatigue

For pumps the reduction in fatigue strength is mainly caused by corrosion. This is due to the chemical reaction of the water to both the pump rod and the rising main, and also due to glue if the risers are cemented.

[26] *Design rules for fatigue life of PVC rising mains and stainless steel pump rods of handpumps*, by P. Beekman and J. de Jongh, Report R 993 D, Wind Energy Group, Laboratory of Fluid Dynamics and Heat Transfer, Faculty of Physics, Eindhoven University of Technology, IADHPP89.03, 1989

Corrosion causes surface damages that initiate many fatigue cracks, the growth of which is, moreover, accelerated by the chemical activity. Corrosion causes an earlier fatigue failure, but also a larger scatter in the S-N diagrams, thereby again reducing the allowable stresses.
The reduction in fatigue strength caused by corrosion has to be determined experimentally. S-N curves in corrosive environments can also be found in literature. Such data has to be used with caution, however, as the influence of corrosion is often determined during accelerated tests lasting only a few months. It is not clear whether such results are entirely representative for the actual situation, whereby corrosive influences act on the structure for 5 to 10 years.

5.3.3 Stress concentrations in grooves and at transitions

a. Stress concentrations

For a qualitative estimate of stress concentrations a (not entirely perfect) analogy between stresses and liquid flows can be used. In a pipe restrictions or enlargements produce local increases in flow velocities somewhat similar to the local increase in stresses caused by changes in cross section. To visualize these stress concentration, 'stream lines' are drawn in such a way that the local stress is proportional to the distance between 'stream lines'. This is illustrated in Figure 5.3.

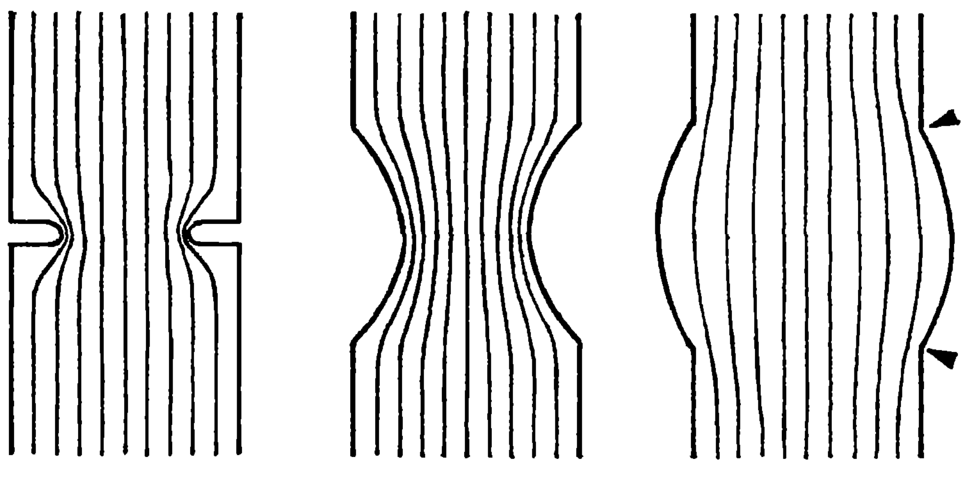

a. b. c.

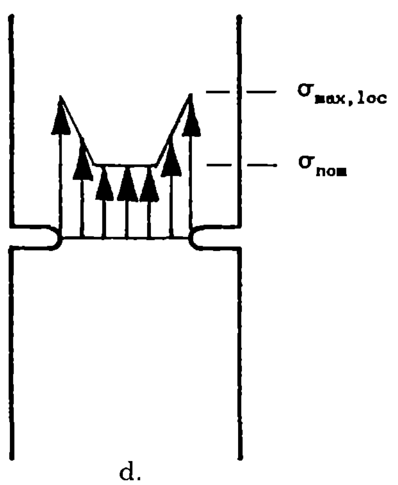

d.

a. The crowding of 'stream lines' helps to visualize the concentration of stress near notches;
b. Streamlining an obstruction decreases the stress concentration (The waist of the obstruction is the same as in (a);
c. Also enlargements of the cross section can cause stress concentrations;
d. Stress profile; definition of maximum local stress and nominal stress.

Figure 5.3 Analogy between 'stream lines' and stress concentration near notches

To calculate the stress concentrations the *stress concentration factor* K_t is introduced:

$$K_t = \frac{\text{maximum local stress}}{\text{nominal stress}} \quad \text{(see Figure 5.3)} \tag{5.1}$$

Charts of stress concentration factors are available in literature[27].

b. *Transitions*

In most structures the stress concentrations that finally lead to fatigue failures occur at transitions between parts of the structure. In handpumps these are pump rod connectors, rising main couplings, the pump rod hanger and the rising main suspension. The simple pump rod connection will be used as an example, see Figure 5.4.

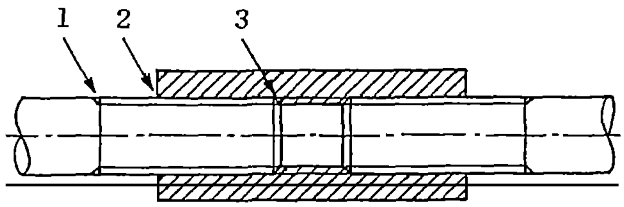

Figure 5.4 *Simple pump rod connection. Arrows indicate stress concentrations, occurring at:*
1. *the first groove;*
2. *the first loaded groove of the pump rod;*
3. *the first loaded groove of the coupling*

At the first groove (1) the stress concentration factor can be calculated, using data books. At the first loaded grooves (2 and 3) this is very difficult. Improvements of the fatigue strength can be obtained by 'streamlining', as shown in Figure 5.5.

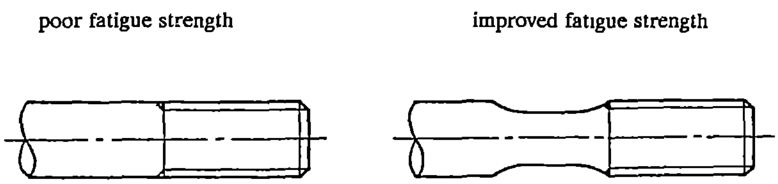

a. First groove of thread

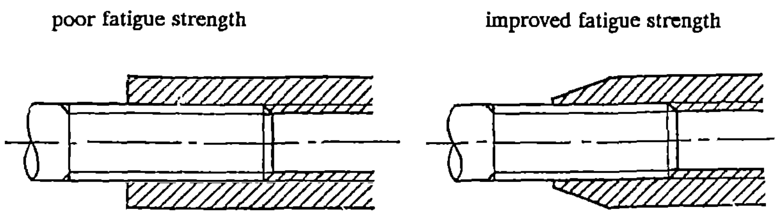

b. First loaded groove of thread

Figure 5.5 *Examples of fatigue stress reduction by 'streamlining'*

[27] *Stress Concentration Factors*, by R.E. Peterson, John Wiley & Sons, New York, 1977

5.3.4 Fatigue strength reduction; notch sensitivity

The *fatigue strength reduction factor* is defined as:

$$K_f = \frac{\text{fatigue strength of a notched specimen}}{\text{fatigue strength of an unnotched specimen}} \tag{5.2}$$

A generally used equation is:

$$K_f = 1 + q\,(K_t - 1) \tag{5.3}$$

in which K_t is according to equation (5.1) and q is the *notch sensitivity*, its value depending on the material and the mean stress level. The parameter q can be found in data books, where q is usually given together with the corresponding S-N curves.

Examples of fatigue strength estimation[28]

a. Introduction

In this paragraph some estimations of fatigue strength will be discussed very briefly. At this point it is repeated that the best way to determine the fatigue strength is to actually test a sample in a testing machine. The procedure pointed out here results in preliminary, necessarily rough, estimates.

b. Fatigue strength of annealed AISI 304 stainless steel

Data on AISI 304 stainless steel is given below. The fatigue strength of a pump rod with threads is estimated. The strength of rod and joint can be found best by testing.

Tensile strength:	580 MN/m^2 ($\approx$ 58 kgf/mm^2)
Yield strength:	289 MN/m^2 ($\approx$ 29 kgf/mm^2)
Fatigue limit:	230 MN/m^2 ($\approx$ 23 kgf/mm^2)
Fatigue strength in fresh water, 10^8 cycles:	170 MN/m^2 ($\approx$ 17 kgf/mm^2)
Cut M10 thread:	K_t = 3
Notch sensitivity	q = 0.35
$K_f = 1 + q(K_t - 1)$	= 1.7
Reduced fatigue strength: 170 / 1.7 =	100 MN/m^2 ($\approx$ 10 kgf/mm^2)
Safety factor:	2
Allowable stress fluctuation amplitude: 100 / 2 =	50 MN/m^2 ($\approx$ 5 kgf/mm^2)

c. Fatigue strength of the PVC rising main

In literature very little information is available on the fatigue behaviour of PVC. Neither S-N curves for PVC in water, nor values of the notch sensitivity could be obtained. Only fatigue data of PVC that was severely notched could be found: root radius 10 μm (the root radius of M10 thread is about 0.9 mm). These values were used to estimate the fatigue strength of PVC rising mains.

[28] see also Appendix IV

Tensile strength:	50 MN/m^2 ($\approx$ 5 kgf/mm^2)
Fatigue strength, 10^8 cycles:	15 MN/m^2 ($\approx$ 1.5 kgf/mm^2)
Fatigue strength of notched PVC, 10^8 cycles:	2.5 MN/m^2 ($\approx$ 0.2 kgf/mm^2)
Allowable stress fluctuation amplitude:	2.5 MN/m^2 ($\approx$ 0.2 kgf/mm^2)

d. *Fatigue strength of the joints*

Due to the complex geometry of the joints it is very difficult to estimate the stress concentration in the joints. Still, by using the 'streamline method' problem areas can be found.

It may be expected that only by collecting extensive experience gained in (simply) testing joints sufficient information can be obtained to allow joints to be designed that meet the requirements.

5.3.5 Residual stresses

To avoid fatigue failures one should try to avoid tensile (mean) stresses, especially at the surface. This can be achieved by inducing compressive internal (or: residual) stresses at highly fatigue-sensitive places[29]. The most common mechanical process to generate residual stresses is surface rolling. This technique is widely used in the production of threads.

5.4 Three-dimensional stress fields

So far we only had the tools to calculate the fatigue stress in one-dimensional stress fields. However, there are three stress components: axial, radial and tangential stress. In the pump rod both the tangential and the radial stress may be neglected so the one-dimensional approach is certainly valid.
In the rising main, however, the axial and the tangential stress can be of the same order of magnitude.

In this section a tool is presented to calculate a one-dimensional reference stress from a stress field, in such a way that the consequences for the fatigue life of the material are the same, whether using the reference stress or the stress field.

Two theories are commonly used to determine a so-called reference stress amplitude from a two- or three-dimensional stress field[30 31]:

Mohr's theory:

$$\sigma_{ref\ Mo} = \sigma_1 - \sigma_3 \qquad (5.4)$$

with σ_1 and σ_3 representing the largest and the smallest of the three stress amplitude components:

$$\sigma_1 > \sigma_2 > \sigma_3$$

---

29 see *Metal fatigue in engineering*, by H. Fuchs and R. Stephens, John Wiley & Sons, New York, 1980

30 *Technische Mechanik*, by G. Holzmann, H. Dreyer and H. Faiss, B.G Teubener, Stuttgart, 1975

31 The reference stress may be used in S-N curves in the same way as one-directional stresses.

Deformation energy hypothesis:

$$\sigma_{ref\,de} = \sqrt{\tfrac{1}{2}\{(\sigma_1 - \sigma_2)^2 + (\sigma_1 - \sigma_3)^2 + (\sigma_2 - \sigma_3)^2\}} \tag{5.5}$$

The formulas show that perpendicular (positive) stresses compensate each other. This is based on the idea that damage is caused by strain and not by stress. Applying perpendicular stresses results in a smaller strain than applying only one (the largest) stress.

Generally $\sigma_{ref\ Mo}$ is larger than $\sigma_{ref\ de}$, as is illustrated in Figure 5.6 for the static situation of a pump at rest. For safety $\sigma_{ref\ Mo}$ can therefore be used best. Because furthermore the smallest stress component σ_{rad} may usually be neglected compared to σ_{ax} or σ_{tan} , (5.4) can be written as:

$$\sigma_{ref} = \sigma_{ref\ Mo} = \max(\sigma_{tan}, \sigma_{ax}) \tag{5.6}$$

which means that using the largest of the three stresses, in a one-dimensional approximation, is allowable.

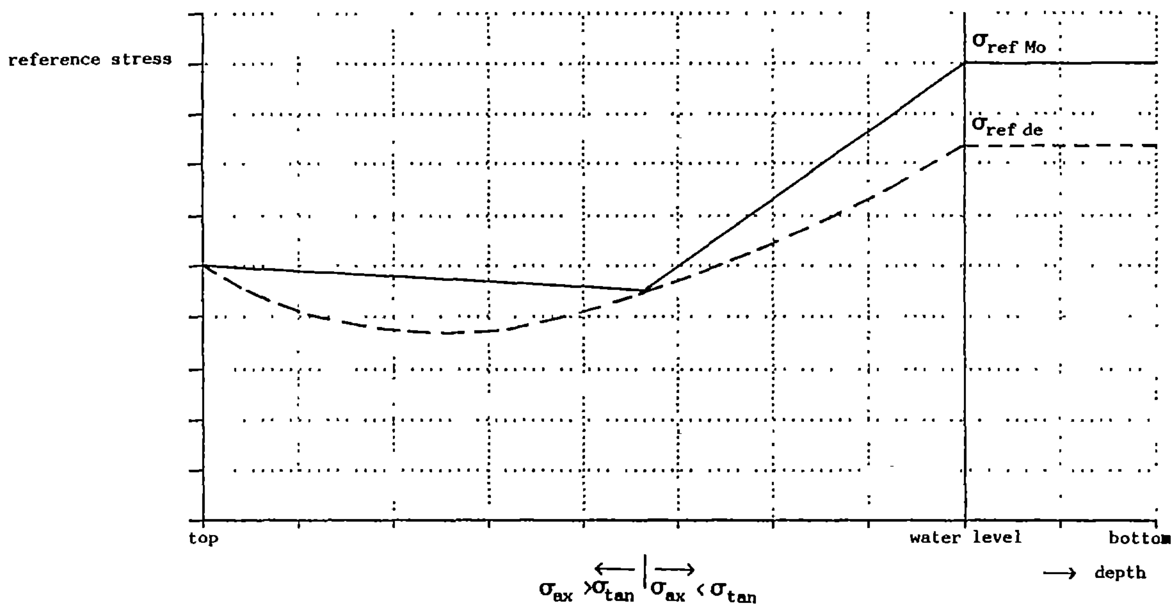

Figure 5.6 Reference stresses along the rising main when the pump is at rest

Note:
Whenever stress concentrations occur, formulas (5.4 - 5.6) should be used with care. E.g.: Consider the joint at the bottom end of the rising main. Due to the geometry of the joints the local *axial* stresses near the edges are increased. The tangential stresses in the rising main, just outside the joint, are not influenced by the joint. Therefore, to calculate the reference stress at this location not the global axial stress should be considered, but the increased local axial stress.

6 BEHAVIOUR AND FAILURES OF HANDPUMPS IN FIELD SITUATIONS

6.1 Introduction

In field situations handpumps have to endure more loads and deformations than the ones mentioned so far: before and after installation! This chapter will concentrate on those in the riser and pump rod.

Apart from axial and tangential stresses that have already been mentioned, important bending stresses may occur in the riser and the pump rod during pumping, due to:
- non-aligned rods, riser pipes and joints;
- inclined and/or curved boreholes;
- inclined pump stand;
- non-aligned fulcrum and rod hanger bearing;
- friction in the rod hanger bearing;
- friction between piston and cylinder;
- swinging;
- buckling and 'snaking'.

Some of the causes may induce bending stress fluctuations that even exceed the axial stress fluctuations! They may considerably reduce the fatigue lifetime of the pump parts.

Also the 'history' of the parts may further reduce their lifetime. This refers, for example, to:
- the use of inferior materials, and rough manufacturing;
- degradation by heat transfer (welding), UV light, (accumulated) glue;
- plastic deformations during transport, installation and maintenance.

Part of these causes can be overcome by better manufacturing and handling methods. Others can be reduced by - sometimes simple - design modifications.

Some examples of design modifications aimed at reducing bending stresses and/or stress concentrations at the joints will be discussed. It is impossible, however, to give more than general design considerations in relation to fatigue: this matter can be solved only in practice!

The last paragraphs will discuss the relation between the loads and issues such as:
- power input;
- pumping against the stops;
- handle versus flywheel drive;
- hand drive versus mechanical drive;
- centralizers, flexible rod and riser hangers, and
- cylinder support.

6.2 Bending stresses in the riser and the pump rod: causes and remedies

a. Non-alignments

Non-alignments of the riser and the pump rod, due to inclined threaded or cemented joints, bent rods, out-of-plumb stands, inclined or curved boreholes, etc. will result in bending stresses in these parts. Not only static, but fluctuating bending stresses as well, because the fluctuating axial tensile load will try to straighten the non-aligned parts each pump cycle.
Larger axial loads (related to pump heads) will therefore lead to larger bending stresses.

These bending stresses will be at their maximum in the weakest spots, such as the thread: a reduction of the cross section because of the thread (- 20%) causes an even larger (relative) reduction of the resistance against bending (about - 30%)! The maximum bending stresses (and fluctuations) are thus about 30% larger than in the non-threaded parts.

This underlines the importance of cutting/rolling straight threads and of preventing accidental bending of the threaded parts during transport, installation and repairs.

b. Friction

Especially the ends of the rod may have to endure increased bending loads:

- top end: due to friction in the rod hanger bearing (if any) the top end (threaded?) has to withstand the friction moment in the bearing;
- bottom end: due to friction between the piston and the cylinder; mainly when sediment builds up in the cylinder, the friction at the return stroke may soon lead to rods broken by buckling[32].

Larger axial loads (related to pump heads) will increase the bending stress fluctuations.

In the top end of the rod bending stresses have been measured that largely exceed the axial stress fluctuations! (see Figure 6.1) This underlines the importance of good bearings and proper maintenance. A stronger top rod will help to reduce fractures, moreover.

At the upward piston stroke the friction between the piston and the cylinder may lead to buckling of the rising main.

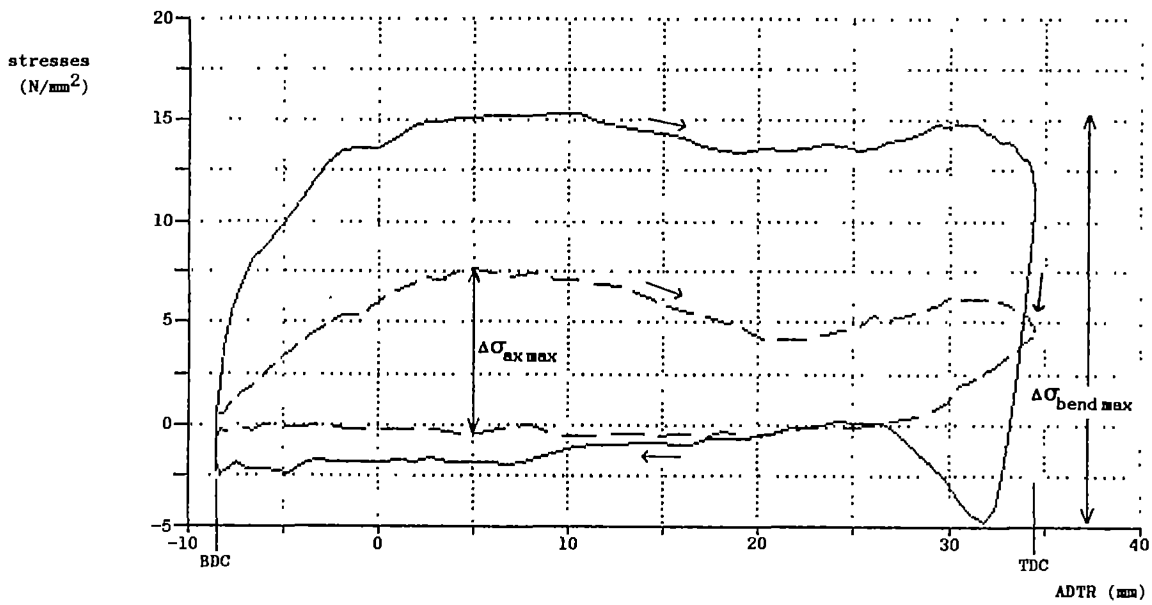

Figure 6.1 Bending stress fluctuations in the top end of the pumprod (mainly due to friction in the hanger bearing) and axial stress fluctuations, against the axial displacement of the top of the rod (ADTR).
(From experimental observations)

32 buckling = bending of the centreline, caused by an excessive axial compressive force.

c. *Buckling*

When compressive axial loads occur in the rising main and the pump rod, they may buckle during each pump cycle, especially near the bottom end of the pump. Buckling of the rod[33] may result from increased friction between piston and cylinder at the return stroke. Buckling of the riser may occur during the upward piston stroke, due to friction between the piston and the cylinder, but also when the piston diameter exceeds the inside diameter of the riser (see also Figure 4.3). This phenomenon has regularly been measured! Bent pipes will accelerate its occurrence.

The pump rod, inside the riser, will prevent a full collapse of the rising main while causing extra friction between the two, and vice versa. Therefore, the resulting bending stresses are limited.

The critical buckling stress can be found by way of Euler's column formula (see Appendix III.4). When the compressive axial stress exceeds the critical buckling stress, buckling will occur.
Non-retained PVC rising mains will buckle as soon as compressive stresses occur! Even with provisions such as riser centralizers or pump rod guides retaining the riser at regular intervals, only in large-diameter rising mains buckling may be prevented. The tests have shown that even with such provisions (a riser centralizer every 3 m) buckling will occur in risers of about 50 mm diameter at riser lengths of 20 m and more.

Buckling can thus hardly be prevented by retaining the rising main. *Reducing the piston diameter (resulting in a decreased "cylinder roof" area and therefore reducing the compressive stress in the rising main) is an effective way to prevent buckling and to limit the bending stress fluctuations in the rising main. Using a piston seal with less friction, such as in the Volanta pump, will also help.*

Buckling of the rod is best prevented by reducing the friction between the piston and the cylinder (return stroke!) and by limiting the maximum pump frequency (< 3 Hz).

Buckling of the rising main will increase axial cylinder displacements during pumping. This will reduce the effective (relative) piston stroke and thus the discharge of the pump.

d. *Swinging*[34]

Swinging is not important for the bending stresses, because the curvature of the riser is small. It may lead to shattering or wear of the cylinder when large displacements lead to regular contact with the wall of the well. At normal immersion depths of the cylinder, however, this plays no role.

e. *Snaking*[35]

Snaking, which is probably caused by travelling transfer waves in the rising main, may induce more frequent and serious bending stress fluctuations. Buckling is presumed to be the 'engine' for both snaking and swinging. Wave amplitudes of 10 cm have been observed, causing increased curvatures and bending stress fluctuations that may equal the axial stress fluctuations.

Especially the top joint is loaded by these waves as they reflect against the (stiff) suspension. Bending stresses here can be reduced by a flexible suspension of the riser (Afridev) or by a protecting tube around the top part of the riser (SWN). Also retaining the rising main at the antinodes of the waves seems a good solution.

---

33 Also when pumping at high frequencies (more than about 3 Hz), when the downward acceleration of the rod may induce compressive forces.

34 swinging = the riser moving like a pendulum

35 snaking = undulating because of transverse waves, of which buckling is probably the engine (see also Appendix IV.4).

f. Conclusions

Various effects may lead to important bending stress fluctuations; in the riser these may become equal to the axial stress fluctuation, and in the rod even to twice that value. These bending stresses will markedly reduce the fatigue lifetime, especially in threaded parts that are subjected to loads.
The bending stresses relate to the axial stress fluctuations: the larger the head of water, the larger, in general, the bending stresses will become.

As soon as compressive axial loads occur, buckling will take place in the riser and the rod. Buckling of the riser can be limited by reducing the piston diameter, buckling of the rod by limiting the friction between the piston and the cylinder.

Large bending stress fluctuations may be induced by the rod hanger bearing. Strengthening the top rod may be necessary in that case.

Centralizers or guides for the rising main will limit the bending stress fluctuations, except when these are due to buckling. The stress fluctuations are normally higher in the bottom part of the riser.

6.3 The 'history' of the pump parts

Apart from the stress fluctuations that weaken the material during pumping, thus shortening its lifetime, other factors may accelerate this process. One of these is the way the material has been treated before installation, thus being part of its 'history'.

The acidity of the pumped water and presence of notches will reduce the safe fatigue stress fluctuations for steel, as will welding of stainless steel and over-stressing (bending and re-bending) of the rod ends.

In the field it has been observed that the 'milder' stainless steel qualities (such as AISI 304), when medium pre-stressed, will last longer than harder qualities.

PVC is weakened by direct sunlight (UV rays) and by glue! Both result in brittle material and cracks. Especially at places where glue has accumulated (e.g. where the ends of the riser pipes meet in the joint) this may occur[36]. Extended storage at high temperatures will lead to similar effects.

It is obvious that the composition of the PVC (for example the length of the molecules and fillers) and its processing (temperature, homogeneity) are of critical importance for its lifetime[37].
High-impact PVC (obtained by adding a few percent of PE to the UPVC) will better resist rough handling during transport and installation. The increased toughness prevents fractures.

It is obvious that re-using old parts (such as cemented joints!) for repairs will result in early breakdowns, as these parts are often the heaviest loaded ones.

Handling of excessively long parts (risers of more than about 6 m and rods of more than 3 m) should be prevented, as this would probably lead to plastic strains in the rod joints and cracks in the PVC joints.

---

[36] see also section 6.4

[37] see *Investigation into the fatigue life expected from uPVC rising mains used for Handpumps for the Developing World*, by P.R. Lewis, the Open University, Walton Hall, Milton Keynes.

6.4 Design adaptations to minimize extra stresses in the joints

In the field some favourable designs (from the point of view of fatigue) have been observed, which are worth mentioning.

Figure 6.2 shows two versions of the hook of a hook-and-eye connection. The original version (I) cracked after some time, especially at larger installation depths. Version (II)[38] has a smoother shape, reducing the internal stresses of the manufacturing process, and reducing the bending stresses due to the axial tensile load.

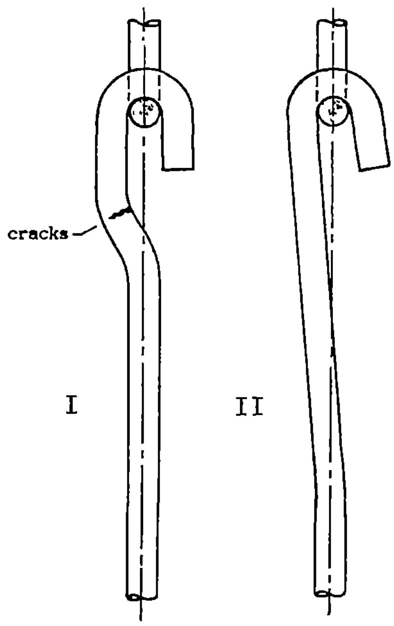

Figure 6.2 The original (I) and an improved pump rod hook (II)

Figure 6.3 shows two versions of a threaded pump rod joint. In version (II) the bending stresses are smoothly led around the thread, preventing bending stress fluctuations in the thread. However, the welded connection with the rods may be the weakest spot as welding induces extra stresses in the material (and weakens stainless steel, moreover).

Figure 6.4 shows two versions of a cemented riser joint. Version (I), the standard factory-made tulip end, cracks rather soon. Version (II), with a more gradual transition[39], will last longer because of the reduced bending stress fluctuations and stress concentrations under identical (axial) loads.

[38] Volanta, manufactured in Saaba, Burkina Faso

[39] Afridev, Kenya

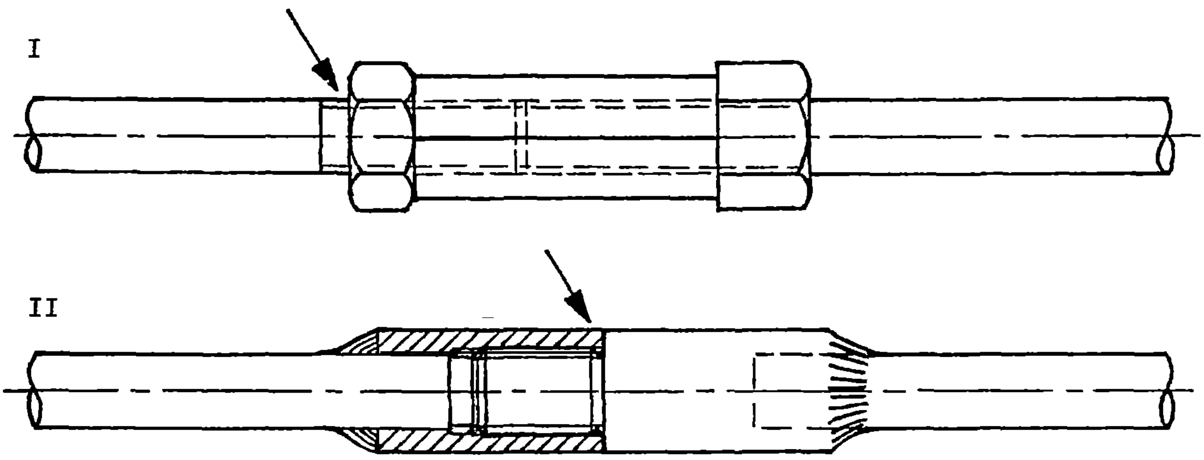

Figure 6.3 Bending stresses through the thread (I) and led around it (II)

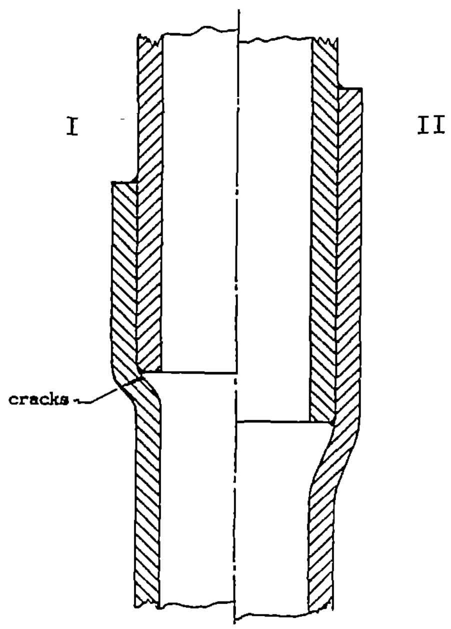

Figure 6.4 Standard (I) and improved (II) cemented riser joint

Centralizers, flexible rod and riser hangers

Centralizers will limit the amplitudes of the radially moving riser, and thus of the bending stress fluctuations. Buckling cannot be prevented in this way, however.
A flexible riser hanger to a limited extent reduces the bending stress fluctuations in the riser that are caused by buckling and snaking.

A flexible rod hanger will limit bending stresses in the top end of the rod that are due to non-alignments of the bearings and between the plane of the moving crank and the centre line of the rod. Bending stresses caused by friction in the rod hanger bearing cannot be prevented in this way, however.

Nevertheless, reductions of a factor 4 (!) of the bending stresses caused by friction in the rod hanger bearing have been realized. The high bending stresses were probably due to the fact that non-alignments had increased the friction in the rod hanger bearing. Without the flexible rod hanger bending stress fluctuations of twice the axial stress fluctuations have been measured in the top end of the rod!

6.5 Extra stresses due to the pump drive

The following paragraphs will discuss the consequences for the stresses in the riser and pump rod, for different power input, drives and pump configurations.

a. *Power input*

The power input is related to the water pressure head, the gross pump stroke, the pumping frequency and the elasticity of the substructure of the pump. These relationships are far from linear, however!
For example: It has been measured that the power need sometimes decreased with increasing pumping frequency.

At large installation depths the axial forces in the rod and the riser increase, but so does the axial elasticity of the pump. In practice this leads to the strange phenomenon that it will be hard to put extra power in the pumping. This is due to the limited volume of water pumped and the fact that a part of the energy that was put in during the upward piston stroke is regained at the downward pump stroke[40], especially with a flywheel-driven pump.

Apart from that, the pressure waves in the water column in the riser will influence the energy that can be accumulated by the pump. This depends on the riser length, the elasticity of the riser and the pumping frequency, but again this relation is not at all linear!

It can therefore be stated that in general the power necessary for pumping water will increase with greater depth, but it will be impossible to predict by exactly how much.

b. *Pumping against the stops*

Figure 6.5 clearly shows the consequences for the crank rotation of pumping against the stops, for a handle-driven pump (SWN with rubber crank stops). The sudden reversal in direction of rotation induces extra accelerations in the pump. Comparing the axial stresses in the pump rod and the riser while pumping against the stops, with the situation while just not touching the stops (at the same pumping frequency), however, shows that the increase in axial stresses by bumping against the (rubber) stops is negligible! This is probably due to the axial elasticity of the riser.

---

[40] as explained in section 4.6 and Appendix III.3

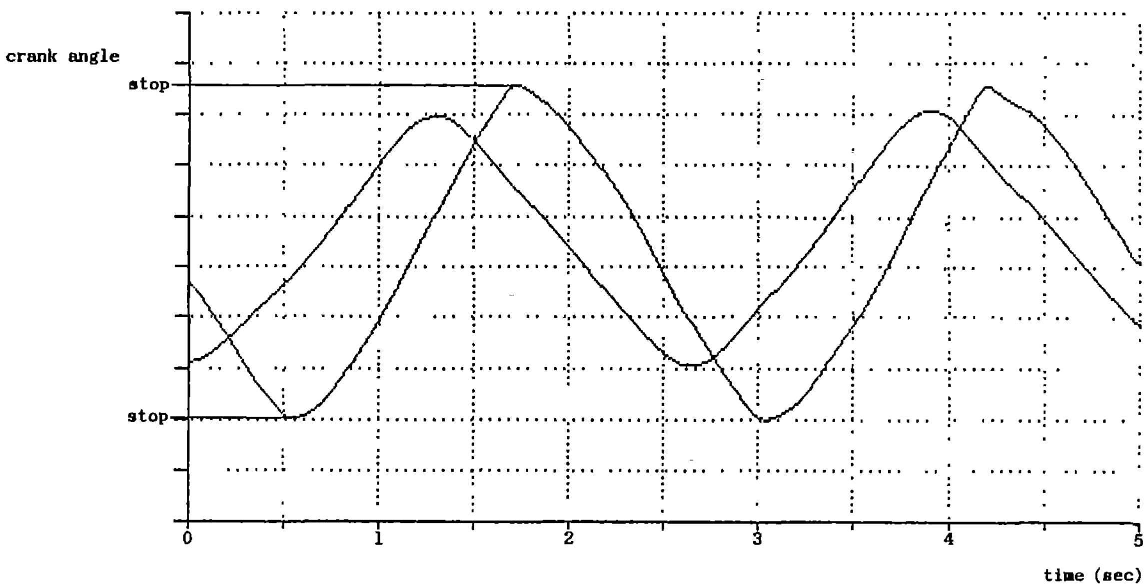

Figure 6.5 Crank rotation: pumping with and without touching the stops

c. Handle versus flywheel drive

Although the flywheel guarantees a smoother pump cycle when compared with a handle-driven pump (remember Figure 6.5!), the consequences for the axial stress fluctuations are negligible.

d. Hand versus mechanical drive

Differences are negligible. There is the danger of (mechanical) pumping at/near the resonance frequencies, without noticing, because with a mechanical drive increased pumping frequencies can be maintained.

6.6 Cylinder support

Some handpump manufacturers prescribe cylinder support as a way to increase the discharge of the pump and to reduce the axial stress fluctuations in the rising main.

The IADHPP tests have shown that cylinder support from the bottom of the well/borehole is effective in the sense that it will reduce axial cylinder displacements, and so increase the relative piston stroke and thus the volumetric efficiency.

However, very much increased bending stress fluctuations in the bottom part of the rising main will be the result. Tests with a SWN 81 handpump showed that in fact the total stress fluctuations are actually larger because of this cylinder support. The tests also showed that, even when supported, the cylinder would still move axially, as can be seen in Figure 6.6. Even clamping of the rising main between the pump stand and the cylinder support could not prevent the cylinder from moving axially!

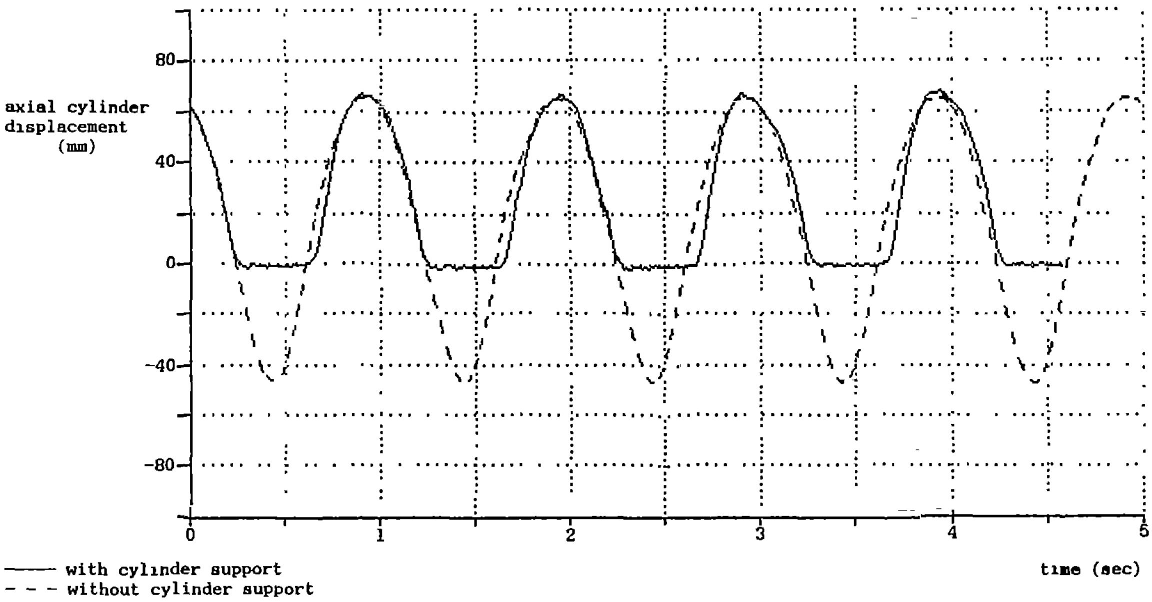

Figure 6.6 Axial cylinder displacement for a pump with and without supported cylinder
(From experimental observations; SWN handpump with a riser length of 96 m)

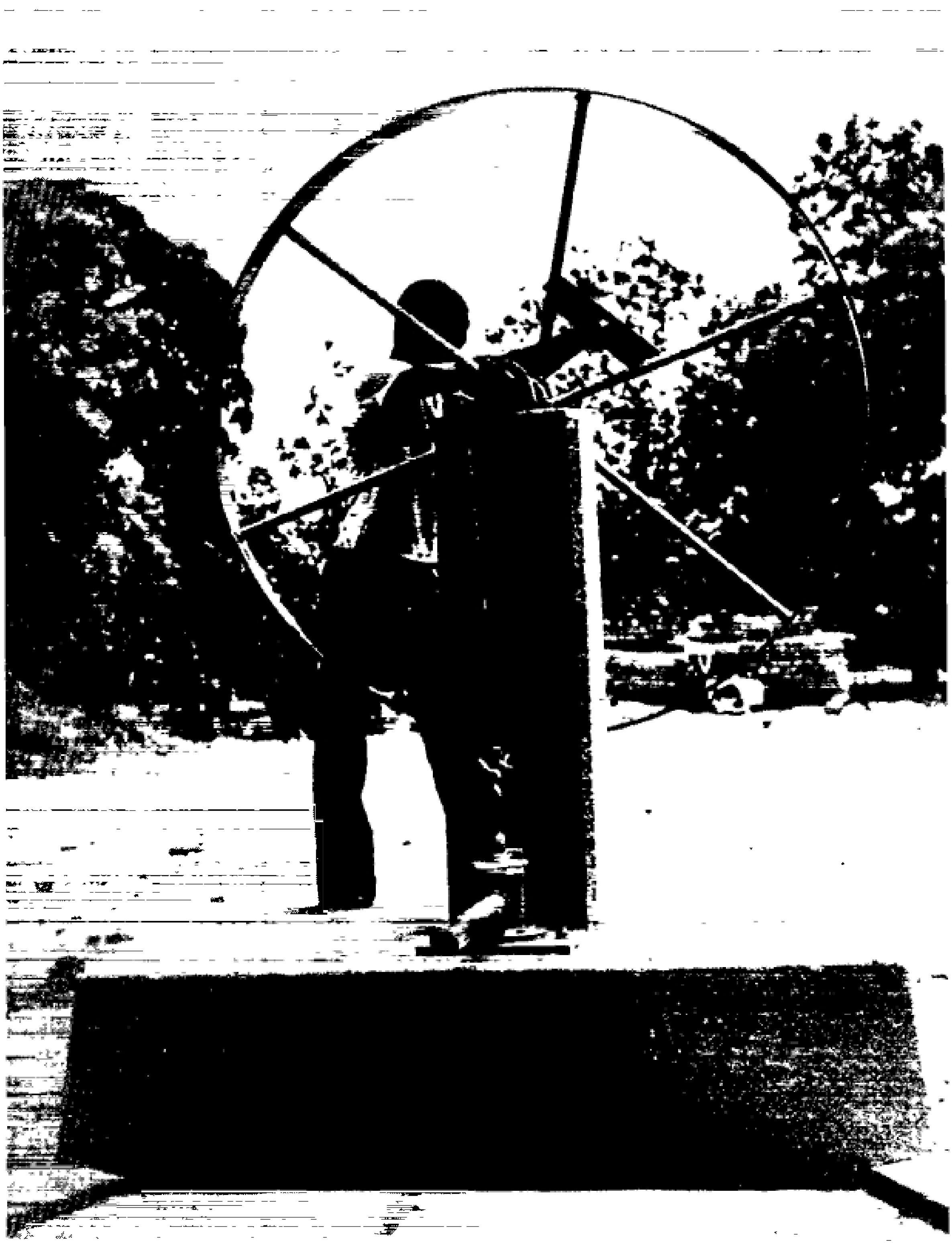

7 CONCLUSIONS

a. **Principal differences exist between piston pumps with stiff and with elastic rising mains:**
- The elasticity of the rising main induces axial displacements of the cylinder that result in reduced discharges and (considerably) lower volumetric efficiencies;
- The elastic rising main has an important effect on the dynamic behaviour of the deepwell handpump. Resonances of pressure waves occur already at much lower pumping frequencies (due to much lower propagation speeds of pressure waves in the elastic rising main);
- During the pump cycle the axial load in the pump is gradually transferred from the rising main to the pump rod, and vice versa;
- Valve dynamics have no significant influence on the pump behaviour and efficiency once (axial) elastic elements form part of the pump substructure.

b. **For low pumping frequencies the stress[41] and strain fluctuations in the rising main and the pump rod can be accurately predicted by quasi-static approximations. Only at frequencies of more than half the resonance frequency[42] dynamic effects will become important:**

- The axial load on the rising main is at a maximum at the top end. The total load is at its maximum in the immersed part of the riser, mainly because of the tangential load;
- The load fluctuation amplitude on the rising main is at a maximum at the extreme ends: at the top end due to axial stress and bending stress fluctuations; at the bottom end due to axial, tangential and bending stress fluctuations;
- Misalignments in the rod and riser and the joints may increase bending stress *fluctuations*. Friction in the rod hanger bearing may induce high bending stress fluctuations in the rod as well;
- When axial compressive stresses occur in the rising main of deepwell handpumps, buckling will develop. This can hardly be prevented by means of retaining facilities for the rising main. Preventing these axial compressive stresses themselves is a better remedy (piston diameter smaller than riser inside diameter). Buckling of the riser is limited by the presence of the pump rod, so that bending stress fluctuations because of buckling will not reach yield stresses;
- For long rising mains axial creep of the riser has to be taken into account. In fact this is true for all long-term loaded plastic parts;

c. **The pump yield (volumetric efficiency) is directly influenced by the elasticity of the rising main:**
- Mainly the axial strain in the (elastic) rising main is responsible for the loss of effective (relative) piston stroke length, and thus for low volumetric efficiencies. This efficiency can be predicted by quasi-static approximations;
- Increasing the riser wall thickness and/or the gross stroke length will improve the volumetric efficiency. Careful dimensioning of the piston diameter, while taking account of the riser length, may further raise the output of the pump; selecting a smaller piston diameter always results in a higher volumetric efficiency;
- Cylinder support is effective as a means of increasing the volumetric efficiency, but at the expense of considerably increased bending stresses in the bottom part of the rising main.

---

41 this excludes bending stress fluctuations

42 This resonance frequency can be simply calculated

d. **The dynamic effects are mainly due to interfering pressure waves in the PVC rising main. These pressure fluctuations develop during the whole pump cycle and result from accelerations forced on to the water column by piston and cylinder movements:**
   - The resonance frequency of the water column (i.e. the pressure waves) can be predicted; the amplitude (at the current state of the art) cannot;
   - Dynamic effects occurring as resonances may cause failure of pump components;
   - Valves have no significant influence.

e. **The measurements have indicated that bending stress fluctuations may occur that exceed the axial stress fluctuations. Most of these stresses can be prevented (or at least limited) by relatively simple design adaptations.**

f. **Fatigue is probably the main cause for early fracturing of pump rods and rising mains.**
   - Fatigue may be caused by fluctuating loads and corrosion;
   - The safe fatigue design stress fluctuations are much lower than was expected. Reasons for this are the occurrence of high stress concentrations at abrupt changes of shape (joints), and the sensitivity of the materials for notches and glue. The quantitative aspects of the stress concentrations and the effects of notches and glue on fatigue in PVC are not clear, however.

g. **The physical models that have been developed during the project give a good qualitative agreement with the measured data. This means that now the dynamics of the piston pump with an elastic (PVC) rising main are largely understood.**
   - The models have a reasonable quantitative prediction value, but the results of the calculation very much depend on the damping factor, which has to be chosen to fit the results. Predicting this damping factor requires fundamental research;
   - Also 'snaking' has not been fully clarified, but is probably caused by buckling.

h. **It is expected that design optimizations that can be derived from this publication, will help making handpumps with PVC rising mains more lasting and reliable under field conditions.**

8 RECOMMENDATIONS AND DESIGN RULES[43]

a. Fatigue is the limiting factor for the lifetime of the PVC rising main. Therefore the (combined) stress fluctuations must be limited, as must the factors that reinforce fatigue such as the effects of glue, of cut thread and of fine scratches, to which PVC is very sensitive.
   - For PVC the combined stress amplitude[44] must not exceed 2.5 N/mm^2 (calculated for the full section); aggressive glue (e.g. containing THFs) is detrimental!
   - For threaded stainless steel the safe fatigue stress amplitude is about 50 N/mm^2 (calculated for the full section). As fatigue is probably also the limiting factor for the lifetime of the stainless steel pump rods, it is important to limit fluctuating stresses and to be aware of fatigue enhancing factors, such as welding of rods. Rolled thread provides better resistance against fatigue than cut thread.

b. Extra friction in the pump rod hanger bearing increases bending stresses and therefore may lead to fatigue fracture in the top end of the rod.
   Reducing the bearing friction (greasing, adjusting play) or strengthening the pump rod top end may be necessary.

c. The riser and pump rod should be straight and joints should be in line (screw threads). Otherwise fluctuating axial stresses will induce bending stress fluctuations, which are probably maximal in the relatively weak joints.

d. When driving the pump mechanically, be aware of the possible occurrence of pressure wave resonances. Pumping at or near the resonance frequency(ies) may drastically shorten the lifetime of the PVC rising main and the stainless steel pump rod.

e. The valve weight and valve lift are not critical for piston pumps with PVC risers, so use (commercially available) standard valves.

f. Centralizers for the riser effectively minimize the bending stress fluctuations in the rising main that are caused by swinging and snaking.

g. Buckling will occur in the riser when compressive stresses occur. This is generally the case when the piston diameter is larger than the internal diameter of the rising main. As centralizers will not prevent buckling, the only remedy may be to reduce the diameter of the piston in relation to the inside diameter of the riser.

h. Normally the axial displacement of the cylinder during pumping, caused by the strain of the riser, reduces the volumetric efficiency, sometimes dramatically, especially for pumps with long risers. Reducing the piston diameter also reduces the axial cylinder displacement. This results in increased volumetric efficiencies and for PVC risers longer than about 50 metres sometimes even in increased net output per stroke.

   A smaller diameter piston also reduces the axial stress fluctuation in riser and pump rod, and so limits the danger of fatigue.
   Increasing the gross stroke length boosts the volumetric efficiency more than proportionally.

---

[43] As endurance testing was not a part of the IAD Handpump Project, the recommendations could not be tested for their long-term consequences. The authors/project team therefore do not accept any responsibility, direct or implied, for the consequences of following these recommendations.

[44] i.e. half the stress fluctuation magnitude

i. Cylinder support clearly improves the volumetric efficiency of a pump, but at the expense of considerably increased bending stresses in the lower end of the rising main. Axial stress fluctuations are hardly affected.

j. The PVC rising main will continue to stretch under the load of its own weight and the water pressure. This so-called 'creep' is a function of the stress in the material and the temperature, as well as time. For deepwell handpumps a creep of 0.5% after 10 years must be counted with (i.e. not less than 400 mm in case of a 80 m long rising main!).

k. The manner of driving the pump (by hand or mechanically, with a handle or a flywheel) hardly influences the stress and pressure fluctuations in the pump. Both the pumping frequency and the gross pump stroke length are far more important. (The mechanical efficiency of a handpump with flywheel is expected to be greater than in the case without flywheel, however. See Appendix III.3)

REFERENCES

Arlosoroff, S., Tschannerl, G., Grey, D., Journey, W., Karp, A. Langenegger, O. and Roche, R. (1987), *Community Water Supply: The Handpump Option.* The World Bank, Washington, USA.

Beekman, P. and de Jongh, J. (1989), *Design rules for fatigue life of PVC rising mains and stainless steel pump rods of hand pumps.* Report R993D, Wind Energy Group, Laboratory of Fluid Dynamics and Heat Transfer, Faculty of Physics, Eindhoven University of Technology, The Netherlands, IADHPP89.03.

Besselink, J. (1989), *Measuring Program IAD.* Arnhem, The Netherlands, InterAction Design, IADHPP89.01.

Besselink, J. (1989), *Second interim report Volanta measuring program.* Arnhem, The Netherlands, InterAction Design, IADHPP89.05.

Forrest, P.G. (1962), *Fatigue of metals.* Pergamon

Fuchs, H. and Stephens, R. (1980), *Metal fatigue in engineering.* John Wiley & Sons, New York, USA.

Grupa, J. (1989), *The dynamical behaviour of man driven piston lift pumps.* Report R991D, Wind Energy Group, Laboratory of Fluid Dynamics and Heat Transfer, Faculty of Physics, Eindhoven University of Technology, The Netherlands, IADHPP89.02.

Grupa, J. (1989), *Fatigue of the pump rod and the rising main of the Volanta handpump.* Wind Energy Group, Laboratory of Fluid Dynamics and Heat Transfer, Faculty of Physics, Eindhoven University of Technology, The Netherlands, IADHPP89.06.

Holzmann, G., Dreyer, H. and Faiss, H. (1975), *Technische Mechanik.* B.G. Teubener, Stuttgart, Germany.

IRC (1988), *Handpumps, Issues and concepts in rural water supply programmes.* Technical Paper No. 25, IRC, International Water and Sanitation Centre, The Hague, The Netherlands.

Lewis, P.R. (1989), *Investigation into the Fatigue Life expected from u-PVC rising mains used in Handpumps for the Developing World.* Overseas Development Administration, London, UK.

Peterson, R.E. (1977), *Stress Concentration Factors.* John Wiley & Sons, New York, USA.

Schuchmann, B., Bonnier, C.J. and Besselink, J. (1989), *Towards an understanding of the dynamic behaviour of the below ground level parts of two handpumps with a PVC riser*, World Water, April 1989.

APPENDIX I

APPENDIX I.1 LIST OF PARAMETERS USED

Parameter	Explanation	Dimension
a	propagation speed	m/s
A	cross section	m^2
D	diameter	m
e	wall thickness	m
E	Young's elasticity modulus	N/m^2
f	frequency	Hz (= 1/s)
F	force	N
g	gravitational acceleration	m/s^2
K_f	strength reduction factor	-
K_t	stress concentration factor	-
L	length (of rising main/pump rod)	m
ΔL	elongation (of rising main/pump rod)	m
m	mass	kg
N	number of cycles	-
p	pressure	Pa (= N/m^2)
q	notch sensitivity	-
r	radius	m
S	stroke length	m
S_a	stress fluctuation amplitude	N/m^2
μ	transverse contraction ratio (Poisson's ratio)	-
ω	angular velocity	rad/s
η	efficiency	-
ρ	density	kg/m^3
λ	slenderness ratio	-
σ	stress	Pa (=N/m^2)
Δ	fluctuation	-

MISCELLANEOUS DATA:

gravitational acceleration:		$g \approx 9.8\ m/s^2$
gravity force on body with mass of 1 kg:		$F_g = m.g \approx 9.8$ Newton
Young's elasticity moduli:	PVC:	$E_{PVC} \approx 2.5 - 3$ GPa
	stainless steel:	$E_{ss} \approx 200$ GPa
Mass densities:	water:	$\rho_{water} = 1000\ kg/m^3$
	PVC:	$\rho_{PVC} = 1380\ kg/m^3$
	stainless steel:	$\rho_{ss} = 7800\ kg/m^3$

APPENDIX I.2 INDICES

a	amplitude
ax	axial
b	bottom
cyl	cylinder
div	diverse
eff	effective
gross	gross
i	inner
loc	local
m	mean
max	maximum
nom	nominal
pis	piston
pr	pump rod
rad	radial
ref de	reference, deformation energy hypothesis
ref Mo	reference, Mohr's theory
rel	relative
res	resonance
rm	rising main
stat	static
u	outer
vol	volumetric

APPENDIX I.3 ABBREVIATIONS AND ACRONYMS

ABS	acrylonitryl butadiene styrene
ADTR	axial displacement of top of pump rod
BDC	bottom dead centre (lowest piston position)
DHV	DHV Consultants
DPO/OT	Section for Research and Technology, Ministry of Development Cooperation, The Hague, The Netherlands
HDPE	high-density poly ethylene
IAD	InterAction Design
IADHPP	InterAction Design Handpump Project
JVI	Jansen Venneboer International B.V.
PVC	poly vinyl chloride
SWN	Sociale Werkplaats Nunspeet
SWNV	Sociaal Werkvoorzieningsschap Noordwest-Veluwe
TDC	top dead centre (topmost piston position)
uPVC	unplasticized poly vinyl chloride
UV	ultra violet
WEG/EUT	Wind Energy Group, Eindhoven University of Technology

APPENDIX I.4 GLOSSARY

Bottom dead centre (BDC)	The lowest piston position.
Buckling	Collapsing under an excessive (or eccentric) axial load while bending laterally.
Creep	Continuing strain in a material with time under (continuous or fluctuating) load (influenced by the ambient temperature).
Cylinder displacement	The absolute axial displacement of the cylinder.
Fatigue	The effect that a material fails under a considerable lower stress when loaded in a cyclic manner than under a continuous static load.
Fatigue strength	The maximum stress fluctuation a material (or component) can withstand during a given number of stress cycles.
Fatigue strength reduction factor	The quotient of the fatigue strength of a notched specimen and the fatigue strength of an un-notched specimen.
Fluttering	Pumping with short, quick strokes (at about half the resonance frequency).
Gross pump cycle	The cycle as induced by the crank/lever. Referred to as a crank angle rotation of 360 degrees.
Gross pump stroke	The maximum axial displacement of the top end of the pump rod as induced by the crank drive or lever/handle.
Mean stress	Time average of stress: $(\sigma_{max} + \sigma_{min})/2$
Net pump cycle	The pump cycle based upon the effective piston displacement relative to the cylinder.
Notch sensitivity	Parameter defining the relation between the stress concentration factor and the fatigue strength reduction factor.
Piston displacement	The absolute axial piston displacement: equals the axial displacement of the top of the rod (ADTR) reduced by the fluctuating elongation of the pump rod itself.
Quasi-static	Situation in dynamic systems where the effect of inertia may be neglected (generally at low frequencies).
Relative piston stroke	The maximum relative piston displacement during a pump cycle; equals the gross pump stroke reduced by the maximum elongation of the rising main and the pump rod during a pump cycle.
Relative piston displacement	The displacement of the piston relative to the (moving) cylinder.
Snaking	Undulating, possibly because of travelling transverse waves.
Static pressure	Water pressure in the cylinder at rest.
Stress range	Difference between maximum and minimum stress: $\sigma_{max} - \sigma_{min}$.
Stress ratio	Quotient of maximum and minimum stresses: $R = \sigma_{max}/\sigma_{min}$.
Stress amplitude	Half of the stress range: $\sigma_a = (\sigma_{max} - \sigma_{min})/2$
Stress concentration factor	Quotient of maximum local stress and nominal stress.
Swinging	Movement of the riser comparable to that of a pendulum.
Top dead centre (TDC)	The highest piston position.
Transverse contraction	The phenomenon that the cross section of a material will decrease under tensile axial stress.

APPENDIX II

APPENDIX II DETAILS OF EXPERIMENTAL PROGRAMME

II.1 EXPERIMENTAL SET-UP

At the premises of one of the partners in the IAD Handpump Project[1] tests have been carried out on SWN 81 and Volanta handpumps, and on a hybrid in which the SWN 81 superstructure was joined to the below-ground part of the Volanta.
The pumps were installed on a 100 metres deep tubewell with watertight lining and bottom, and with an inner diameter of 170 mm, in which the water level could be varied at will. This allowed testing of the pumps with lifts varying between 20 and 96 metres. The water that was pumped from the well was circulated back into it.

During testing the pumps were driven either by hand or mechanically. A mechanical drive was attached to the pump handle by a connecting rod. The Volanta was driven by means of a leather belt around the flywheel. The speed of the mechanical drive could be adjusted, allowing a pumping frequency to be selected between 0.4 and 2.0 Hz[2].

II.2 MEASURING PROGRAMME

The measuring programme covered the following:

a. SWN 81:
- hand-driven and mechanically driven
- riser lengths of 21, 39, 60, 81 and 96 m
- with and without flexible rod hanger ('swivel')
- with and without flexible riser hanger
- with and without superstructure out of plumb
- with and without centralizers and/or cylinder support (for 96 m riser length only)
- with different immersion depths (20, 10, 5, 2 and 0 m)

The results and insight obtained during the SWN 81 testing programme allowed a drastic reduction of the number of tests in the (subsequent) Volanta testing programme:

b. Volanta:
- hand-driven and mechanically driven
- 78 m riser length only
- standard flywheel (1.5 m diameter) and smaller flywheel (0.75 m diameter)
- also tested with pump-handle drive
- with and without reduced piston valve lift
- with and without reduced piston valve weight

c. Hybrid:
- hand-driven and mechanically driven
- 78 m riser length only
- with and without swivel

All combinations were tested at stepwise increased frequencies, from 0.6 Hz to 1.6 Hz and 2.0 Hz (the last option for reduced heads only).

---

1 Sociaal Werkvoorzieningsschap Noordwest-Veluwe, Industrieweg 47, 8071 CS Nunspeet, The Netherlands

2 (= strokes per second)

The effects tested are summarized in Table II.1:

Table II.1 Summary of effects tested[3]

Effects measured	SWN 81	Volanta	Hybrid
- centralizers for rising main	96 m	-	-
- cylinder support	96 m	-	-
- flexible riser fixing	20/40/60/80/96 m	-	-
- stand out of plumb	20/40/60/80/96 m	-	-
- swivel	20/40/60/80/96 m	-	78 m
- mechanical and hand drive	20/40/60/80/96 m	78 m	78 m
- flywheel of 1.5 m and 0.75 m diam.	-	78 m	-
- flywheel and pump handle	-	78 m	-
- immersion depth	20/40/60/80/96 m	-	-
- piston valve weight	-	78 m	-
- piston valve lift	-	78 m	-

II.3 MEASURING EQUIPMENT

Object	Equipment used
crank angle	digital absolute encoder + DA-converter
strain	strain gauges + analog conditioner
pressure	absolute pressure transducer + built-in analog conditioner
axial displacements	strain gauges + analog conditioner
valve displacements	magnetic field sensor + bar magnet in valve + analog conditioner
water delivery	water pumped during a given number of pump strokes was measured using household scales

The absolute strain was always measured simultaneously by 4 strain gauges, glued at 90° intervals around the circular section of the riser and rod, permitting both the axial stress and bending stress to be calculated. To compensate for contraction caused by pressure fluctuations inside the riser,

[3] The table indicate the riser length(s) for which the relevant effect was studied

tangentially placed strain gauges were added to the axially placed gauges at the bottom end of the rising main.

The analog conditioners were based upon the Analog Devices AD 693 chip, giving a current that is directly proportional to the signal, of 4 - 20 mA (current loop principle), and not influenced by fluctuations in the power supply (voltage), temperature or length of the measuring cables.

The analog signals were multiplexed and digitized with a Lab Master board, controlled by the data acquisition and processing software package ASYSTANT+ (at a maximum of 16 signals simultaneously).
The project used two AT-compatible computers with mathematical co-processors and hard disks.

II.4 MEASURED AND DERIVED PARAMETERS

Parameters measured as a function of time:

- crank angle
- axial strain near top end of riser and pump rod
- axial and tangential strain near bottom end of riser
- axial strain at about 12 m and 13.5 m above the bottom end of the riser (SWN 81 only)
- pressure inside the cylinder and above the piston
- axial displacement of the piston relative to the cylinder position
- axial displacement of the cylinder
- displacement of the valves
- water delivery

Parameters that were either derived mathematically or determined by means of the ASYSTANT+ package:

- angular velocity and acceleration of the crank
- axial, tangential and bending stresses in the rising main (top and bottom)
- axial and bending stresses in the top of the pump rod
- valve opening and closing angles and delays
- axial displacements of piston and cylinder, and volumetric efficiency
- mechanical efficiency
- pressure waves and resonances
- 'snaking'
- buckling of the rising main
- (predictions for the) fatigue lifetime of the pump rod and riser

Figure II.1 shows the experimental set-up, for the SWN 81 handpump, with the locations of the various transducers.

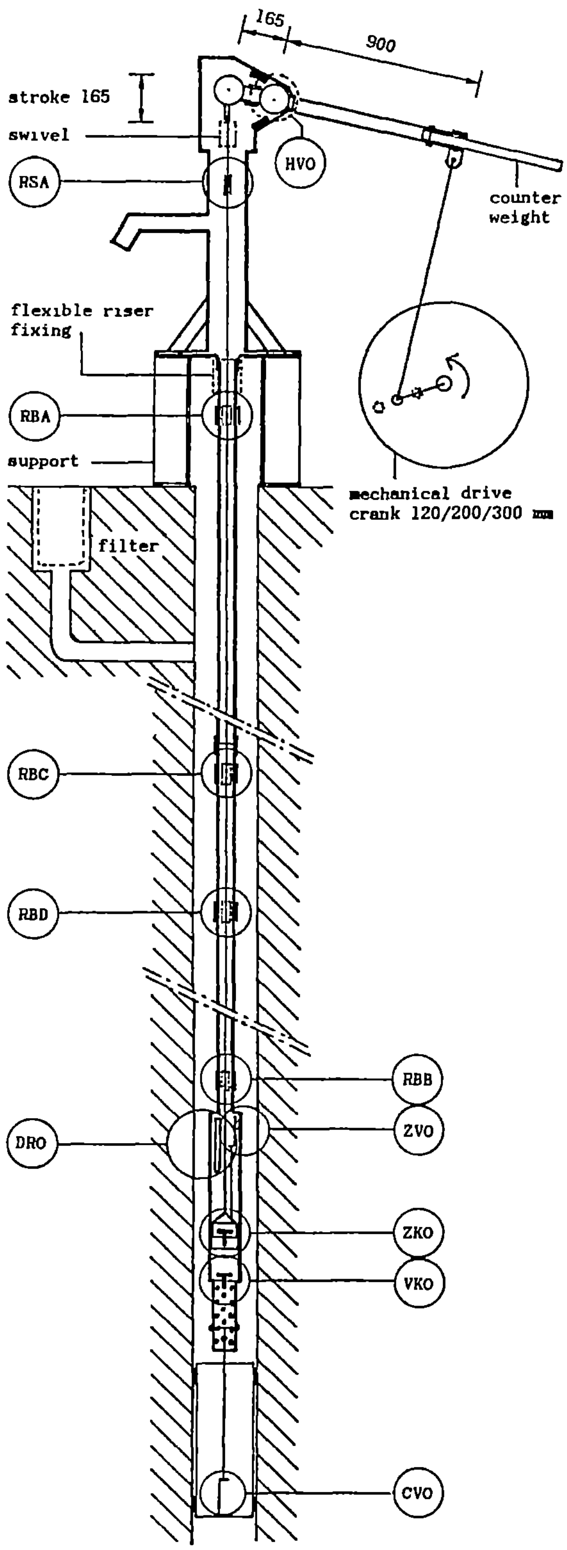

Figure II.1 Experimental set-up for SWN 81 handpump

RBA	strain gauges in axial direction, glued to outside of riser, 0.25 m from the upper end
RBB	4 strain gauges in axial direction + 1 in tangential direction, glued to outside of riser at 0.2 m from the lower end
RBC	strain gauges in axial direction, glued to outside of riser, 0 3 m below riser coupling
RBD	strain gauges in axial direction, glued to outside of riser, 1.3 m below the RBC group, halfway on riser section
RSA	strain gauges in axial direction, glued to pumprod, at 0.2 m below the pumprod bearing
ZKO	magnetic field sensor, centrally under the piston valve, reacting to the displacement (both axially and radially) of a bar magnet in the foot valve
VKO	as ZKO, centrally under the foot valve
ZVO	strain gauge assembly fitted in the cylinder, above the piston, to measure the relative piston displacement
CVO	as ZVO, but located in a PVC tube under the cylinder, to measure axial displacement of the pump cylinder
DRO	absolute pressure transducer, placed in the cylinder, above the piston
HVO	digital absolute encoder, connected to pump handle

APPENDIX III

APPENDIX III BACKGROUND MATERIAL/FORMULAS

III.1 CALCULATION OF STATIC AND QUASI-STATIC STRESSES AND DEFORMATIONS IN THE RISING MAIN AND PUMP ROD

Pump at rest:

The *axial strain* in the rising main, caused by the static load is:

$$\Delta L_{rm} = \frac{L_{rm} \cdot F_{stat}}{E_{rm} \cdot A_{rm}} = \frac{L_{rm} \cdot (F_{int} + F_{ext} + G_{rm} + G_{div})}{E_{rm} \cdot A_{rm}} \qquad \text{(III.1)}$$

in which:

L_{rm}	=	length of rising main [m]
E_{rm}	=	elasticity modulus of rising main material [Pa]
F_{stat}	=	total static axial load at top of the rising main [N]
F_{int}	=	resultant axial force of water pressure inside the pump
	=	$\pi/4 \cdot p \cdot D_{i\,rm}^2$ [N]
F_{ext}	=	upward force by the water in the well
	=	resultant axial force of water pressure outside the pump
	=	$-\pi/4 \cdot p_u \cdot D_{u\,rm}^2$ [N]
G_{rm}	=	weight of the rising main = $L_{rm} \cdot A_{rm} \cdot \rho_{rm} \cdot g$ [N]
A_{rm}	=	cross section of rising main = $\pi/4\,(D_{u\,rm}^2 - D_{i\,rm}^2)$ [m^2]
ρ_{rm}	=	density of rising main material [kg/m^3]
g	=	gravitational acceleration ($\approx$ 10 m/s^2)
G_{div}	=	weight of cylinder, riser centralizers, etc. [N]

The static axial stress in the rising main, as a function of the distance x from its suspension point (which is approximately the same as the outflow level of the water), is:

$$\sigma_{ax\,rm}(x) = \frac{F_{stat}(x)}{A_{rm}} = \frac{F_{stat} - x \cdot A_{rm} \cdot \rho_{rm} \cdot g}{A_{rm}} \qquad \text{(III.2)}$$

in which F_{stat} (x) = static axial load in the rising main at position x
= total static load minus weight of riser part above position x

During pumping:

The *axial stress* in the pump rod and rising main, without taking inertia effects into account, is:

$$\sigma_{ax\,pr} = \frac{p \cdot (D_{pis}^2 - D_{pr}^2) - p_b \cdot D_{pis}^2}{D_{pr}^2} \qquad \text{(III.3)}$$

$$\sigma_{ax\,rm} = \frac{p_b \cdot D_{pis}^2 - p \cdot (D_{pis}^2 - D_{i\,rm}^2)}{D_{u\,rm}^2 - D_{i\,rm}^2} \tag{III.4}$$

in which

p = the pressure above the piston
= static pressure at low pumping frequencies

p_b = pressure under the piston, above the cylinder bottom, varying between p and p_u.

The radial and tangential stresses in a thick walled pipe are given by:

$$\sigma_{rad\,rm}(x,D) = \frac{p(x) \cdot D_{i\,rm}^2}{D_{u\,rm}^2 - D_{i\,rm}^2}\left(1 - \frac{D_{u\,rm}^2}{D^2}\right) - \frac{p_u(x) \cdot D_{u\,rm}^2}{D_{u\,rm}^2 - D_{i\,rm}^2}\left(1 - \frac{D_{i\,rm}^2}{D^2}\right) \tag{III.5}$$

The first part of (III.5) is zero for $D = D_{u\,rm}$, the second part is zero for $D = D_{i\,rm}$.

$$\sigma_{tang\,rm}(x,D) = \frac{p(x) \cdot D_{i\,rm}^2}{D_{u\,rm}^2 - D_{i\,rm}^2}\left(1 + \frac{D_{u\,rm}^2}{D^2}\right) - \frac{p_u(x) \cdot D_{u\,rm}^2}{D_{u\,rm}^2 - D_{i\,rm}^2}\left(1 + \frac{D_{i\,rm}^2}{D^2}\right) \tag{III.6}$$

in which:

p(x)	=	$10^4\,x$	when pumping at very low speed [Pa]
$p_u(x)$	=	0	(for $x < h$)
	=	$10^4\,(x - h)$	(for $x \geq h$) (under same conditions) [Pa]
x	=	distance from the top end of the pump rod (≈ from pump spout); $0 < x < L_{rm}$ [m]	
h	=	pump head [m wc]	

For $D = D_{u\,rm}$ and $p_u = 0$ (above water level in the well) the tangential stress becomes:

$$\sigma_{tang\,rm}(x, D_{u\,rm}) = \frac{2p(x) \cdot D_{i\,rm}^2}{D_{u\,rm}^2 - D_{i\,rm}^2} \tag{III.7}$$

The tangential stress in the immersed part of the rising main is constant and about equal to the value just above the water (quasi-static!). Figure 4.1 shows the static stresses in the rising main, as a function of the riser length, calculated with equations (III.2), (III.5) and (III.6).

Even when p fluctuates eq. (III.3) through (III.7) still hold, but all stresses and the pressure will be a function of time.

III.2 DISCHARGE AND VOLUMETRIC EFFICIENCY

The discharge depends mainly on the effective piston stroke (the piston stroke relative to the cylinder, as explained in section 4.5). The discharge equals the effective (relative) piston stroke length multiplied by the piston cross section.

The relative piston stroke length can be found by deducting the strain in the rising main and pump rod from the gross pump stroke. Equations (III.8) and (III.9) give the strain in the rising main and the pump rod as a function of the pressure above and below the piston. In the quasi-static situation the pressure above the piston will not change. Therefore when calculating the maximum strain *differences* in the riser and pump rod only that part of equations (III.3) and (III.4) that relate to the changing p_b (between p and p_b) has to be taken into account.

$$\Delta L_{rm}(\Delta p_b) = \frac{L_{rm} \cdot \Delta p_b \cdot D^2_{pis}}{E_{rm} \cdot (D^2_{urm} - D^2_{irm})} = \frac{L_{rm} \cdot (p - p_u) \cdot D^2_{pis}}{E_{rm} \cdot (D^2_{urm} - D^2_{irm})} \qquad \text{(III.8)}$$

Similarly:

$$\Delta L_{pr}(\Delta p_b) = \frac{L_{pr} \cdot (p - p_u) \cdot D^2_{pis}}{E_{pr} \cdot D^2_{pr}} \qquad \text{(III.9)}$$

The volumetric efficiency thus becomes:

$$\eta_{vol} = \frac{S_{gross} - (\Delta L_{rm} + \Delta L_{pr})}{S_{gross}} = 1 - \frac{\Delta L_{rm} + \Delta L_{pr}}{S_{gross}} \qquad \text{(III.10)}$$

The discharge per pump cycle will be:

$$q = (S_{gross} - (\Delta L_{rm} + \Delta L_{pr})) \cdot \frac{\pi}{4} \cdot D^2_{pis} \qquad \text{(III.11)}$$

Note: This simplification is permissible only for low pumping frequencies, where $p \approx p_{star}$

III.3 MECHANICAL EFFICIENCY

The mechanical efficiency decreases due to mechanical losses, such as:
- friction in the bearings,
- friction between the piston seal and the cylinder,
- friction between the rod (guides) and the cylinder, and
- hydraulic losses.

These losses are difficult to calculate and vary to a large extent, depending on the type of pump. But even without taking these losses into account, some important conclusions can be drawn in relation to the mechanical efficiency and the axial elasticity of the substructure of the deepwell piston pump.

The axial elasticity of the substructure of the pump (i.e. the difference between the gross pump stroke and the effective piston stroke) will reduce the mechanical efficiency. Friction between the piston seal and the cylinder will further reduce the effective piston stroke.

In this section only the effects of the axial elasticity will be taken into account.

While pumping during the upward piston stroke the force required is:

$$F = p_{lift} \cdot A_{pis} \qquad \text{(III.12)}$$

where p_{lift} = pumping head = $p_{stat} - p_{submerged}$

The energy represented by the water pumped during the upward stroke is:

$$E = F \,.\, S_{rel} = p_{lift} \cdot A_{pis} \,.\, S_{rel} \qquad \text{(III.13)}$$

Before water is pumped, a load transfer takes place from the riser towards the pump rod, during the first part of the upward piston stroke. During this load transfer, F increases from F = 0 (at the beginning of the upward piston stroke) to $F = p_{lift} \cdot A_{pis}$

Meanwhile, the riser is shortened by ΔL_{rm} and the pump rod stretched by ΔL_{pr}. (see Sections 4.3 and 4.4)

$$\Delta L = \Delta L_{rm} + \Delta L_{pr} = S_{gross} - S_{rel}$$

ΔL may be further increased (i.e. the relative piston displacement reduced) by friction between the piston seal and the cylinder and by buckling. Both effects increase with larger pumping heads.

Hence the energy required to realize the load transfer equals:

$$E \approx \tfrac{1}{2} F \,.\, \Delta L = \tfrac{1}{2}\, p_{lift} \cdot A_{pis} \,.\, \Delta L \qquad \text{(III.14)}$$

When pumping with a handle or a flywheel driven deepwell pump, this load transfer is felt like loading a spring.
During the beginning of the downward piston stroke the 'unloading of the spring' can be felt: thus the energy of the spring is released again. With a flywheel drive this helps to accelerate the pump drive after passing the TDC (top dead centre) of the crank. It may help to increase the mechanical efficiency.

With a handle drive it also helps to lift the handle. However, if the handle 'bounces' up (i.e. if the counterweight is too light), it may cost extra energy to slow down the handle (to dissipate the energy of the unloading spring!) to prevent injury. This in fact decreases the mechanical efficiency!

The total energy required during the upward piston stroke (for a handle driven pump) thus amounts to:

$$E_{tot} = p_{lift} \cdot A_{pis} \left(S_{rel} + \tfrac{1}{2}\,\Delta L\right) \qquad \text{(III.15)}$$

Hence the mechanical efficiency is as follows:

$$\eta_{mech} = \frac{S_{rel}}{S_{rel} + \frac{\Delta L}{2}} = 1 - \frac{\Delta L/2}{S_{gross} - \frac{\Delta L}{2}} = 1 - \frac{\Delta L}{2S_{gross} - \Delta L} = 1 - \frac{\frac{\Delta L}{S_{gross}}}{2 - \frac{\Delta L}{S_{gross}}} \qquad \text{(III.16)}$$

Compare with the volumetric efficiency:

$$\eta_{vol} = 1 - \frac{\Delta L}{S_{gross}} \qquad \text{(III.10)}$$

The volumetric and mechanical pump efficiencies are shown in Figure III.1, as function of the ratio $\Delta L/S_{gross}$. Friction losses have not been taken into account.

As Figure III.1 shows, a flywheel-driven deepwell pump will have a mechanical efficiency close to 100%, independent of the axial elasticity of the substructure of the pump (for $\Delta L < S_{gross}$). A handle-driven pump will have a mechanical efficiency closer to the curved line, strongly depending on the axial elasticity of the substructure and the effect of the counterweight.

However, for both types the volumetric efficiency decreases with increasing elasticity.

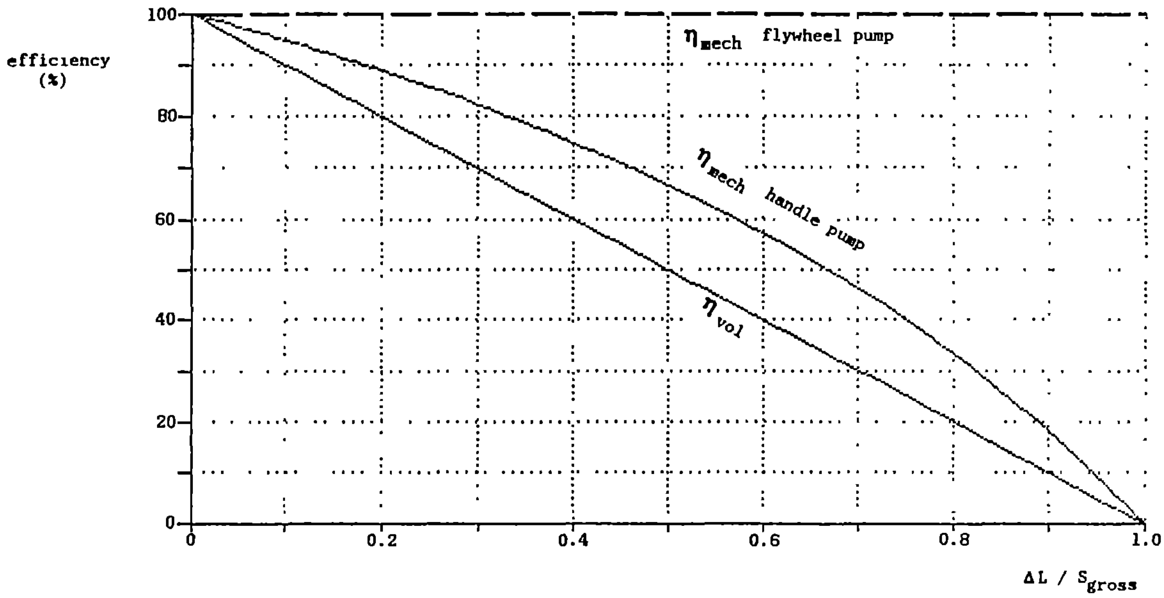

Figure III.1 Volumetric and mechanical pump efficiency, neglecting friction losses

III.4 BUCKLING

The critical buckling stress can be found with Euler's column formula:

$$\sigma_{crit} = \frac{n \cdot \pi^2 \cdot E}{\lambda^2} \tag{III.17}$$

in which

n = coefficient that counts for the fixation conditions of the particular rising main part:
- = 1 if pivoted at both ends
- = 2 if pivoted at one end
- = 4 if fixed at both ends

λ = l/i = slenderness ratio

l = unsupported length of the rising main part that can bend (see Figure III.2)

i = least radius of gyration

$= \sqrt{I_{min}/A}$ or: $1/4\sqrt{D_{urm}^2 + D_{irm}^2}$ for the rising main

I_{min} = moment of inertia = $\pi/64 \cdot (D_{u\,rm}^4 - D_{i\,rm}^4)$ for the rising main

A = A_{rm} = cross section = $\pi/4 \cdot (D_{u\,rm}^2 - D_{i\,rm}^2)$ for the rising main

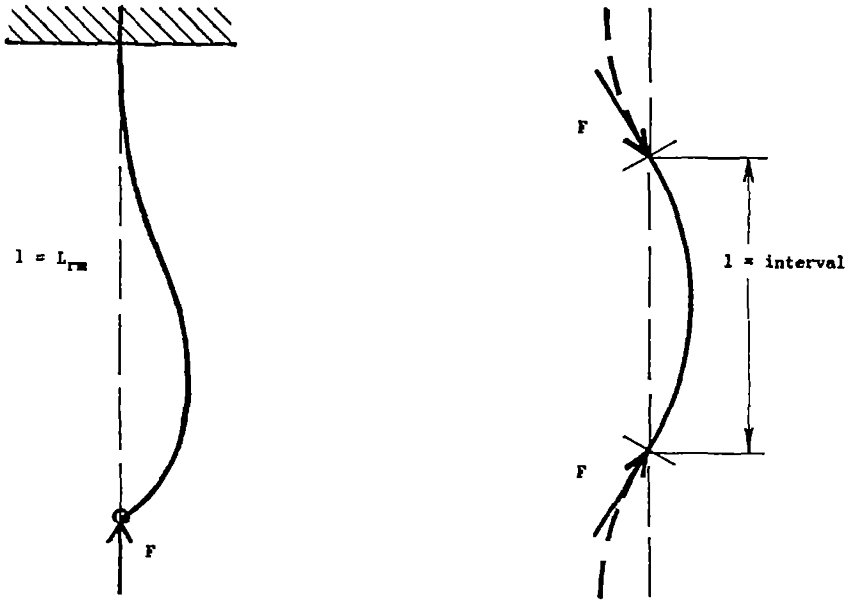

Figure III.2 Buckling in the rising main

When the compressive axial stress exceeds the critical buckling stress, buckling will occur. Taking as unsupported length the entire riser length L_{rm} and taking n = 2 (fixed suspension at one end, viz. the top end), shows that the PVC riser will buckle as soon as compressive stresses occur.

With provisions such as riser centralizers or pump rod guides retaining the rising main at regular intervals, the unsupported length equals such interval. In that case the value 1 should be substituted for n (no fixed suspension).

The experiments have shown that even with these provisions buckling may occur for rising mains with a length of 20 metres and more.

For calculating buckling of the pump rod equation (III.17) can be used as well. In this case, however, for l the length of the pump rod, L_{pr}, should be taken or the interval between two rod guides where applicable. For the pump rod n = 1 and $I_{min} = \pi/64 \cdot D_{pr}^4$.

III.5 PROPAGATION SPEED

The propagation speed *a* can be calculated as follows:

$$a = \sqrt{\frac{\frac{K}{\rho}}{1 + \frac{A_{irm}}{A_{irm} - A_{pr}} \cdot \frac{K}{E} \cdot \frac{D}{e} \cdot c_1}} \tag{III.18}$$

where:

a	=	propagation speed [m/s]
K	=	bulk modulus of elasticity of water (= 2.2 10^9 N/m^2)
ρ	=	density of water (= 1000 kg/m^3)
$A_{i\,rm}$	=	internal cross section of the rising main [m^2]
A_{pr}	=	cross section of pump rod including coating [m^2]
E	=	Young's elasticity modulus of the rising main material; for PVC: E ≈ 2.5 10^9 N/m^2
D	=	internal diameter of rising main [m]
e	=	wall thickness of the rising main [m]

and

$$c_1 = \frac{2e}{D}(1 + \mu) + \frac{D}{D + e} \tag{III.19}$$

III.6 Formulas describing the dynamic behaviour of the water column

To be completer the exact formulas describing the dynamic behaviour are given in this section. However, much physical and mathematical knowledge is required to understand these formulas.

The dynamic behaviour of the water column is modelled by deriving a relation between (1) the water velocity at the bottom end of the rising main induced by piston and cylinder movements and (2) the dynamic part of the pressure at the bottom end of the rising main (which simply has to be added to the static pressure to find the actual pressure).

This means that if the piston and the cylinder movements are known in detail (so the water displacement is known; see Chapter 3), the pressure fluctuations can be calculated using this sub model.

In section 3.4 it was already suggested that pressure disturbances behave like waves. This is permitted because we proved this using general flow equations. This proof[4] resulted in a quantitative description of the propagation of pressure waves. Also the propagation speed was determined in this exercise, turning out to be an important parameter. To complete the model we also need to know (apart from the propagation mechanism of the waves) the reflection mechanism of the waves at the

---

4 see publication IADHPP89.07

top end of the rising main and the production mechanism of the waves at the bottom end of the rising main. This results in a set of differential equations describing the dynamic behaviour:

$$\frac{\partial p}{\partial x}(A_{i\,rm}-A_{pr})+\tau_{0,rm}\,\pi D+\tau_{0,pr}\,\pi\, d_{pr}+\rho\, g\sin\alpha+\rho\,(A_{i\,rm}-A_{pr})\frac{dv}{dt}=0 \tag{III.20}$$

$$\frac{1}{\rho}\frac{dp}{dt}+a^2 v_x=-a^2\frac{2\mu\, A_{i\,rm}}{A_{i\,rm}-A_{pr}}\frac{v_{cyl}}{L} \tag{III.21}$$

with:

p	$= p(x,t)$	(pressure at time t and place x in the rising main)
v	$= v(x,t)$	(velocity at time t and place x in the rising main)
v_{cyl}	$= v_{cyl}(t)$	(velocity of the cylinder at time t)
D	$= 2\, r_{i\,rm}$	(inside diameter of the rising main)
d_{pr}	= diameter of the pump rod plus coating	
$A_{i\,rm}$	= internal cross section of the rising main	
A_{pr}	= cross section of pump rod plus coating	
L	= length of the riser	
$\tau_{0,pr}$	= wall friction coefficient, pump rod	
$\tau_{0,rm}$	= wall friction coefficient, rising main	
ρ	= density of water (1000 kg/m^3)	
μ	= transverse contraction ratio (μ_{pvc}= 0.35)	
a	= velocity of sound (see equation III.18)	

Equations (III.20) and (III.21) are similar to the so-called water hammer equations. The presence of the pump rod inside the rising main has been taken into account. The Poisson contraction of the rising main, which occurs when the riser is strained, is included in equation (III.21) in a quasi-static manner. For details see publication IADHPP89.07.

Damping caused by wall friction is included in equation (III.20). There are many more damping processes, but we have not been successful in finding the theories predicting the damping. This problem was solved partially by introducing an empirical damping term in the equations, whereby the damping coefficient has to be chosen to fit best with the experimental observations.

Since we try to model the dynamic behaviour of the water column, we assume to know the water velocity at the bottom end of the rising main, which enables us to solve the differential equations (III.20) and (III.21). The solution is an explicit relation between pressure and velocity.

We transform the equations to the frequency domain by substituting the so-called flat wave in (III.20) and (III.21). The flat wave can be found by Fourier transforming pressure and velocity:

$$p=\int_{-\infty}^{\infty}\tilde{p}(\omega)\cdot e^{i(\omega t+kx)}\,d\omega \tag{III.22a}$$

$$v = \int_{-\infty}^{\infty} \tilde{v}(\omega) \cdot e^{i(\omega t + kx)} d\omega \tag{III.22b}$$

Substituting (III.22) and the boundary conditions in (III.20) and (III.21) finally results in:

$$\tilde{p}(x=0) = Z_{rel}(\omega) \cdot \tilde{v}_{rel}(x=0) + Z_{cyl}(\omega) \cdot \tilde{v}_{cyl}(x=0) \tag{III.23}$$

where the so-called impedances Z_{cyl} and Z_{rel} are given by:

$$Z_{cyl}(\omega) = i\rho a \left\{ \tan\left(\frac{\omega L}{a}\right) - \frac{a\alpha}{\omega L} \cdot \left(\frac{1}{\cos\left(\frac{\omega L}{a}\right)} - 1 \right) \right\} \tag{III.24a}$$

where

$$\alpha = \frac{2\mu A_{irm}}{A_{irm} - A_{pr}}$$

and

$$Z_{rel}(\omega) = i\rho a \tan\left(\frac{\omega L}{a}\right) \tag{III.24b}$$

The measurements, from which pressure and velocities were derived, were used to check the model (see publication IADHPP89.07).

The results plotted in Figure 3.11 were obtained in the following way:
From the measured $v_{rel}(t)$ and $v_{cyl}(t)$ the coefficients $\tilde{v}_{rel}(\omega)$ and $\tilde{v}_{cyl}(\omega)$ were derived by means of the FFT (Fast Fourier Transform) algorithm. With these values, and using equation (III.23) $\tilde{p}(\omega)$ was calculated. Using the inverse FFT algorithm, p(t) was derived.

APPENDIX IV

APPENDIX IV SUMMARIZED DESIGN RULES FOR HANDPUMPS UNDER FATIGUE CONDITIONS

IV.1 STAINLESS STEEL

IV.1.1. Stainless steel AISI 304

For pump rods that are normally submerged in fresh water the fatigue strength goes down with an increasing number of cycles. The ultimate fatigue strength of both annealed and 98% cold worked stainless steel AISI 304 is given in Figure 5.1.

The ultimate fatigue strength[5] of smooth stainless steel AISI 304 in fresh water[6] is

	200,000 cycles	100 million cycles
annealed AISI 304	240 N/mm^2	170 N/mm^2
98% cold worked AISI 304	860 N/mm^2	790 N/mm^2

For a type of stainless steel that has only been partly cold worked, the fatigue strength can be found by linear interpolation between the values of 0% and 98%.

IV.1.2. Notched stainless steel AISI 304

The notches for which the pump rods generally have to be designed are notches formed by grooves of a thread.
As a rule of thumb the following values can be used:

- for mechanically cut thread $K_t \approx 3$ (IV.1)
- for rolled thread $K_t \approx 2$ (IV.2)

For *annealed stainless steel AISI 304* $q = 0.3$ for $K_t < 4$ (IV.3)

For *cold worked (98%) stainless steel AISI 304*
$q = 0.7$ for $K_t < 4$ (IV.4)

In all cases: $K_f = 1 + q(K_t - 1)$ (see paragraph 5.5.5) (IV.5)

Safety factor

In view of the range of values for K_f found in literature, as well as the incompleteness of data about notches, it is preferable to take a safety factor of 2 for thread under load:

safety factor = 2

5 This is valid for alternating axial stresses (combined tension and bending) in the pump rod, which is normally the case. It is not valid for torsion.

6 In aggressive water lower values apply.

IV.1.3. Summarized design procedure

To obtain the design strength of stainless steel AISI 304 with thread, the following procedure can be followed:

Data to be given:
- the material, stainless steel AISI 304
- the treatment: annealed or cold worked, in %
- the plain fatigue stress
- the type of thread, with K_t value

In most cases, the value for K_t of thread is given in handbooks; if not, determine:
- K_t using equations (IV.1) or (IV.2)
- K_f using equations (IV.3), (IV.4) or (IV.5)

Choose a desirable lifetime for the pump rod, say 10 years. With Figure 5.6 this gives a number of cycles of about 10^8 (100 million cycles) supposing the pump is used as indicated. With the same figure the plain fatigue strength can be found, using the lines for fresh water (which take the corrosion effect into account only partly). The ultimate fatigue strength and design fatigue strength can then be calculated, as follows:

- ultimate fatigue strength $= \dfrac{\text{plain fatigue strength}}{K_f}$

- design fatigue strength $= \dfrac{\text{ultimate fatigue strength}}{\text{safety factor}}$

IV.1.4 Example calculation

Assume mechanically cut thread BSF (r = 0.135) on annealed stainless steel AISI 304 pump rods. From data books the value $K_t = 3.3$ can be derived, resulting in a factor $K_f = 1.7$, according to equation (IV.5)[7].

At a lifetime of 10 years (10^8 cycles) the plain fatigue stress then is found to be 170 N/mm^2.
This gives an ultimate fatigue strength of 170/1.7 = 100 N/mm^2.
Taking into account a safety factor of 2, as recommended by Beekman and de Jongh, the design fatigue strength becomes: 100/2 = 50 N/mm^2.

---

[7] When no data books are available, the value proposed under (IV.1) and equation (IV.5) would give $K_t = 3$ and $K_f = 1.6$, or: a negligible difference.

IV.2 PVC

Strength criteria

The brittle strength criteria for uPVC and rigid PVC for rising mains in handpumps, protected against direct sunlight[8] are:
fatigue strength (for 10^8 cycles):

- for smooth pipe 16.5 N/mm^2 (IV.6)
- for glued/threaded pipe 6.0 N/mm^2

For the S-N curve of smooth PVC see Figure 5.2.

Note:
For a threaded riser connection it is possible to estimate a fatigue strength, based upon the geometrical data of the thread cut on the pipe ends. First the stress concentration is calculated, and then, by using the notch sensitivity, the fatigue strength reduction factor. In the case of the SWN pump this results in a fatigue strength of about 6 N/mm^2.
However, it is very probable that during cutting of the thread small cracks have developed, with a root radius of about 10 μm. As a consequence, the fatigue strength will have been reduced to 2.5 N/mm^2!

Also in a cemented rising main similar cracks may occur, due to the action of the solvent in the glue. Since we have no information on the strength reduction factor in relation to the chemical activity of the glue in a period of 10 years (or 10^8 cycles), we propose to use the value of 2.5 N/mm^2 also for the fatigue strength of a cemented rising main. (Field experience indicates that this value is not too low.)

The maximum allowable load fluctuation amplitude on the riser can be found by multiplying the fatigue strength by the cross-sectional area of the riser.

---

[8] If PVC pipe is subjected to direct sunlight, the ultraviolet rays in the sunlight cause a vastly accelerated loss of strength of the pipe, which becomes brittle and discoloured (brown/blackish).

APPENDIX V

APPENDIX V EXAMPLE OF A DYNAMIC SYSTEM: THE MASS-SPRING SYSTEM

As an illustration the simplest dynamic system will be discussed here: the mass-spring system.

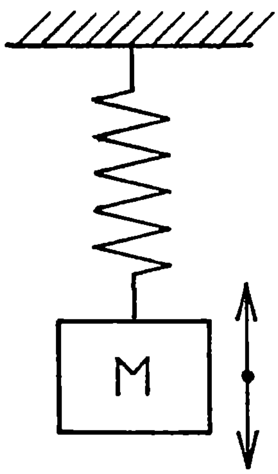

Figure V.1 Schematics of mass-spring system

When the mass is thrust a vibrational motion will start. The vibration is due to the exchange of energy between the elongation of the spring and the kinetic energy (due to inertia) of the mass. Such continuous motion without interaction with the environment is called a *free* oscillation. The frequency of the free oscillation is called the *resonance frequency*.

The counterpart of the free oscillation is the *forced oscillation*: this means that a periodic force acts upon the mass. This also results in a vibration, which has the same frequency as the periodic force. During pumping only forced oscillations occur, the external force imposed by the piston movement. The parameter of interest is the amplitude of the vibration.

Suppose a sinusoidal force with a very low frequency acts on the mass. Then the inertia will be much smaller than the force due to the elongation of the spring. This situation is called *quasi-static*. The amplitude of the vibration is determined by the amplitude of the force and the stiffness of the spring, the elongation being proportional to the force.

Increasing the frequency will increase the accelerations. At very high frequencies the accelerations are so large that the mass will hardly move from its equilibrium position. The force due to inertia will then be much larger than the force due to the elongation of the spring.

Between very high and very low frequencies lies the resonance frequency. When the force is applied with the resonance frequency, the mass starts an oscillating motion with this frequency. Suppose we now stop applying the force (for a moment). We know from free oscillations that the vibration will continue with exactly the resonance frequency and with the same amplitude. So when the force is

applied again the amplitude will even grow. In fact, the amplitude would become infinite if not the friction or another damping mechanism would dissipate the energy supplied by the force.
It should be mentioned that more complicated systems (e.g. multiple mass-spring systems) do have more than one resonance frequency.

Summarizing the typical behaviour of dynamic systems (see also Figure V.2):

Free oscillations: vibrations with resonance frequency
Forced oscillation:
- If the driving frequency is much lower than the lowest resonance frequency: the system behaves quasi-statically;
- If the driving frequency is (almost) equal to (one of) the resonance frequencies: the oscillation amplitude may become very large;
- If the driving frequency is much larger than the resonance frequencies: the inertia dominates the response. In fact, the higher the frequency, the less the system responds (i.e. the smaller the amplitude becomes).

The amplitude ratio (Figure V.2) equals $\dfrac{\text{displacement amplitude at frequency f}}{\text{displacement at zero frequency}}$,

both being brought about by a force with equal amplitude.

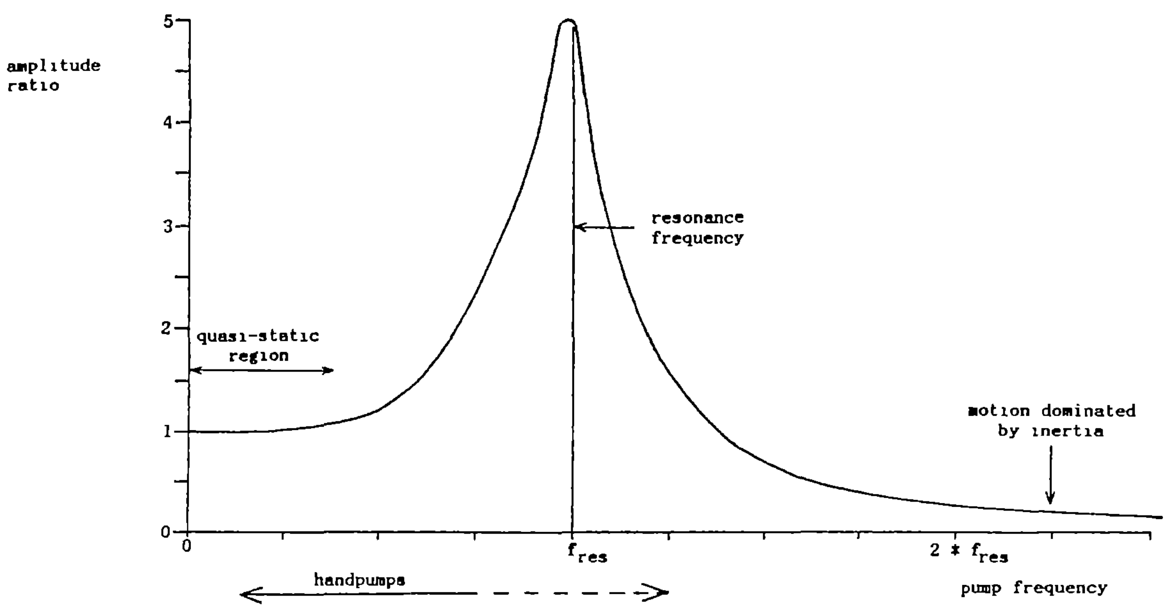

Figure V.2 Typical behaviour of a mass-spring system (forced oscillation)